NOVEL MEDIATORS OF PLATELET-MEDIATED HEMOSTASIS

by

Nima Mazinani

B.Sc., University of British Columbia, 2013

A THESIS SUBMITTED IN PARTIAL FULFULLMENT OF

THE REQUIREMENT FOR THE DEGREE OF

DOCTOR OF PHILOSOPHY

in

THE FACULTY OF GRADUATE AND POSTDOCTORAL STUDIES

(Biochemistry and Molecular Biology)

THE UNIVERSITY OF BRITISH COLUMBIA

(Vancouver)

July 2020

The following individuals certify that they have read, and recommend to the Faculty of Graduate and Postdoctoral Studies for acceptance, the dissertation entitled:

Novel mediators of platelet-controlled hemostasis

submitted by Nima Mazinani in partial fulfillment of the requirements for the degree of Doctor of Philosophy in Biochemistry and Molecular Biology

Examining Committee:

Dr. Christian J. Kastrup, Associate Professor, Biochemistry and Molecular Biology
Supervisor

Dr. Ed Pryzdial, Clinical Professor, Biochemistry and Molecular Biology, UBC
Supervisory Committee Member

Dr. Joerg Gsponer, Associate Professor, Biochemistry and Molecular Biology, UBC
Supervisory Committee Member

Dr. Hugh Kim, Associate Professor, Biochemistry and Molecular Biology, UBC
University Examiner

Dr. Jay Kizhakkedathu, Associate Professor, Biochemistry and Molecular Biology, UBC
University Examiner

Abstract

Platelets are small, discoid, anucleate blood cells that circulate in the blood. The primary role of platelets is to mediate various aspects of hemostasis, but platelets are also key mediators in inflammation, host defense, and tumor growth and metastasis. In hemostasis, platelets work in concert with the endothelium and blood coagulation enzymes to sense and respond to injury and hemostatic challenges. Platelets elicit their functions through activation of a plethora of surface receptors and release of a vast array of granule contents. However, there are substantial gaps in knowledge with various abundant platelet contents with regards to their roles and interactions in hemostasis. This thesis examines the contribution of short-chain polyphosphate (PolyP) on clotting, inactivation of coagulation factor XIII (FXIII) by plasmin, cross-linking of amyloid beta (Aβ) by FXIII, regulation of amyloid precursor protein (APP) processing by FXIII activity, and the contribution of APP to hemostasis.

Short-chain polyP is released from platelets upon platelet activation, but it is not clear if it contributes to thrombosis. In this thesis, the ability of localized polyP, as particles or on surfaces, to clot flowing blood plasma was examined using a microfluidic device. Localized polyP of all lengths was more effective at triggering clotting than when solubilized in solution or as nanoparticles. In particular, surface localized short-chain polyP, previously not considered as a hemostatic agent, was able to clot flowing blood plasma at sub-micromolar concentrations at shear rates typical of large veins or valves, where thrombosis usually occurs. These results indicate that platelet-length short-chain polyP can modulate thrombosis when localized onto surfaces.

Transglutaminase FXIII circulates in plasma (bound to fibrinogen) and in platelets, and is critical for various hemostatic and platelet functions. However, the mechanism by which FXIII

becomes inactivated is unknown. This thesis examined the potential role of the fibrinolytic system in the inactivation of FXIII. Plasmin preferentially cleaves and degrades the active enzyme, FXIIIa, but not the zymogen, FXIII.

Lay Summary

Platelets are small cells that are required to stop the flow of blood during injury. Platelets stick to the site of injury and release various molecules to help with the blood clotting and healing process. The function of several molecules within platelets is not clear, and identifying their roles can be of great interest in developing tools to help stop bleeding. This thesis examines several different abundant molecules within platelets with functions that are unclear or ambiguous, and investigates their roles in various aspects of blood clotting. Here we show polyphosphate released by platelets can trigger clotting, only if localized to a surface. This thesis shows that coagulation factor XIII can be inactivated by the fibrinolytic system, but also that it can covalently cross-link amyloid beta released by platelets. Furthermore, factor XIII can also covalently modify amyloid beta precursor protein on platelets and modulate its processing.

Preface

Approvals for the study were given by the research ethics boards of the University of British Columbia and Vancouver Coastal Health Research Institute. The UBC Ethics Certificate is H14-01581 for human blood collection and A16-0176 for mouse blood collection. The reuse and reprint of all published work is with permission from all journals referenced.

A modified version of Chapter 2 has been published in *Scientific Reports*: J.H. Yeon, N. Mazinani, T.S. Schlappi, K.Y.T. Chan, J.R. Baylis, S.A. Smith, A.J. Donovan, D. Kudela, G.D. Stucky, Y. Liu, J.H. Morrissey, C.J. Kastrup (2017). Localization of short-chain polyphosphate enhances its ability to clot flowing blood plasma. J.H.Y. and N.M. were co-first authors on the paper. N.M., J.H.Y., T.S.S., K.Y.T.C., J.R.B., S.A.S., A.J.D., and D.K., performed experiments and analyzed data; N.M., J.H.Y., T.S.S., C.J.K., J.H.M., Y.L., and G.D.S. conceptualized and planned experiments; N.M., J.H.Y., and C.J.K. wrote the manuscript; and all authors reviewed and edited the manuscript before submission. N.M. performed experiments to collect data for Figures 2.2B, 2.3B-C and 2.4A-D., and contributed to 40% of this paper.

A modified version of Chapter 3 has been published in *Blood*: W.S. Hur, N. Mazinani, X.J. Lu, H.M. Britton, J.R. Byrnes, A.S. Wolberg, C.J. Kastrup (2015). Coagulation factor XIIIa is inactivated by plasmin. W.S.H. conceived the idea, designed experiments and performed experiments, analyzed and interpreted data and wrote the paper. W.S.H. performed experiments to collect data specifically for Figures 3.1, 3.2A-E, 3.3, 3.4, 3.5, 3.7, 3.8, 3.9, 3.10, 3.10A-B and 3.11. N.M. designed and performed experiments to collect data for Figure 3.2F, 3.6, 3.10C-E, analyzed and interpreted data, and wrote the paper. N.M. contributed to 20% of this paper. C.J.K. helped design experiments, interpret data and write the paper. Collaborators and undergraduate

thesis students contributed to different aspects of the paper, such as methods development (J.R.B.), performing preliminary experiments (X.J.L. and H.M.B.) and data analysis (A.S.W.).

A modified version of Chapter 4 has been published in *Journal of Biological Chemistry*: W.S. Hur, N. Mazinani, X.J. Lu, L.S. Yefer, J.R. Byrnes, L. Ho, J.H. Yeon, S. Filipenko, A.S. Wolberg, W.A. Jefferies, C.J. Kastrup (2018). Coagulation factor XIIIa cross-links amyloid β into dimers and oligomers and to blood proteins. W.S.H and N.M. were co-first authors on the paper. W.S.H. designed, performed experiments, analyzed and interpreted the data and wrote the paper. W.S.H. performed experiments to collect data for Figure 4.1A-B, 4.2C-D, 4.3, 4.4, 4.5A, 4.7A and 4.7C-D. N.M. performed experiments to collect data for Figure 4.1C, 4.5B-C, 4.6A-C and 4.7B and wrote the paper. N.M. contributed to 40% of this paper. J.B. performed experiments for Figure 4.2A-B. C.J.K. helped design and analyze experiments and write the paper. Collaborators and undergraduate thesis students contributed to other aspects of the paper such as preliminary data collection (X.J.L., L.S.Y., L.H., J.H.Y, S.F.), and data analysis and editing of the paper (A.S.W. and W.A.J.).

A modified version of Chapter 5 has been prepared for publication. W.S. Hur, N. Mazinani, L.J. Juang, W.A. Jefferies, C.J. Kastrup (2020). Post-translational modifications of platelet-derived amyloid precursor protein regulated by transglutaminase coagulation factor XIII-A*. W.S.H. designed, performed experiments, analyzed and interpreted the data and wrote the paper. W.S.H. performed experiments to collect data for Figure 5.1A-C, 5.2A, 5.2C-F, and 5.4A-C. N.M. performed experiments to collect data for Figure 5.2B and 5.3A-D and edited the paper. N.M. contributed to 40% of this paper. L.J.J. is currently performing experiments to supplement Figure 5.4A-C. C.J.K. and W.A.J. helped design and analyze experiments and write the paper.

A modified version of Chapter 6 has been published in *Research and Practice in Thrombosis and Haemostasis*: N. Mazinani, A.W. Strilchuk, J.R. Baylis, W.S. Hur, W.A. Jefferies, C.J. Kastrup (2020). The absence of amyloid precursor protein in a mouse model measurably increases bleeding. N.M. designed, performed experiments, analyzed and interpreted the data and wrote the paper. N.M. performed experiments to collect data for Figure 6.1, 6.2 and 6.3. N.M. contributed to 75% of this paper. A.W.S. performed experiments to collect data for Figure 6.4A-C. J.R.B. performed experiments to collect data for part of Figure 6.1 and 6.3. C.J.K. and W.A.J. helped design and analyze experiments and write the paper. W.S.H. analyzed data and edited the paper.

Table of Contents

List of Tables

List of Figures

List of Symbols

α alpha

β beta

γ gamma

ε epsilon

μ micro

List of Abbreviations

Aβ	Amyloid-β
AD	Alzheimer's disease
ADP	Adenosine diphosphate
AICD	Amyloid precursor protein intracellular domain
AP	α2-antiplasmin
APC	Activated protein C
APP	Amyloid precursor protein
APTT	Activated partial thromboplastin time
AT	Antithrombin
ATP	Adenosine triphosphate
B.D.	Below detection
BK	Bradykinin
CAA	Cerebral amyloid angiopathy
CD39	ADPase
CD40L	CD40 ligand
CD42b	Glycoprotein Ib
cFXIII	Cellular FXIII
CGS	Citrate glucose saline buffer
CNS	Central nervous system
COL	Collagen
COX-1	Cyclooxygenase-1
CSF	Cerebrospinal fluid

DAG	1,2 diacylglycerol
DAPI	4′,6-diamidino-2-phenylindole
DLS	Dynamic light scattering
D-polyP	Dispersed polyphosphate
DHPE	1,2-dihexadecanoyl-sn-glycero-3-phosphoethanolamine
DMSO	Dimethylsufoxide
DTT	Dithiothreitol
DVT	Deep vein thrombosis
EACA	ε-aminocaproic acid
ECM	Extracellular matrix
EDTA	Ethylenediaminetetraacetic acid
EPCR	Endothelial protein C receptor
FAD	Familial Alzheimer's disease
FDP	Fibrinogen degradation products
FGN	Fibrinogen
FITC	Fluorescein isothiocyanate
FV(a)	(Activated) coagulation factor V
FVII(a)	(Activated) coagulation factor VII
FVIII(a)	(Activated) coagulation factor VIII
FIX(a)	(Activated) coagulation factor IX
FX(a)	(Activated) coagulation factor X
FXI(a)	(Activated) coagulation factor XI
FXII(a)	(Activated) coagulation factor XII

FXIII(a)	(Activated) coagulation factor XIII
FXIIID	Coagulation factor XIII deficiency
GP	Glycoprotein
HEPES	4-(2-hydroxylethyl)-piperazineethanesulfonic acid
HK	High molecular weight kininogen
HMWP	High molecular weight protein
ICH	Intracranial hemorrhage
IP3	Inositol 1, 4, 5-triphoshate
KO	Knock-out
LPS	Lipopolysaccharide
NET	Neutrophil extracellular trap
NFT	Neurofibrillary tangles
NP-polyP	Nanoparticle polyphosphate
ns	Not significant
OCS	Open canicular system
PAI	Plasminogen activator inhibitor
PAMP	Pathogen-associated molecular pattern
PAR	Protease-activated receptor
PBS	Phosphate buffered saline
PC	Phosphatidylcholine
PDMS	Polydimethylsiloxane
PE	Pulmonary embolism
PF4	Platelet factor 4

pFXIII	Plasma FXIII
PK	Plasma kallikrein
PLCγ2	Phosholipase Cγ2
PLT	Platelet
Pn	Plasmin
PolyP	Polyphosphate
PPK	Plasma prekallikrein
PRP	Platelet-rich plasma
PT	Prothrombin time
PS	Phophatidylserine
P2Y	Purogenic receptor
RANTES	Regulated on activation normal T cell expressed and secreted
RBC	Red blood cell
sAPP	Soluble amyloid precursor protein
SEM	Standard error of mean
SDS	Sodium dodecyl sulfate
SI-polyP	Surface-immobilized polyphosphate
SMC	Smooth muscle cell
SNP-polyP	Polyphosphate-coated silica nanoparticles
TAFI	Thrombin activated fibrinolysis inhibitor
TEG	Thromboelastography
TF	Tissue factor
TFPI	Tissue factor pathway inhibitor

TG	Transglutaminase
TGF-β1	Transforming growth factor beta 1
THR	Thrombin
TLR	Toll-like receptor
TP_{α}	Thromboxane receptor
tPA	tissue-type plasminogen activator
TXA	Tranexamic acid
TxA_2	Throboxane A_2
uPA	Urokinase-type plasminogen activator
uPAR	uPA receptor
vWF	von Willebrand factor
WT	Wild type

Acknowledgements

Thank you to all current and past members of the Kastrup lab. In particular, the following members have contributed significantly or provided support for data collection for this dissertation: W. Hur, V. Chan, S. Novakowski, J. Baylis, J. Yeon and A. Strilchuk. I thank my supervisor, Dr. Christian Kastrup, and my supervisory committee Dr. Ed Pryzdial and Dr. Joerg Gsponer, for their support and research guidance. I also thank our collaborators, Drs. Wilf Jefferies and Alisa Wolberg, and the members of their labs for their contributions.

Thank you to the donors and the staff at the Canadian blood Services' netCAD facility, as well as all my fellow graduate students and co-workers who donated their time (and blood) to our lab.

Dedication

To my father, Davoud, and my brother, Hajeir, for their continual support.

Chapter 1: Introduction

1.1.1 Thesis overview

Platelets are key players in a multitude of physiological and pathological processes, including during hemostasis, thrombosis, inflammation, host defense, and tumor growth [1]. The primary function of platelets is to stop hemorrhage following vascular damage, and they are indispensable to the process [2]. Platelets circulate in the blood and can detect and respond to vascular damage through its surface receptors and release of various bioactive granule contents that aid in the process of hemostasis and thrombosis [2]. Many of these molecules are well characterized and their direct roles to clotting are understood. However, traumatic hemorrhage and uncontrollable bleeding remains a leading killer of young healthy people worldwide, accounting for 10% of the world's deaths [3-5]. There remains a need to further understand the mechanisms modulating hemostasis, particularly with platelets due to their many roles within and outside of blood clotting.

Platelets are an attractive area of research as they contain and release a plethora of surface proteins, receptors, small molecules, bioactive lipids, proteins, peptides, hormones, growth factors and other biologically active molecules [6]. Platelet releasate and mass spectrometry proteomics analysis has extensively categorized these molecules; however, several platelet molecules still have no clear physiological or pathophysiological functions in hemostasis. For platelet molecules with unknown or ambiguous roles that are released upon platelet activation, it would not be unsurprising for their biological roles to be in relation with clotting, as it is the primary platelet role. As such, the focus of this thesis was to investigate the novel functions and interactions of several abundant platelet proteins and molecules with unclear roles in hemostasis and thrombosis. Specifically, this thesis examines and explores novel

interactions and roles of platelet-length polyphosphate, coagulation factor XIII, amyloid beta, and amyloid beta precursor protein. All of which are contained in high concentrations within platelets, and released or externalized upon platelet activation following vascular injury.

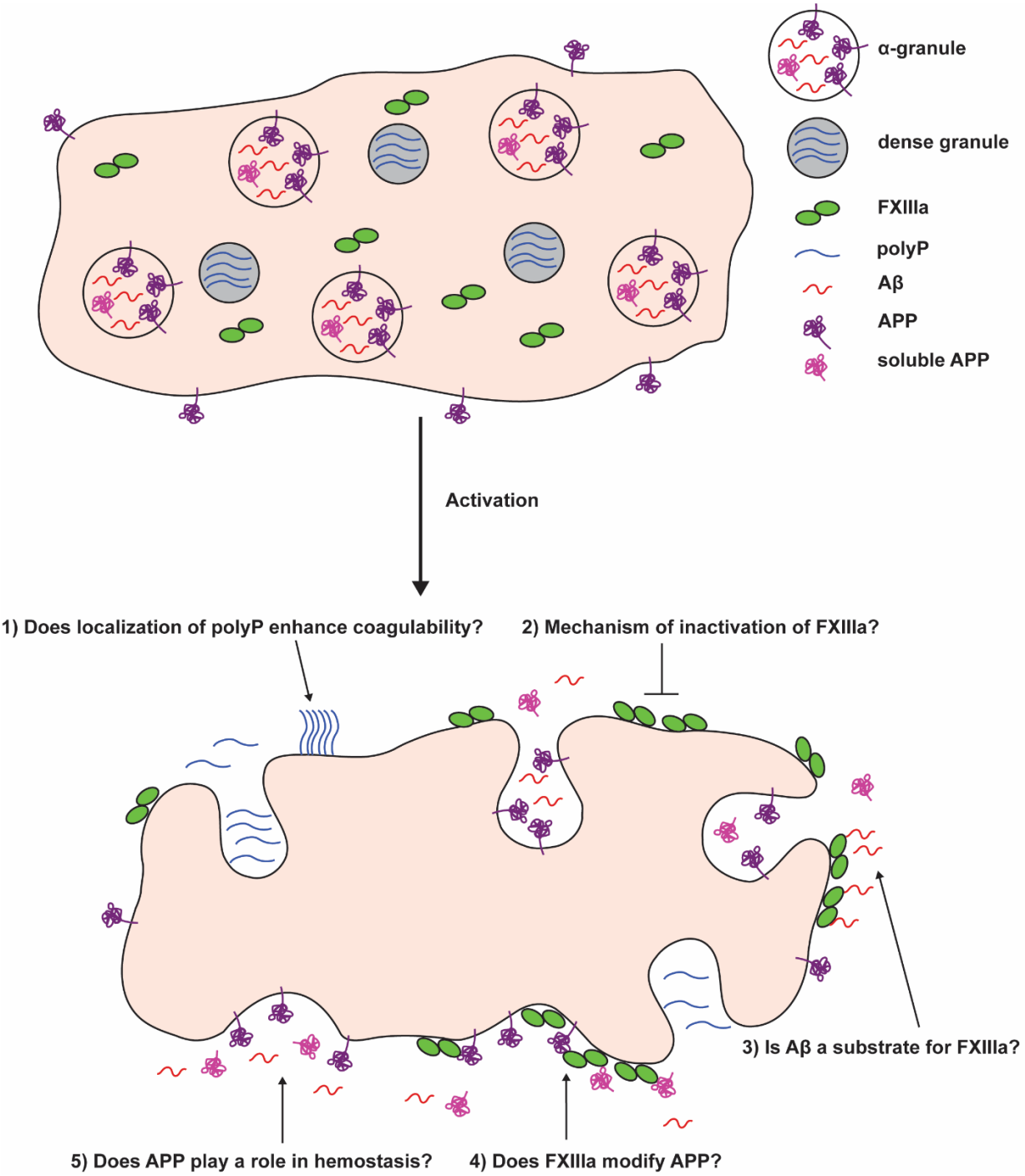

Figure 1.1 Thesis overview of examined questions.

The overarching theme of this thesis is then to identify novel functions in hemostasis in relation to each of these abundant platelet components. Each of these molecules have been extensively studied, however, their specific roles in hemostasis have been difficult to decipher likely due to their multifaceted and typically disparate functional plurality. Each specific question in the figure above come together to further our understanding of platelets in hemostasis and pathophysiological processes: 1) Does localization of polyP enhance coagulability? 2) What is the mechanism of inactivation of FXIIIa? 3) Is Aβ a substrate for FXIIIa? 4) Does FXIIIa modify APP? 5) Does APP play a role in hemostasis? In addition, these specific questions lend themselves in illuminating current gaps in knowledge regarding various pathophysiological processes. For example, question 1 can also help our understanding of polyP mediated thrombosis in humans, as well as develop novel targets and therapies against unwanted thrombosis. Question 2 furthers our understanding of the effect of fibrinolysis on anti-fibrinolytics, and is relevant in various coagulopathies which include hyperfibrinolysis. Questions 3-5, which are the bulk of this thesis, maintains an effort to address several long-neglected aspects of platelet biology and molecules historically only appreciated in the context of the brain in Alzheimer's disease. These last questions in particular are aimed to further strengthen the relationship and overall appreciation of the links between Alzheimer's disease pathology and various aspects of hemostasis.

1.2 Rationale and objectives

1.2.1 Examine the role of platelet polyphosphate in thrombosis

Polyphosphates (polyP) are inorganic linear polymers of phosphate residues which are ubiquitous in nature [7]. Long-chain polyP (hundreds to thousands of residues long), generally found in microbes, is a potent activator of clotting via the intrinsic pathway [8, 9]. By contrast, short-chain polyP (60-100 residues long) is found in high concentrations in platelet dense granules and released upon activation, but do not appear to trigger clotting at physiological concentrations [10]. The different propensities of short- and long-chain polyP to trigger clotting is likely due to the ability of long-chain polyP to spontaneously aggregate into particles, thereby increasing its local concentration [10]. Thus it is unclear if there is a physiological role for short-chain polyP released by platelets in thrombosis [11].

In chapter 2, I determined spatial localization of short-chain polyP increases its propensity to trigger clotting. Numerical simulations predicted the effect of localization of polyP under flow. Microfluids were used to test this prediction *in vitro*. Surface localized short-chain polyP was evaluated for its ability to trigger clotting at various shear rates, compared to solubilized short-chain polyP.

1.2.2 Identify the mechanisms of inactivation of coagulation factor XIII

Coagulation factor XIII (FXIII) is a transglutaminase that cross-links fibrin and other proteins to seal and strengthen the blood clot [12]. In addition to regulating clot stability, FXIII is also abundant in platelets and modulates several platelet functions [13]. The synthesis, localization, and activation of FXIII have been well characterized [13]; but a clear physiological mechanism of inactivation has remained elusive. Activated FXIII (FXIIIa) is a promiscuous transglutaminase [14], and presumably systemic unregulated circulation of activated FXIIIa

would result in deleterious effects. As fibrin and FXIII are co-localized at the site of clotting[13], a candidate for the inactivation of FXIII is plasmin, which is normally tasked with degrading fibrin [15]. This was previously ruled out [16], but these studies were extended to further evaluate how the fibrinolytic system regulates FXIIIa inactivation.

In chapter 3, I determined plasmin degrades FXIIIa, while unactivated FXIII is resistant. The rate of proteolytic cleavage was quantified, and the primary cleavage sites were determined to further characterize the reaction. Both plasma and platelet FXIIIa were tested for their sensitivity to plasmin degradation. Situations during the hemostatic process where this reaction might be relevant were assessed.

1.2.3 Examine the role of FXIIIa in cerebral amyloid angiopathy

Cerebral amyloid angiopathy (CAA) is a common pathological hallmark of Alzheimer's disease, where amyloid beta (Aβ) peptides deposit along the cerebrovascular lumen and lead to degeneration and dysfunction of the surrounding tissue [17]. The mechanism of Aβ deposition in CAA has not been determined [17], however FXIIIa has been found to co-localize with Aβ in CAA deposits [18]. Additionally, platelets are implicated in AD progression and contain both FXIIIa and Aβ, which are externalized/released upon platelet activation [19]. However, the ability of FXIIIa to cross-link Aβ has not been demonstrated.

In chapter 4, I determined the ability of FXIIIa to covalently cross-link Aβ. The kinetic parameters of the reaction were quantified in a purified system using a spectrometric assay. The ability of FXIIIa to cross-link Aβ to other blood and platelet proteins was evaluated. Furthermore, the ability of platelet FXIIIa to cross-link Aβ was determined. The effects of FXIIIa-mediated Aβ cross-linking on the mechanical properties of clots was assessed. Finally, the cross-linking of various Aβ mutants relevant in AD progression was examined.

1.2.4 Examine interactions between platelet amyloid precursor protein and FXIIIa

Amyloid beta precursor protein (APP) is a type 1 transmembrane protein that can be proteolytically processed to generate several metabolites including Aβ and soluble forms of APP [20]. APP is highly expressed in the brain, but platelets also contain an abundant source of circulating APP [21]. Platelets APP is primarily stored in alpha granules, and can be processed into metabolites and released upon platelet activation [22]. The physiological function of platelet APP is not well understood. Aβ, a primary metabolite of APP, co-localizes with FXIIIa in CAA plaques [18]. . However, whether FXIIIa can modify full-length platelet APP or its other metabolites has not yet been evaluated.

In chapter 5, I evaluated novel interactions between platelet APP, its metabolites, and FXIIIa. Binding of platelet FXIIIa and APP was evaluated at different platelet activation states using co-immunoprecipitation and mass spectrometry. The effect on FXIIIa biology in the presence or absence of APP was assessed in mouse platelets. The processing of platelet APP was evaluated in the presence or absence of FXIIIa activity. Finally, the ability of FXIIIa to cross-link soluble forms of APP was determined.

1.2.5 Examine if amyloid precursor protein plays a role in hemostasis

While APP is abundant in platelets, its physiological role in hemostasis is not clear. Platelet APP contains a Kunitz-type protease inhibitor (KPI) domain that potently inhibits several coagulation factors *in vitro* [24]. APP and its metabolites also have several procoagulant roles *in vitro,* promoting thrombus formation, platelet adhesion, platelet activation, and resistance to fibrinolysis [25-28]. Some i*n vivo* studies in mice have demonstrated the anticoagulant function of platelet APP in certain situations, but there are discrepancies in the data [29, 30]. The role of APP in hemostasis was further evaluated by examining hemostasis in

multiple mouse models, by selectively inhibiting several aspects of coagulation, and by analyzing coagulation in blood *ex vivo*.

In chapter 6, I identified a bleeding phenotype in mice deficient in APP. Blood loss in APP KO and WT mice were measured in liver laceration and tail transection models of hemorrhage. Blood loss was also measured in tail transection in mice treated with various modulators of coagulation, to determine the mechanism of the bleeding phenotype. Whole blood collected from APP KO and WT mice were also evaluated by thromboelastography to further investigate clotting differences in APP KO blood.

1.3 Background Information

1.3.1 Hemostasis

Hemostasis is the balance between procoagulant and anticoagulant factors, and the process of preventing blood loss by formation of a hemostatic plug at the site of vascular damage. The endothelium of blood vessels serves as an important anticoagulant surface to maintain the fluid state of blood in the absence of vascular damage [31]. However, if the endothelium is damaged, components of the subendothelium become exposed to blood, which activates a cascade of reactions with results in a stable blood clot primarily composed of platelets, fibrin, and red blood cells, at the site of injury [31]. Blood clotting, or coagulation, is primarily divided into 3 stages: 1) Primary hemostasis, or formation of a platelet plug via platelet aggregation, 2) Secondary hemostasis, formation and deposition of an insoluble fibrin network via activation of the coagulation cascade, and 3) Tertiary hemostasis, which initiates at the start of fibrin cross-linking and ends with fibrinolysis, or clot dissolution [32].

1.3.1.1 Primary Hemostasis

Primary hemostasis refers to platelet activation and aggregation at the local site of vascular damage and results in the formation of a platelet plug. Primary hemostasis is initiated within seconds following endothelial injury [31]. Inactive von Willebrand factor (vWF) circulating in the blood binds to newly exposed subendothelial collagen [32]. Under high shear, vWF monomers unfold and polymerize onto immobilized vWF-collagen by binding head-to-head and tail-to-tail to form vWF multimers or strands of 500 to 20,000 kDa in size [33]. The formation of vWF multimers exposes binding sites for high affinity binding of platelets to vWF via glycoprotein receptor Ib (GPIb), as part of the GPIb-V-IX receptor complex, even at arterial shear rates, which results in the deposition of a monocellular platelet layer [33]. At lower venous

shear rates, platelets can bind directly to exposed collagen via GPIa/IIa and GPVI [34, 35]. This initial process constitutes platelet adhesion to the site of vascular damage.

Following initial adhesion of platelets to collagen and vWF, platelets become activated and facilitate recruitment of additional platelets to induce platelet aggregation [36]. Upon activation, platelets undergo morphological changes and extend interlocking pseudopodia to enhance mechanical strength of the growing thrombus [37]. Platelets also release their granular contents, most notably adenosine diphosphate (ADP) and thromboxane A_2 (TxA_2), which act in an autocrine and paracrine manner to further amplify platelet activation in addition to activating nearby circulating platelets [38, 39]. Platelet activation also leads to conformational changes in GPIIb/IIIa, allowing the receptor to bind plasma fibrinogen [40]. Platelet aggregation now occurs through platelet-to-platelet linkages (via activated GPIIb/IIIa and fibrinogen), which leads to further platelet activation, granule release, and recruitment/aggregation of nearby circulating platelets [40]. Feedback activation allows for a rapidly growing platelet plug directly at the site of injury, and completes the final phase of primary hemostasis.

1.3.1.2 Secondary Hemostasis

Secondary hemostasis consists of the activation of the coagulation cascade which results in the deposition of an insoluble fibrin matrix around and among platelets which serves to strengthen the growing thrombus [41, 42]. This process occurs simultaneously with primary hemostasis and platelet aggregation [41, 42]. Secondary hemostasis is initiated when circulating factor VII (FVII) binds to subendothelial tissue factor (TF) [32]. TF is abundantly expressed on extravascular tissues as a transmembrane protein but is absent on endothelial cells [43]. Although some trace amounts of FVIIa (activated factor VII) circulates in blood, most circulates as the proenzyme FVII [45]. Once FVII binds to subendothelial TF, it undergoes autocatalysis to an

active serine protease, FVIIa [45]. The TF-FVIIa complex, termed the extrinsic pathway of coagulation, is a potent activator of FIX and FX [43]. FIXa can also activate FX to FXa in the presence of its cofactor FVIII [46]. FXa also in the presence of its cofactor, FV, binds to an anionic phospholipid membrane surface to form the prothrombinase complex, which converts prothrombin to the active serine protease thrombin [46].

Thrombin is a central mediator of several critical functions in coagulation. Thrombin converts soluble circulating fibrinogen into insoluble fibrin [47]. Fibrin monomers self-assemble noncovalently throughout the growing thrombus to form a matrix of fibrin protofibrils which provide initial mechanical strength [47]. Thrombin also converts essential cofactors FV and FVIII to their active forms, FVa and FVIIIa respectively, which greatly enhances the conversion of prothrombin to thrombin [32]. Thrombin also converts FXI to FXIa, which in turn activates FIX to FIXa, and in concert with FVIIIa generates the prothrombinase complex [48]. This latter FXIa mediated positive feedback of thrombin generation is termed the intrinsic pathway and is critical for clot propagation. The intrinsic pathway of coagulation can be triggered directly by activation of FXII, which can activate via autocatalysis upon binding to a negatively charged surface [49]. The resulting FXIIa converts plasma prekallikrein (PPK) to kallikrein (PK), another activator of FXII [49]. Together, FXIIa and PK can activate additional FXII in a positive feedback fashion, and FXIIa can initiate clotting by activating FXI.

Additionally, thrombin activates FXIII to FXIIIa which is essential for stabilizing fibrin [47], and is referenced during tertiary hemostasis in the following section. The final critical role of thrombin during secondary hemostasis is to activate platelets via cleavage of protease-activated receptor 1 and 4 (PAR1 and PAR4), which is the most potent activator of platelets [50]. It is important to note that the stated functions of thrombin do not happen sequentially, but occur

simultaneously. The cascade of reactions triggered by thrombin during secondary hemostasis serves to propagate and strengthen the growing clot by the generation of the fibrin matrix among other stated roles. The growing thrombus also captures a significant amount of red blood cells (RBCs) which contribute to the structural integrity and mass of the thrombus [51]. Stable cessation of blood loss is typically established at this time.

1.3.1.3 Tertiary hemostasis/fibrinolysis

Tertiary hemostasis is the final phase of hemostasis and typically referred to as fibrinolysis, or the resolution of the thrombus. Tertiary hemostasis begins with covalent cross-linking of adjacent fibrin monomers by the active transglutaminase FXIIIa. The cross-linking of fibrin monomers and other stabilizing factors to the clot strengthens the thrombus and prevents early lysis of the clot [52].

Concurrent to the clot initiation and propagation (primary and secondary hemostasis) are the negative regulators of coagulation (discussed in detail in the next section) which over time become a dominant force and negatively regulates thrombosis. Fibrinolysis is one such negative regulator and is initiated with the conversion of plasminogen to the active serine protease plasmin, which in turn can degrade fibrin and lyse the clot [53]. Plasmin is generated from tissue-type plasminogen activator (tPA) and urokinase-type plasminogen activator (uPA) [53]. tPA is the most potent activator of plasminogen and is released from damaged endothelial cells and binds to fibrin on lysine binding sites and catalyzes the conversion of plasminogen to plasmin [54]. uPA activates plasminogen to a lesser extent by binding to the uPA receptor (uPAR) on the surface of cells [55]. The lysis or degradation of the clot by plasmin generates fibrin degradation products (FDP) which is an indicator of thrombosis and active clot lysis [56].

Fibrinolysis, as in other aspects of coagulation, is tightly regulated to prevent uncontrolled thrombosis as well as premature clot lysis. Negative regulation of fibrinolysis occurs at several levels. Plasminogen activator inhibitors 1 and 2 (PAI-1 and PAI-2) directly inhibit tPA and uPA, and α_2-antiplasmin inhibits plasmin [54]. Additionally, thrombin activated fibrinolysis inhibitor (TAFI) negatively regulates fibrinolysis by removing fibrin lysine residues, which impairs the binding and localization of plasminogen, plasmin and tPA at the site of the clot [57].

1.3.1.4 Negative regulators of coagulation

As discussed earlier, negative regulation of coagulation, to prevent unwanted thrombus formation, is just as important as positive regulation of coagulation to prevent unwanted bleeding. The endothelium is a dynamic organ, and though it secretes procoagulant vWF, the endothelium also serves many essential functions to downregulate coagulation [31]. The intact endothelium serves as a natural barrier to coagulation by preventing the contact of blood to subendothelial procoagulant proteins [31]. Endothelial cells produce prostacylcin and nitric oxide which serve as vasodilators and inhibitors of platelet adhesion and aggregation [58]. Furthermore, endothelial cells express a membrane-associated ADPase (CD39) on their surface which degrades platelet agonist ADP [59].

The endothelium also executes several anticoagulant activities to regulate thrombin generation. Endothelial cells express heparin sulfate proteoglycans (HSPGs) on their surface which bind to circulating antithrombin (AT) and enhance the rate at which AT inhibits thrombin among other coagulation enzymes [60]. Tissue factor pathway inhibitor (TFPI), expressed by endothelium and megakaryocytes, binds to HSPGs and directly inhibits the TF-VIIa complex [61]. Potent inhibition of thrombin is mediated by thrombomodulin and endothelial protein C

receptor (EPCR), both expressed by endothelium and localized on the cell surface [62]. Thrombomodulin binds thrombin and inhibits the procoagulant activity of thrombin and instead converts the thrombomodulin-thrombin complex into an activator of protein C (PC), generating activated protein C (APC) [63]. APC and its cofactor protein S (PS) inhibit coagulation by inactivating cofactors FVa and FVIIIa [63]. EPCR enhances this reaction by binding PC and facilitating its binding to the thrombomodulin-thrombin complex [63]. Interestingly through this mechanism, thrombin is converted from a potent procoagulant to an anticoagulant and facilitates degradation of cofactors it initially activated. The final negative regulator of coagulation is fibrinolysis, which is also mediated by endothelial cells, and has been already discussed above.

1.3.2 Platelet Physiology

Platelets are small (1 to 3 μm in diameter), discoid, anucleate blood cells that circulate at a concentration of 150 x 10^9 to 400 x 10^9 cells/L [64]. Platelets are released directly into the blood following fragmentation of pseudopodial structures extending from megakaryocytes, in either the bone marrow or lung circulation [65, 66]. Once in circulation, platelets have an average lifespan of 7 to 10 days before being cleared by the reticuloendothelial system in the liver or spleen [64]. Besides their established role in hemostasis and thrombosis, platelets are key players in several processes including inflammation, atherogenesis, antimicrobial host defense, and tumor growth and metastasis [67]. These functions are mediated through activation of surface receptors and adhesion molecules through various signaling pathways and release of granule contents.

The surface of platelets is home to various receptors and glycoproteins (GPs) used to detect and respond to an array of stimuli. The most abundant of which are integrin αIIbβ3 (GP IIb/IIIa), GPIb-V-IX complex, GPVI, and GPIa/IIa, which are all primarily involved in the hemostatic function of platelets such as platelet activation, adhesion, and clot retraction [68]. The platelet surface is also studded with openings of a complex network of surface-connected membrane channels which extend inwards referred to as the open canalicular system (OCS) [69]. The major functions of the OCS are to mediate transportation of substances into platelets by endoctytosis for packaging into granules, as well as to mediate transport of substances (primarily granule contents) out of the platelets upon activation [69]. A further function of the OCS is to provide membrane necessary for platelet spreading upon activation [70, 71].

As platelets are anucleate, they have limited capacity to synthesize proteins and derive their granule contents from packaging via megakaryocytes during platelet formation, and by

direct uptake of plasma proteins by mature circulating platelets through the OCS [69, 72]. α-granules are the most numerous organelles in platelets and contain both membrane-associated and soluble proteins [67]. Some of the components of α-granules relating to hemostasis and thrombosis include GPVI, integrin αIIbβ3, vWF, fibrinogen, thrombospondin, FV, prothrombin, FXI, TFPI, protein S, and plasmin(ogen) [72, 73]. The second most abundant secretory vesicles are dense granules, which are less numerous and contain small molecules such as ADP, ATP, GDP, serotonin, histamine, pyrophosphate, polyphosphate, magnesium, potassium, and calcium [67, 72, 74, 75]. The regulation and release of these components executes the multiples roles of these dynamic and critical blood cells.

1.3.2.1 Platelets mediate hemostasis

The main function of platelets is to mediate hemostasis following vascular injury [68]. Normally platelets circulate in an inactive state, not interacting with the endothelium. However, upon vascular injury the subendothelial extracellular matrix (ECM) becomes exposed to blood, which allows platelets to bind molecules such as collagen, vWF, laminin, fibronectin, vitronectin, and thrombospondin via different surface receptors [76]. The binding of platelets to the subendothelium follows a coordinated process of tethering, rolling, activation, and firm adhesion. At high shear rates (>1000 s^{-1}), platelets bind vWF multimers bound to collagen via GPIb, and at low shear rates (<1000 s^{-1}) platelets primarily bind directly to exposed collagen through GPVI and GPIa/IIa [34, 35]. Also at low shear, platelets can directly bind ECM proteins fibronectin via integrin α5β1 and laminin via α6β1 [77, 78].

Platelet adhesion through GPIb, GPVI, and/or GPIa/IIa receptors promotes outside-in-signaling which leads to platelet activation [79-82]. Binding of ligands leads to signal transduction which activates cytosolic phospholipase Cγ2 (PLCγ2) [83, 84]. PLCγ2 then goes on

to hydrolyze phosphatidylinositol 4,5 bisphosphate to liberate 1,4,5 triphosphate (IP3) and membrane bound 1,2 diacylglycerol (DAG) [85]. IP3 serves as a second messenger which leads to the release of intracellular calcium stores from the dense tubular system [85]. The sharp increase in cytosolic DAG and calcium concentrations results in a cascade of activation events which include granule secretion via the OCS, exposure of phosphatidylserine, platelet shape change, and aggregation [68]. The release of ADP, TxA_2, and serotonin from granules recruit additional platelets and enhance activation [67]. Specifically, binding of ADP to purogenic receptors $P2Y_1$, and $P2Y_{12}$, and TxA_2 to thromboxane receptor TP work in an autocrine and paracrine fashion to amplify platelet activation, while binding of serotonin to 5-hydroxytryptamin 2A receptor (5HT2A) works to facilitate the activation signal transduction pathway [86-90]. This positive feedback loop and signal amplification further facilitates release of cytosolic DAG and calcium which causes integrin αIIbβ3 to activate and undergo a conformational change which allows it to bind fibrinogen and induces the ultimate step in platelet activation, platelet aggregation [91-93].

The concomitant generation of thrombin from the coagulation cascade is the most potent activator of platelets. Thrombin activates platelets through cleavage of PAR1 and PAR4, inducing activation events described above which further amplifies aggregation, exposure of phosphatidylserine, granule release and microparticle release [50, 68]. Platelets also assist in the further generation of thrombin and hemostasis through release of calcium, polyphosphate, FV, FXI, FXIII, prothrombin, and by providing a negatively charged surface [94, 95]. The prothrombinase complex, consisting of FXa and FVa, assembles on the platelets' negatively-charged phospholipid surface (termed procoagulant surface) in a calcium-dependent manner to further amplify the coagulation cascade [96, 97]. Released platelet microparticles also presenting

a procoagulant surface and bound TF further facilitate coagulation [100, 101]. Activation of platelets also induces major cytoskeletal rearrangements which trigger the initial discoid shape of platelets to extend lamellipodia and filipodia, leading to platelet spreading [102]. Cytoskeletal rearrangements also mediate clot retraction, whereby the actin cytoskeleton and αIIbβ3 mediate contractile forces whereby the platelet-rich thrombus physically retracts to increase the internal density of the clot thus improving thrombus stability [102, 103].

Platelets mediate several critical functions in hemostasis and are also a major constituent of the resulting thrombus. A stable thrombus has a complex architecture, with a dense core of highly activated and degranulated platelets intercalated with a cross-linked fibrin network, and an outer layer of loosely adhered and less activated platelets. The initial interaction of platelets with exposed ECM components leads to adhesion, activation, granule release, αIIbβ3 externalization and activation, shape change, phosphatidylserine exposure, and finally microparticle formation and release. These activation events (among others outlined above) work together in a step-wise fashion to facilitate the role of platelets in hemostasis. And, although platelets are the first responders to vascular injury, and mediate various aspects throughout hemostasis, they also mediate functions such as inflammation and wound healing after a stable thrombus has formed.

1.3.2.2 Platelet roles and functions outside of hemostasis

Beyond their critical ability to mediate several aspects of hemostasis and thrombosis, platelets also play important roles in several processes including inflammation, host defense, wound healing, tumor metastasis, and other pathophysiological processes [104]. Upon activation, contents of α-granules mediate inflammatory responses by externalization of immune-specific adhesion receptors and secretion of chemokines [72]. P-selectin translocated to the cell surface of

platelets from α-granules facilitates recruitment and activation of monocytes, neutrophils and lymphocyte by binding to P-selectin glycoprotein ligand-1 [105, 106]. Platelets also release several chemokines and cytokines to modulate the immune response, such as CXCL4 (PF4), CXCL7 and CCL5 (RANTES) which also help recruit and activate immune cells [107-109]. PF4 (platelet factor 4) in particular is one of the most abundant α-granule proteins and can induce monocyte recruitment, activation and differentiation, and neutrophil adhesion to the site of injury [107, 110, 111]. In addition, serotonin released from dense granules activates the endothelium and facilitates the recruitment of neutrophils to the site of vascular damage [112]. Platelets can also module the adaptive immune response through release of soluble CD40L, which facilitates immunoglobulin secretion from B-cells, T-cell activation and dendritic cell maturation and secretions [113-115].

Platelets also play a direct role in host defense. Upon activation, platelets secrete antimicrobial peptides such as α-defensins and β-defensins [116, 117]. Platelets can also promote clearance of pathogens by direct internalization and generation of reactive oxygen species [118]. Platelets can also detect pathogen-associated molecular patterns (PAMPS) via Toll-like rectors (TLRs) which allows them to directly sense and communicate processes in host defense [118]. For example, the activation of TLR4 on platelets through interaction with bacteria-bound lipopolysaccharide (LPS) induces platelet-neutrophil interactions which induces release of neutrophil extracellular traps (NETs) [119]. NETs are negatively charged DNA-protein complexes which can ensnare microorganisms and localize components of host defense to their site [120]. In a similar fashion, platelets can also detect pathogens entangled within the fibrin mesh of a thrombus and induce immune cell recruitment and NET formation [121].

Platelets also release a plethora of growth factors, angiogenic regulators and apoptotic regulators which mediate various aspects of wound healing [72]. These factors facilitate proliferation and migration of smooth muscle cells (SMCs), fibroblasts, and endothelial cells to restore the integrity of the vascular wall [122]. The release of platelet derived growth factor (PDGF) is critical for regulating SMC proliferation and migration [123]. Release of stromal cell-derived factor-1 alpha (SDF-1α) by platelets mediates migration and differentiation of endothelial cells progenitor cells, as well as, acts as a potent pro-angiogenic factor to facilitate sprouting and tube formation [124, 125]. Other released pro- and anti-angiogenic factors such as vascular endothelial growth factor (VEGF), platelet factor 4 (PF-4) and endostatin work together to regulate revascularization [122]. In addition, platelets can modulate wound healing by releasing apoptotic regulators such as tumor necrosis factor alpha (TNF-α), CD95, Apo2-L and Apo3-L [126].

Given the wide range of bioactive molecules released from platelets, they have also been implicated in many pathological processes such as chronic inflammatory conditions, sepsis, acute lung injury and cancer growth and metastasis [72]. Most notably, many platelet secretions necessary for wound healing and tissue repair can be utilized by cancer cells to promote survival and growth. VEGF, PDGF, epidermal growth factor (EGF), and transforming growth factor beta 1 (TGF-β1) have all been implicated in cancer stem cell survival, tumor initiation, extravasation and tumor growth [127-129]. While release of anti-angiogenic factors such as PF-4, TSP-1, and endostatin can inhibit cancer progression [130]. Pro-inflammatory mediators released by platelets have been implicated in transplanted graft rejection, acute lung injury, inflammatory bowel disease, asthma and many more pathological processes [131-134].

1.4 Literature Review

1.4.1 Polyphosphate in coagulation

Polyphosphate (polyP) is an inorganic anionic linear polymer of phosphates, ubiquitous in all living organisms and with a wide range of biological functions depending on the polymer length [135, 136]. In humans, polyP is present in platelets, mast cells, and tumor cells. In platelets, short-chain polyP (60-100 phosphate units long) is abundant in dense granules and secreted upon activation [137]. Platelet-derived polyP can enhance hemostasis and thrombosis through various mechanisms. Platelet-derived (short-chain) polyP accelerates FV and FXI activation, inhibits TFPI, and inhibits fibrinolysis [138-140]. These functions of short-chain polyP act to accelerate and enhance clotting reactions. In contrast to short-chain polyP, long-chain polyP (hundreds to thousands of phosphates long) which are abundant in microbes, is a potent activator of the contact pathway and can directly trigger clotting in a FXII-dependent manner [141, 142]. Interestingly, recent findings demonstrate a second pool of polyP in platelets that is retained on the platelet surface in the form of nanoparticles upon activation [143]. The polymer length of membrane-bound polyP nanoparticles greatly exceeds that of secreted short chain polyP, and can directly and potently activate FXII [143].

Due to the intricate involvement of polyP with hemostasis and thrombosis, polyP is seen as an attractive therapeutic target and agent to modulate clotting. Polycationic agents have been developed as polyP inhibitors by preventing the interaction of polyP and clotting enzymes [144]. These polyP inhibitors were shown to be thromboprotective in mouse models, with reduced bleeding side effects compared to heparin [145]. In addition to anti-polyP based antithrombotic therapy, polyP is also being investigated as a novel hemostatic agent. Silica nanoparticles coated

with polyP have been shown to be a potent activator of clotting, and demonstrates proof-of-principle for utilizing polyP as a safe and stable hemostatic agent [146].

1.4.2 Factor XII

Factor XII (FXII, Hageman factor) is a serine protease secreted by hepatocytes as an 80-kDa (596 residues) single-chain zymogen [147]. FXII circulates at a concentration of 30-40 μg/mL, with a half-life of 50-70 hours [148]. Binding of FXII to a negatively charged surface such as DNA/RNA, NETs, polyP nanoparticles, collagen, heparin, amyloid beta (Aβ) aggregates, or artificial surfaces (glass, kaolin) leads to activation of FXII to FXIIa (αFXIIa) [142, 148-152]. This binding promotes conformation changes and autoactivation of a small amount FXII to FXIIa [153, 154]. The newly generated FXIIa cleaves PPK (plasma prekallikrein) to PK (kallikrein), and PK in turn activates additional FXII in a positive feedback loop [154]. Further cleavage of FXIIa by PK releases a 48-kDa fragment (containing the heavy-chain binding domains) to generate βFXIIa [155].

One major function of FXIIa is to activate the pro-inflammatory kallikrein-kinin system. Activation of PK by FXIIa leads to activation of high molecular weight kininogen (HK), and release of the pro-inflammatory mediator bradykinin (BK) [156]. In coagulation, the primary role of FXIIa is to activate the intrinsic coagulation pathway through activation of FXI [157]. *In vitro*, the activation of FXII through anionic activators leads to thrombin generation and subsequent clot formation [157]. However *in vivo*, FXII is disposable for hemostasis as individuals with FXII deficiency clot normally and exhibit no bleeding abnormalities [158]. Instead, *in vivo* FXIIa contributes to thrombus growth and stabilization [49]. Interestingly, depletion of FXII with inhibitors is thromboprotective with little to no associated bleeding risk [159, 160]. In contrast to FXIIa, βFXIIa which lacks the binding domain necessary for binding to anionic surfaces does

not activate the intrinsic coagulation pathway and is only limited to activation of PK [155, 161]. Other functions of FXII is the initiation of fibrinolysis through activation of PK-mediated uPA activation, and activation of the classical complement pathway [162].

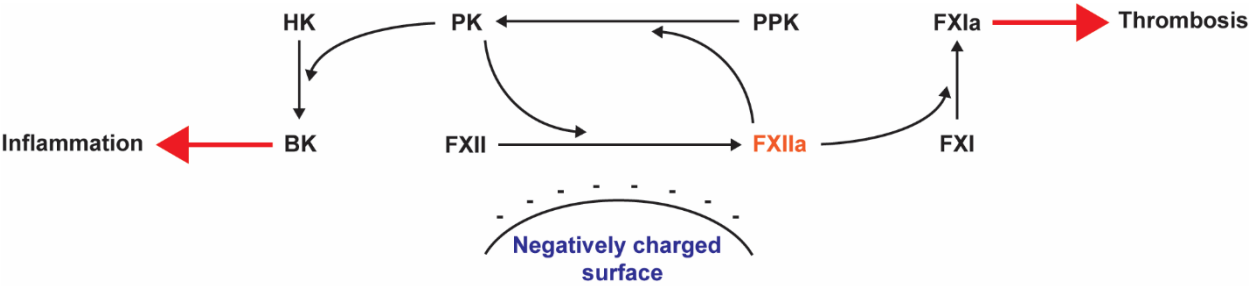

Figure 1.2 FXII activation pathways.

Due to its multifaceted roles, FXII mediates many pathological processes. Through activation of the intrinsic system, FXII contributes to pathological thrombotic conditions such as atherothrombosis, ischemic stroke, venous thromboembolism (VTE), pulmonary embolism (PE), and cancer-driven VTE [150, 159, 163-165]. Through activation of the kallikrein-kinin system, FXII contributes to pathological inflammatory conditions such as sepsis, rheumatoid arthritis, anaphylaxis, hereditary angioedema, and vascular dysfunction in Alzheimer's disease [152, 166-169].

1.4.3 Factor XIII

Coagulation factor XIII (FXIII) is a protransglutaminase and the final enzyme in the coagulation cascade with a primary role of cross-linking fibrin to stabilize blood clots. FXIII circulates as a 320 kDa hetrotetramer (FXIII-A_2B_2), consisting of two catalytic FXIII-A subunits and two regulatory FXIII-B subunits [170]. The protransglutaminase FXIII-A subunit (83 kDa) is primarily expressed by cells originating from the bone marrow and released into circulation, or expressed intracellularly as a dimer (FXIII-A_2) in platelets, megakaryocytes, monocytes, and

macrophages [171]. FXIII-B (80 kDa) is expressed by hepatocytes and strongly binds FXIII-A, serving as a regulatory and stabilizing protein for the catalytic subunit [172]. FXIII (FXIII-A_2B_2) circulates blood complexed with fibrinogen, through FXIII-B, which accelerates cross-linking activity by localizing the protransglutaminase at the site of active clotting [173, 174].

Activation of FXIII consists cleavage of the first 37 residues of the FXIII-A subunit N-terminus, which releases the activation peptide (AP) and exposes the active site, generating FXIII-A_2'B_2 [175]. FXIII-B_2 disassociates and FXIII-A_2', and in the presence of calcium, following a conformational change becomes an active transglutaminase, FXIIIa (FXIIIA_2*) [175]. Covalent cross-linking of molecules by FXIIIa, primarily of fibrin, consists of an acyl transfer reaction mediated by the catalytic triad (Cys314, His373, and Asp396) of the FXIII-A subunit [176]. The reaction proceeds by formation of a thioester bond between the catalytic cysteine and the glutamine of the substrate, resulting in the release of ammonia [176]. Then the acyl group is transferred from the enzyme to a primary acceptor amine, forming an isopeptide bond between the two substrates and releasing the enzyme [176].

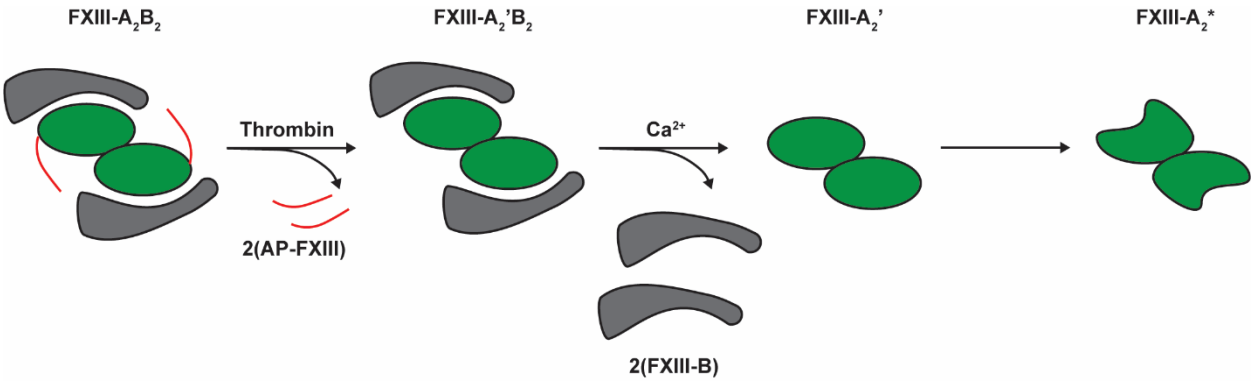

Figure 1.3 Activation of FXIII.

FXIIIa catalyzes the cross-linking of over 140 substrates, including fibrin, fibrinogen, fibronectin, vitronectin, and collagen [14]. Cross-linking of fibrin, the most prominent FXIIIa

substrate, increases clot stiffness and stabilizes the clot against premature fibrinolysis [177]. In addition, FXIIIa can cross-link the antifibrinolytic α_2-antiplasmin to the fibrin clot to provide further stabilization [178]. Other substrates of interest include complement proteins (C3, C4b, C5a), plasminogen, PAI-2, and TAFI, but their roles and significance remain to be investigated [14].

FXIII is also present in high concentrations in the cytoplasm of platelets as a homodimer (FXIII-A_2) [179]. Upon platelet activation, platelet FXIII is translocated to the platelet surface by an unknown mechanism, and can participate in cross-linking reactions [180]. Platelet FXIII can stabilize clots by cross-linking fibrin directly, as well as antifibrinolytics into the clot [181, 182]. Intracellularly, platelet FXIII can cross-link cytoskeletal components and modulate morphological changes of platelets following activation [183]. Platelet FXIII has been implicated in the process of clot retraction, but due to conflicting reports the specific role of platelet FXIII in clot retraction remains to be determined [184]. Platelet FXIII also facilitates the formation of procoagulant coated platelets by cross-linking α-granule proteins to serotonin [186, 187].

FXIII has many roles in physiological processes outside of coagulation. FXIII plays an important role in wound healing by enhancing adhesion of inflammatory cells by cross-linking vitronectin and fibronectin to the wound [171]. FXIII can also promote angiogenesis by cross-linking signaling molecules on the endothelial cell surface [188]. FXIII facilitates bone remodeling and deposition by regulating bone ECM secretions [189]. FXIII also plays a critical role in pregnancy by stabilizing the interaction between the placenta and uterus mediated by cross-linking between fibrin and fibronectin [190, 191].

FXIII deficiency (FXIIID) is a rare hemorrhagic disorder, with an occurrence rate of one per two million people [192]. Diagnosis of FXIIID is difficult as routine coagulation tests such as

bleeding time (BT), activated partial thromboplastin time (APTT), prothrombin time (PT), thrombin time (TT), and platelet count are normal [193]. Manifestations of FXIIID include soft tissue hematomas, recurrent miscarriages, umbilical cord bleeding, delayed wound healing, and intracranial hemorrhage (ICH) which can be life-threatening [193]. Due to these complications, replacement therapy using FXIII concentrates or rFXIII is necessary [194].

1.4.4 Fibrinogen

Fibrinogen is a 340 kDa glycoprotein consisting of two Aα, two Bβ, and two γ chains. Fibrinogen is synthesized by hepatocytes and released into circulation as a homodimer at a concentration of 2-5 mg/mL, and can exceed 7 mg/mL during acute inflammation [195]. Fibrinogen is assembled with each single chain forming a coiled-coil half molecule (Aα/Bβ/γ), before forming a hexameric complex joined together at the N-terminus, referred to as the E domain [196]. Extending outward from the E domain, are the two globular ends of the fibrinogen molecule, referred to as the D domains [196].

Fibrinogen circulates blood in a soluble form until it reaches a site of active coagulation and is converted into insoluble fibrin by thrombin. Thrombin proteolytically cleaves N-terminal regions of the two Aα and Bβ chains, referred to as fibrinopeptide A and B respectively [197]. Cleavage and release of these fibrinopeptides exposes α- and β- "knobs" (on the E domain) that interact with binding pockets on the D domain of the γ and β chains respectively, of another fibrin molecule [197]. This binding conformation results in half-staggered association of fibrin monomers into protofibrils. Further aggregation of protofibrils and self-assembly of fibrin monomers results in branched fibers and a fibrin meshwork that is deposited at the site of clotting [198].

Both fibrinogen and fibrin, fibrin(ogen), have many functions inside and outside of hemostasis. The primary role of fibrin is to deposit in and around a growing thrombus to assist in clotting [47]. Fibrin fibers increase the mechanical strength of the clot and increase resistance to fibrinolysis [47]. The fibrin mesh also traps RBCs into the clot, which contributes to preventing blood loss [51]. Fibrinogen is carrier molecule for plasma FXIII, and aids in localizing FXIII to sites of active coagulation [199]. Fibrin(ogen) mediates platelet aggregation through platelet cross-linking by binding GPIIb/IIIa, and through this interaction also plays a central role in clot retraction [200, 201]. Thrombin can also directly bind to fibrin, in a process termed antithrombin-1 (AT-I), which acts to sequester thrombin and suppresses further thrombin generation [202]. Fibrin(ogen) also plays a significant role in mediating inflammation. Fibrinopeptides A and B act as chemoattractants for monocytes, neutrophils and macrophages [203-205]. Fibrin(ogen) mediates migration of leukocytes through various surface receptors and can directly induce an inflammatory cellular response through binding and activation of leukocytes integrin Mac-1 [206]. As such, fibrinogen has been implicated in chronic inflammatory conditions such as arthritis and multiple sclerosis [207, 208].

The stability of the fibrin meshwork and thus the clot is regulated by various mechanisms. Covalent cross-linking of fibrin chains by FXIIIa is a major contributor to fibrin stability [47]. FXIIIa can rapidly cross-link adjacent γ chains, forming γ-γ dimers [209]. Cross-linking also occurs between adjacent α chains (α-polymers) and between α and γ chains (αγ-hybrids), but at a slower rate [210, 211]. Cross-linking of fibrin chains by FXIIIa induces branching of fibrin fibers and stabilizes the meshwork by increasing stiffness and elasticity [212]. The outcome of these changes results in stable clots resistant to physical detachment and increased resistance to fibrinolysis. FXIIIa can also cross-link antifibrinolytics such as α_2-

antiplasmin directly to the fibrin meshwork to increase clot stability [213]. Thrombin concentration during fibrin formation also contributes to fibrin stability. A high thrombin concentration results in the formation of a highly branched and dense fibrin meshwork, which confers high stability and resistance to fibrinolysis [214]. In contrast, a low thrombin concentration results in less dense and unbranched fibrin fibers, which are more susceptible to fibrinolysis [214]. Clots with abnormally dense fibrin structures have been implicated with increased cardiovascular disease risk [215-217].

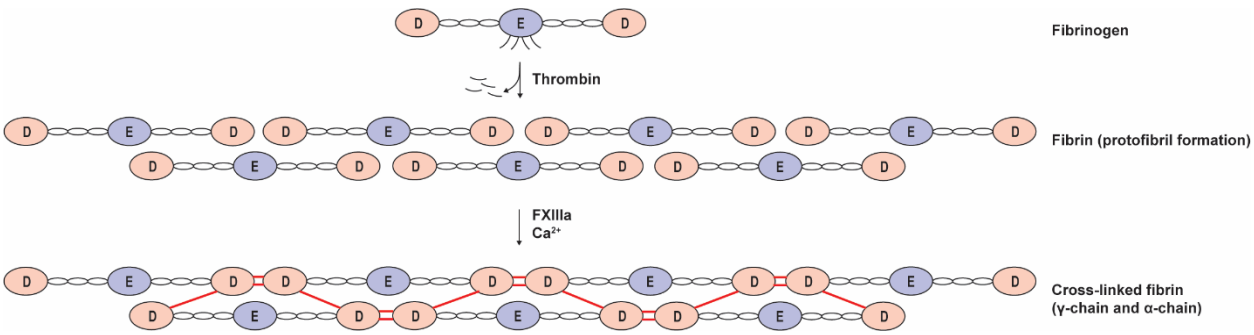

Figure 1.4 Fibrinogen activation and cross-linking.

Due to the abundance and multifaceted roles of fibrinogen, fibrinogen deficiency is associated with several prominent manifestations. Most notably, fibrinogen deficiency is associated with mild-to-severe bleeding [218]. Intracerebral hemorrhages and gastrointestinal bleeding are the most severe and often fatal bleeding manifestations in patients with fibrinogen deficiency [218]. Other symptoms include impaired wound healing, spontaneous splenic rupture, bone cysts, menometrorrhagia, miscarriage and postpartum hemorrhage [219-222].

1.4.5 Plasminogen

Plasminogen is the precursor of the major fibrinolytic enzyme plasmin. Plasminogen is primarily synthesized in the liver and released into circulation as a mature 791-amino acid

protein at a concentration of 200 µg/mL [223, 224]. The modular structure of full-length plasminogen, termed Glu-plasminogen, includes a pre-activation peptide, 5 kringle domains, and a serine protease domain [225]. Plasminogen can adopt two distinct conformations which can or cannot be readily activated, termed open and closed respectively. Glu-plasminogen circulates in a closed conformation and cannot be activated by tPA or uPA [226]. Upon binding of Glu-plasminogen to lysine-like ligands on fibrin or cell surface receptors (mediated through the kringle domains), Glu-plasminogen adopts an open conformation [226]. Alternatively, the active protease plasmin can remove the pre-activation peptide on Glu-plasminogen, generating Lys-plasminogen, which also adopts an open conformation [227]. Both Glu- and Lys-plasminogen in the open conformation can be cleaved and activated by tPA or uPA to generate the active fibrinolytic enzyme plasmin [225].

Plasmin is a serine protease with the primary function of degrading blood clots. Although plasmin has broad substrate specificity, the primary substrate of plasmin is fibrin [228]. Degradation of fibrin-containing clots by plasmin releases previously cross-linked D-dimers into circulation, which is a relevant biomarker for thrombosis/fibrinolysis [56]. Other substrates of plasmin include fibrinogen, complement component 3, complement component 5, vitronectin, factors V, VIII, and X, and aggregated proteins [225]. Plasmin can also cleave and activate plasminogen activators tPA and uPA, which generates a positive feedback loop for further plasmin generation [225].

Plasmin has high enzyme efficiency and a wide substrate specificity which can lead to systemic exhaustion of various coagulation factors if it is released into circulation and left unchecked [229]. Plasmin released from target surfaces is primarily inhibited by the serpin α_2-antiplasmin in a rapid and irreversible reaction [230]. Plasmin can also be inhibited to a lesser

extent by the non-specific serpin, α_2-macroglobulin [231]. Plasmin activity can be indirectly inhibited by TAFI, which removes lysine binding sites from fibrin and other surfaces, and reduces the rate of further plasmin activation [232]. Small molecule lysine-analogs such as tranexamic acid (TXA) and ε-aminoprocaic acid (EACA) inhibit plasmin activation through a similar mechanism by binding the kringle domains and preventing localization of plasmin to the clot surface [233].

Plasmin plays many other important physiological functions outside of hemostasis, such as in wound healing, inflammation, tumor development, and various neurological-related processes [53]. As such, deficiency of plasmin(ogen) often manifests in the inability to remove fibrin deposits and mediate tissue remodeling throughout various physiological processes. Commonly, such patients develop ligneous conjunctivitis, pseudomembranous disease and potentially occlusive hydrocephalus [234, 235]. Other manifestations of plasminogen deficiency include pulmonary fibrosis, and exacerbation of rheumatoid arthritis [224]. Interestingly, although fibrinolytic defects are notable in plasminogen deficient patients, there is no increase in risk of thrombotic disorders [236].

1.4.6 Tissue plasminogen activator

The primary role of tPA is to activate plasminogen to the active protease plasmin and facilitate dissolution of blood clots [237]. Outside thrombolysis, tPA is involved in important physiological functions such as in cell migration, tissue remodeling, and various aspects of central nervous system (CNS) physiology and pathophysiology [237]. tPA is constitutively released into circulation by endothelial cells as a single-chain 70 kDa (527 amino acids) mature protein [53]. The circulating concentration of tPA is approximately 70 pM, but local secretion levels can be acutely increased in response to various stimuli [238]. tPA can activate

plasminogen by cleavage of a single polypeptide chain, in a reaction that occurs 1000-fold more efficiently in the presence of fibrin [239]. Fibrin acts as a cofactor for plasminogen activation by providing bindings sites for both plasminogen and tPA via their kringle domains [239]. Plasmin can in turn cleave single-chain tPA to generate two-chain tPA, which both have similar activities in the presence of fibrin [240].

As with plasmin, the activity of tPA is regulated through various mechanisms to prevent premature clot lysis. The three main inhibitors of tPA are PAI-1, PAI-2, and neuroserpin, a brain-specific serpin [53]. These inhibitors rapidly bind to form irreversible complexes with tPA to inhibit the enzyme and facilitate its clearance. These inhibitory mechanisms result in a circulating half-life of free tPA of only 4 minutes, and 2 minutes for tPA complexed with a serpin [241, 242]. Deficiency of tPA, unlike plasminogen, leads to increased risk of thrombosis, particularly in the cerebrovasculature [243]. In contrast, tPA can be administered locally as a thrombolytic therapy to recanalize a blood vessel following an obstructive thrombotic event [244].

tPA also has many functions in CNS physiology and pathophysiology that are independent of fibrin. tPA is highly expressed in the CNS and involved in mediating synaptic plasticity and long-term potentiation, which are important for memory and learning [245-247]. In addition, tPA can facilitate the clearance of misfolded protein aggregates through binding of the cross-β structure common to aggregated proteins [248]. One such protein aggregate common to the CNS and Alzheimer's disease (AD) is Aβ, and tPA has been shown to modulate deposition of Aβ, likely though activation of plasmin, which can degrade Aβ aggregates *in vitro* [249-251]. In line with these findings, knockdown of PAI-1 reduces Aβ burden in AD mice [252]. However,

there are conflicting reports that demonstrate plasmin deficiency does not alter endogenous Aβ levels in a murine model of AD [253].

1.4.7 Alzheimer's disease and cerebral amyloid angiopathy

Alzheimer's disease (AD) is a progressive neurodegenerative disease and the most common form of dementia worldwide. Patients with AD suffer from impaired cognitive function and memory formation, the severity and scope of which increases as the disease progresses [254]. The vast majority (95-98%) of the incidence of AD are described as sporadic, while the remaining are termed familial AD (FAD), with known etiology [254]. The neuropathological hallmarks of AD are amyloid plaques, cerebral amyloid angiopathy (CAA), and neurofibrillary tangles (NFTs) [254]. Amyloid plaques are extracellular aggregates of Aβ with primarily 40 or 42 amino acids (Aβ40 and Aβ42), which are generated from the metabolism of amyloid precursor protein (APP) [20]. CAA involves the deposition and accumulation of Aβ along the cerebrovasculature [254]. NFTs are intracellular aggregates of hyperphosphorylated tau [254]. These pathologies can coexist in different variations, but the consequences of these toxic processes leads to neuroinflammation, synaptic dysfunction and accompanying neuronal loss [255]. The molecular mechanisms that lead to these pathologies and eventually AD are not fully understood, but APP and particularly its metabolite, Aβ, have been determined to be critical in disease progression [254]. There are currently no effective treatments for AD.

APP is a type 1 transmembrane glycoprotein that is expressed highly in the brain, as well as various extraneuronal tissues including platelets [256]. The three major isoforms of APP in humans are APP695, APP751, and APP770 [20]. The former (APP695) is expressed in the CNS, while the latter two (APP751 and APP770) are expressed extraneuronally (particularly in platelets) [256]. APP can be proteolytically processed by two alternative pathways termed

amyloidogenic and non-amyloidogenic. In the amyloidogenic pathway, APP is cleaved by β-secretase and γ-secretase to release the ectodomain soluble APPβ (sAPPβ), Aβ (typically 40 or 42 residues in length), and an intracellular C-terminal fragment (AICD) [257]. The non-amyloidogenic involves concerted action of α-secretase and γ-secretase to release the ectodomain soluble APPα (sAPPα), peptide p3, and an identical AICD [257]. The precise physiological function of APP and its metabolites are not yet fully understood. However in the brain, APP appears to modulate cell growth, motility and neurite outgrowth, while Aβ regulates synaptic scaling and synaptic vesicle release [258-261].

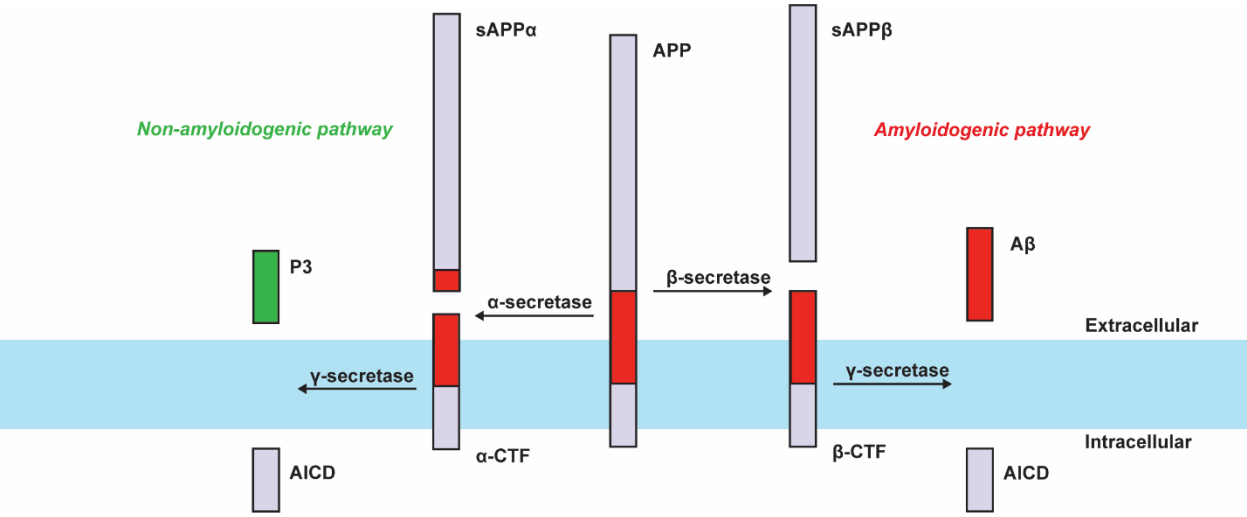

Figure 1.5 APP processing.

CAA is characterized as pathology of the cerebrovasculature and present in 98% of AD patients [262]. Deposition of Aβ (primarily Aβ40) in and along cerebral blood vessels induces degeneration of vessel wall components leading to smooth muscle cell loss which can trigger microaneurisms and intracranial hemorrhages [263]. These pathologies lead to vascular dysfunction and reduced cerebral blood flow which often exacerbate and aggravate other existing

pathological processes in the AD brain [262]. The exact mechanism of Aβ deposition along the cerebrovasculature is not fully understood, but components in the blood have been implicated [262]. Deposition of fibrin(ogen) has been observed along with Aβ in CAA positive blood vessels, which can encourage a prothromhotic environment and subsequent vascular dysfunction [264]. Platelet adhesion and activation along Aβ (and fibrinogen) deposited vasculature has been implicated in mediating the onset and progression of CAA by contributing more Aβ and a prothrombotic state, leading to a positive feedback loop and further thrombosis and vascular pathology [262, 265]. Furthermore, other blood components such as FXIII and thrombin have also been identified within CAA deposits, suggesting blood components play an important role in CAA pathology [266].

1.4.8 Amyloid precursor protein and amyloid beta in hemostasis

Beyond the functions of APP and Aβ in the brain, several interactions have been identified for APP and Aβ in hemostasis, generally mediated by platelets. Platelets contain over 90% of circulating APP, with a copy number of 9300 APP molecules/platelet [267, 268]. In contrast to brain-derived APP (APP695), platelet APP isoforms (APP751 and APP770) contain a Kunitz-type serine protease inhibitory (KPI) domain [269]. Platelets also express all the enzymes necessary to process APP (α, β, and γ-secretases) into its metabolites. About 10% of full-length APP is retained on the plasma membrane, while the majority of platelet APP is processed into metabolites (sAPPα, sAPPβ, and Aβ) and stored in α-granules, which can be released upon platelet activation [270]. Platelets are considered the major source of Aβ in plasma, and have been implicated in AD pathology [19]. The physiological function of platelet APP or Aβ is not yet fully understood.

Several functions of platelet APP in hemostasis have been identified, primarily through the interaction of the KPI domain and coagulation factors. Through *in vitro* studies, the KPI domain was shown to be an effective inhibitor of coagulation FXa, FIXa, FXIa, and FVIIa:TF complex [271-274]. Further *in vivo* studies demonstrated platelet APP to be a negative regulator of cerebral thrombosis in mice via the inhibitory effect of the KPI domain [275, 276]. More recently, in a mouse model of venous thromboembolism, APP KO mice developed larger thrombi through reduced negative regulation of FXIa [30]. In contrast to the demonstrated anticoagulant properties, platelet APP also acts as an adhesion molecule, capable of mediating platelet adhesion to deposited Aβ peptides and initiating thrombus formation [277].

Aβ peptides also interact with several coagulation factors and are capable of modulating hemostasis. Aβ peptides can support platelet adhesion and directly induce activation, which allows for more Aβ release through α-granules and promotion of a prothrombotic state [277, 278]. Aβ can trigger thrombin generation through activation of FXII and the intrinsic system [25]. Binding of Aβ to fibrin(ogen) induces structural changes which render the clot more resistant to fibrinolysis [28]. Stable complexes of Aβ and FXIII have been identified within CAA, but whether Aβ is a substrate for FXIII has not yet been established [266].

Despite the many interactions of APP and Aβ with components of the coagulation system, whether APP or Aβ contribute to hemostasis is not clear. The problem is compounded by the rapid processing of platelet APP, and the pro- and anticoagulant effects of APP and Aβ. APP KO mice have normal platelet aggregation, activation, and secretion [30]. However, APP KO platelets are 20% fewer in number and slightly larger [30]. Tail-bleeding times in APP KO mice appear to be longer compared to WT mice, but resulted in no significant increase in blood loss [30].

Chapter 2: Localization of short-chain polyphosphate enhances its ability to clot flowing blood plasma

2.1 Contribution

This research was a collaborative project published in *Scientific Reports*. N.M. and J.H.Y contributed equally to this work. N.M., J.H.Y., T.S.S., K.Y.T.C., J.R.B., S.A.S., A.J.D., and D.K., performed experiments and analyzed data; N.M., J.H.Y., T.S.S., C.J.K., J.H.M., Y.L., and G.D.S. conceptualized and planned experiments; N.M., J.H.Y., and C.J.K. wrote the manuscript; and all authors reviewed and edited the manuscript before submission. I performed experiments to collect data specifically for Figures 2.1A-B, 2.2, 2.4B, 2.5B-C 2.6A-D, 2.7, 2.8 and 2.9. I contributed to 40% of this paper.

2.2 Introduction

PolyP is an activator of blood coagulation through its ability to accelerate the activation of coagulation factors XII, XI, and V [142, 154], and by abrogating tissue factor pathway inhibitor (TFPI) function [11, 279]. Long-chain polyP (hundreds to thousands of residues long) appears to be a much more potent activator of clotting, via activation of factor XII and the contact pathway, than short-chain polyp [8-10]. Short-chain polyP (60-100 phosphate residues long) is found in dense granules of human platelets and mast cells granules (acidocalcisomes) and released upon their activation, while long-chain polyP occurs in microbes but also in some mammalian cells, such as in prostate cancer [10, 165, 280, 281]. A characteristic of long-chain polyP is its ability to aggregate into particles, and this spatial localization may possibly contribute to its propensity to accelerate clotting [282]. It is less clear if there is a pathophysiological role for polyP released from human cells in thrombosis [11]. Short-chain endogenous polyP facilitates activation of FXII *in vitro*, albeit at supraphysiological

concentrations [153]. It can also contribute to clotting *in vitro* under flow when tissue factor (TF) is present [283]. It is well-known that the local concentration of activators can profoundly influence their ability to initiate the clotting of blood [284]. Localization of polyP onto particles also accelerates coagulation under stagnant conditions [285]. Thus, we hypothesized that short-chain polyP may be a more effective activator when spatially localized onto surfaces, capable of accelerating clotting of flowing blood *in vitro* without participation of TF.

Initiation of blood coagulation is triggered when the local concentration of activators reaches a critical threshold, upon which the proteolytic cascade amplifies the local concentration of active enzymes to form a cross-linked fibrin mesh [286, 287]. The spatial localization of activators to surfaces effectively increases their local concentration, allowing coagulation to be triggered with less total amount of activator [288, 289]. Several activators have displayed this effect of spatial localization in microfluidic models of clotting, including TF, glass, and bacteria that activate prothrombin and factor X [290]. Flow influences coagulation in a variety of ways and enhances the effects of spatial localization [291]. Flow continuously strips clotting factors from catalytic surfaces, preventing activators from achieving a critical threshold and ultimately preventing clot initiation [292, 293]. To accelerate clotting of flowing blood, greater amounts of activator need to be localized in order to achieve a higher local concentration [294]. In this study, we used numerical simulations and a microfluidic model of thrombosis to investigate whether the ability of localization to enhance clotting extends to short-chain polyP *in vitro* under flow. The shear rates used in this study range from low to sub-physiological (i.e. pathological) shear. These low shear rates mimic those typical of where thrombosis occurs in large veins and valves, such as in deep vein thrombosis (DVT) or those associated with airplane economy class syndrome [295-300]. This microfluidic model of thrombosis enabled clotting of plasma, or lack

thereof, to be monitored over many hours in the absence of TF. In contrast to coagulation that occurs from acute injury to vessels, such as from puncture that exposes large amounts of TF, thrombosis may initiate over longer periods of time and can be potentiated by factor XII [154, 301-305]. Our experiments were designed to determine if localization of physiologically-relevant concentrations of platelet-length polyP could contribute to coagulation *in vitro* at low to sub-physiological shear, but do they do not validate whether or not localization of platelet-length polyP contributes to thrombosis *in vivo*.

2.3 Methods

2.3.1 Numerical Simulations

Thrombin generation was modeled with the *Transport of Diluted Species* module of Comsol Multiphysics 4.4 by adding diffusion and convection to a previously reported kinetic model [290]. Changes to the model included the addition of three rate equations to describe the activity of polyP: 1) the binding and inhibition of TFPI; TFPI + polyP ↔ TFPI-polyP; k_{on} = 4.0 x 10^5 $M^{-1}s^{-1}$, k_{off} = 1.0 x 10^{-2} s^{-1}, 2) the activation of factor V; V + Xa + polyP → Va + Xa + polyP; k = 8.0 x 10^{12} $M^{-2}s^{-1}$, 3) the activation of factor XI; XI + IIa + polyP → XIa + IIa + polyP; k = 8.8 x 10^9 $M^{-2}s^{-1}$ [8, 10, 142, 279, 290]. The diffusion coefficient for all soluble species was 5 x 10^{-11} m^2/s and the velocity profile varied with the shear rate, $v_z(r) = \frac{\gamma_w R}{2}\left(1 - \frac{r}{R}\right)^2$, where v_z is the velocity in the axial direction at each radial coordinate r, R is the cylinder radius, and γ_w is the shear rate at the cylinder wall. The chemical species were flowed into a cylindrical geometry of radius 2 mm and length 20 mm. For each shear rate, [thrombin] was sampled after the incoming flow had displaced the channel volume 12.5 times. Both the experiments and simulations were performed in the same mass-transfer regime ($Pe \gg 1$ and $Gz > 3000$).

2.3.2 Preparing soluble polyP (D-polyP), self-assembled polyP nanoparticles (NP-polyP), polyP-coated silica nanoparticles (SNP-polyP), and surface-immobilized polyP (SI-polyP)

To make D-polyP (dispersed polyp), polyP was solubilized and diluted first in water and then added to citrated plasma (frozen citrated normal control plasma, Affinity Biologicals Inc.) prior to entering the microfluidic device. NP-polyP was generated as described previously [282]. To generate polyP nanoparticles, powdered polyP was first solubilized in dH_2O to a final concentration of 1 M. The polyP stock solution was then diluted in a calcium solution (10 mM polyP, 5 mM $CaCl_2$, 8 mM Tris, pH 6.0) which was immediately followed by vortexing for 10 seconds, during which polyP self-assembled into nanoparticles tightly bound to Ca^{2+} cations [282]. The formation and size of the nanoparticles were verified after adding them to this calcium solution by observing the scattering intensity and hydrodynamic diameter, as measured by dynamic light scattering (Zetasizer Nano ZSP, Malvern Instruments). NP-polyP formulations were added and diluted in calcium-saline solution, rather than the citrated-plasma, prior to entering the microfluidic device. The NP-polyP were stable for over 6 hr in these solutions. SNP-$polyP_{70}$ were made by covalently attaching $polyP_{70}$ onto silica nanoparticles as previously described [146]. Synthetic PolyP was generated by solubilization from Maddrell salts and biotinylated as previously described [10, 306]. Synthetic polyP has been previously characterized, including its chain length, counterions and clotting activity [10, 282]. Long-chain NP-polyP contained a heterogeneous preparation of very long, non-biotinylated polyP polymers ranging from around 200mers to 1300mers, referred to here as NP-$PolyP_{>1000}$. Some experiments with SI-polyP employed heterogeneous long-chain biotinylated polyP consisting of chains 50 to 400 units in length, referred to here as biotin-$polyP_{400}$. Some experiments employed fractionated

material of narrower sizes ($polyP_{70}$ and $polyP_{160}$) [10]. All polyP concentrations are stated with respect to the concentration of phosphate monomer.

2.3.3 Preparing microfluidic devices with SI-polyP

Microfluidic devices were prepared from polydimethylsiloxane (PDMS) as previously described [307]. Channel dimensions are listed as follows (length x width, 125 µm height for all channels): 1.67 mm x 1000 µm (1 s^{-1}), 3.33 mm x 500 µm (3 s^{-1}), 5.83 mm x 286 µm (10 s^{-1}), 8.33 mm x 200 µm (22 s^{-1}), 12.50 mm x 133 µm (55 s^{-1}), 16.67 mm, 100 µm (110 s^{-1}). The devices were incubated in saline and kept under vacuum overnight to hydrate and remove air from the channels. Devices remained soaked in saline throughout the experiment to aid in coating the surfaces with lipids, and to reduce convective flow during experiments in the absence of flow. The devices were coated with phosphatidylcholine (PC) vesicles to prevent activation of clotting on the PDMS surface. In devices that were not coated with SI-polyP, vesicles were prepared with egg PC (Avanti Polar Lipids, Alabaster, USA) and fluorescent Texas Red 1,2-Dihexadecanoyl-*sn*-Glycero-3-Phosphoethanolamine (DHPE) (Invitrogen) in a 99.5:0.5 molar ratio. Lipids were extruded through a 100 nm membrane using a Lipex Thermobarrel Extruder (Northern Lipids, Burnaby, Canada). The vesicle solution (10 mg/mL in dH_2O) were flowed through microfluidic channels at a rate of 1 µl/min for 15 min and rinsed out with saline. The coating of PC on the channels was stable for at least 10 hours (Figure 2.1). For devices where polyP was surface-immobilized, the channel was first coated with biotinylated lipids (1 µl/min, 15 min) and rinsed out with saline. To prepare biotinylated vesicles, 1-oleoyl-2-[12[biotinyl(aminododecanoyl)]-sn-glycero-3-phosphocholine (biotinylated-PC, Avanti Polar Lipids) was mixed with Egg PC and Texas Red DHPE in a molar ratio of 5.0:94.5:0.5 and extruded. Next, streptavidin (100 µg/mL) conjugated to Alexa Fluor® 488 (Molecular Probes,

Inc.) was flowed through the device (1 µl/min, 40 min) and then rinsed with saline to wash away the unbound, excess streptavidin. Finally, a solution of biotin-polyP (50 µg/mL) and biotinylated-polyethylene glycol (biotin-PEG) (either 0 or 99 molar equivalents to biotin-polyP) was flowed through the device (1 µl/min, 40 min), binding to the patterned streptavidin followed by a saline rinse, which resulted in SI-polyP being selectively patterned on the walls of the microfluidic device shear chambers. Liposomes and saline were flowed into the device through a combination of inlet and outlet channels to achieve laminar flow patterning, such that the parallel streams of fluids were at low Reynolds number (<<1) and maintained sharp boundaries and excluded the possibility of turbulent flow [308, 309]. This patterning allowed specific channel walls of the device to be coated, either all channels in the device, the channels in the shear chambers, or one wall of the chambers. To measure the amount of polyP, it was stained by flowing DAPI (40 µg/mL in 15 mM Tris acetate, 300 mM NaCl, 30 mM EDTA, and 0.02% NaN_3) into the device. Thrombin generation during clotting was detected by adding 125 µg/mL of fluorescent peptide substrate for thrombin (Boc-Val-Pro-Arg-4-methylcoumaryl-7-amide, Peptide Institute Inc.) into normal plasma.

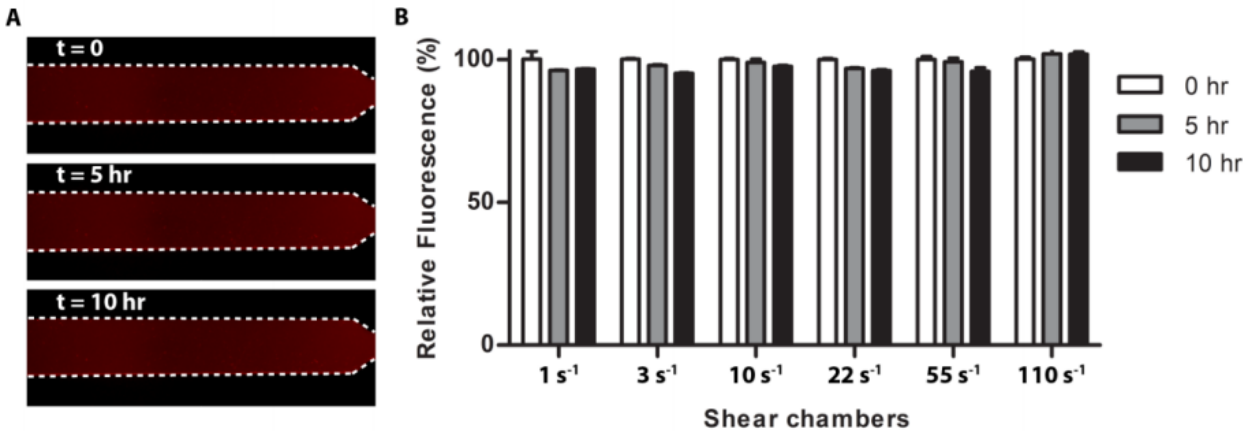

Figure 2.1. PC channel coverage and stability. (A) Representative time lapse images of a channel (white dashed lines) coated with PC/Texas Red DHPE (red) with citrated normal plasma

flowing through it. (B) Fluorescence intensities in different regions of each shear chamber. Data indicate mean ± SEM.

2.3.4 Flowing plasma and calcium into devices and measuring clotting

Flow rates were controlled using a syringe pump (Harvard Apparatus PHD 2000) by withdrawing solutions out of the outlets of the device at a rate of 1 µl/min. Shear rates in different channels were controlled by the width of each channel, while the residence time of plasma within the shear chambers were kept constant (~10 sec) by varying their respective lengths. Tubing connected to the outlets of the device were charged with 50 µl of Egg PC vesicles to prevent clotting from initiating in the tubing or syringes. A solution of sodium citrate (10 mM in dH_2O) was initially pulled into both inlet channels to wash out the device and further charge the outlet tubing. Normal citrated human plasma (7 mM citrate) and calcium-saline solution (40 mM $CaCl_2$ and 90 mM NaCl) were simultaneously pulled into the device and mixed at a ratio of 3:1 to recalcify the plasma, yielding a final free calcium concentration of 4-5 mM [310]. To measure clotting times, fluorescent beads (2.5 µg/mL, Fluoresbrite Plain YG 1.0 Micron Microsphere, Polysciences Inc.), and in some experiments 125 µg/mL fluorescent thrombin substrate, were mixed into the plasma and time-course imaging of each channel was performed using an epifluorescence microscope (Leica DMI6000B). The fluorescent beads did not influence clotting times (Figure 2.2). Clotting was determined by the immobilization of the fluorescent beads and in some experiments also by the generation of blue fluorescence upon cleavage of the thrombin substrate. In experiments where the effect of nanoparticle polyP (NP-polyP) on clotting was tested, the activators were mixed with the calcium solution prior to entering the device. For experiments with soluble polyP (D-polyP), polyP was added to the

plasma instead to prevent nanoparticle formation. For experiments at zero shear, normal or congenital FXII-deficient plasma (Geroge King Bio-Medical, Inc.) and calcium were mixed together immediately before flowing them into the device and blocking all outlets to create stagnant plasma.

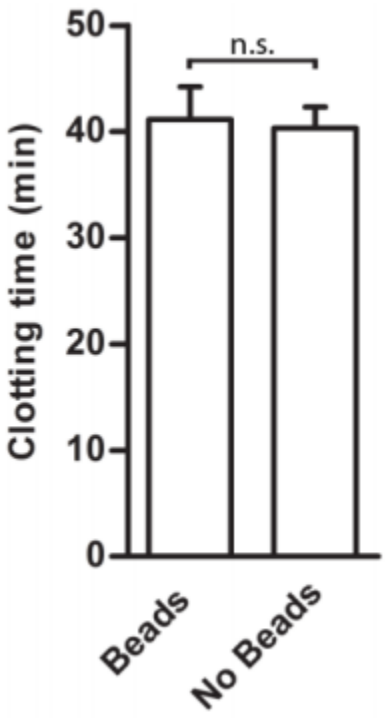

Figure 2.2. Fluorescent beads do not influence clotting. Normal recalcified plasma (with or without beads) was flowed into the device and clotting times at zero-shear were measured by bright-field microscopy. Data indicate mean ± SEM, n=3.

2.4 Results

2.4.1 Numerical simulations predict the localization of polyP will increase its coagulability at low shear rates

To initially examine how localizing polyP onto surfaces affects thrombin generation, we used a two-dimensional numerical simulation that considered diffusion, convection, and the rates

of 41 reactions of the coagulation cascade. An established kinetic model for the coagulation cascade was used with the addition of $polyP_{>1000}$ in three reactions that were previously characterized in kinetic assays [8, 10, 142, 279, 290]. PolyP was either spatially localized onto the surface of a cylindrical channel or dispersed throughout its volume. Shear rates were from 1 s^{-1} to 110 s^{-1}, a range that encompasses sub-physiological shear rates (< ~10 s^{-1}) and shear rates in the inferior vena cava, venous valves, and large veins [295-297, 311]. When polyP was localized onto the surface of the channel with a shear rate of 1 s^{-1}, the local thrombin burst was 782-fold higher than when an equal amount of polyP was dispersed throughout the volume (1.83 x 10^{-8} M versus 2.34 x 10^{-11} M) (Figure 2.3A). The amount of polyP in the simulations was 7.54 x 10^{-9} mol, which equates to 30 μM (with respect to phosphate monomer) when the total volume of the simulation was considered. The resulting thrombin burst was a consequence of the higher local concentration of polyP, which led to increased positive feedback from the coagulation cascade. Simulations showed that differences in thrombin generation persisted over various shear rates, up to 60 s^{-1} (Figure 2.3B). However, at a set distance, the difference decreased as shear rate increased, because thrombin was rapidly transported down-stream.

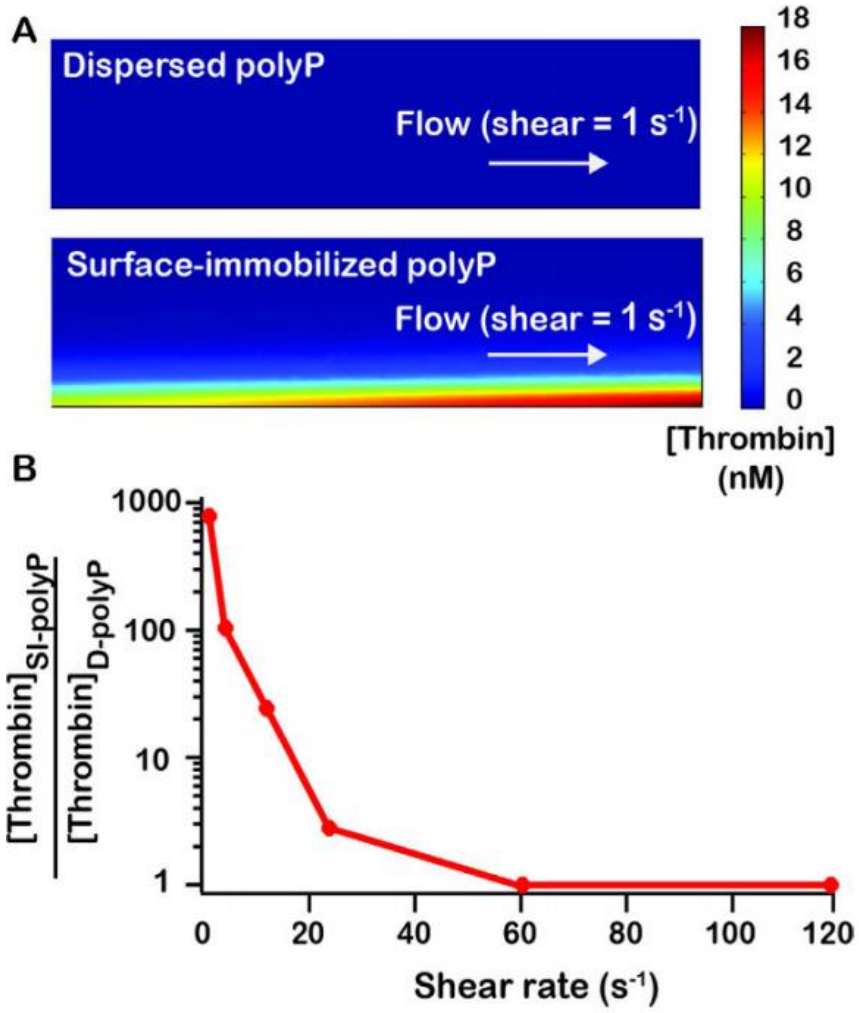

Figure 2.3. Numerical simulations predict localization of polyP accelerates thrombin production at low shear rates. Two-dimensional numerical simulations of the human blood coagulation cascade, comparing the generation of thrombin by polyP dispersed throughout a cylindrical channel versus polyP immobilized on the channel surface. The channel was 20 mm long with a radius of 2 mm. The overall number of polyP molecules was the same in all simulations (7.54×10^{-9} moles). (A) Plots show [thrombin], which is the sum of concentrations of thrombin and meizothrombin, for a two-dimensional longitudinal cut of the cylinder at 500 s into the simulation. (B) The fold difference in the maximum [thrombin] generated in the channel

when polyP was surface-immobilized (SI-polyP) versus dispersed (D-polyP) at varying shear rates.

2.4.2 Surface-immobilized polyP accelerates clotting of flowing blood plasma

To determine if SI-polyP was able to accelerate clotting of flowing blood plasma, synthetic $polyP_{400}$ was immobilized onto the walls of microfluidic channels (Figure 2.4A). Half of each chamber was patterned with biotinylated lipids followed by an excess of streptavidin (Figure 2.4B). Biotinylated-$polyP_{400}$ was then flowed through the channel, becoming immobilized onto streptavidin. The surface concentration of SI-$polyP_{400}$ was varied by diluting biotinylated-$polyP_{400}$ in a solution of biotin-PEG before coating the channel. The concentration of polyP was determined by DAPI staining. Fluorescence intensities from known concentrations of stained D-polyP, which was soluble and dispersed throughout the channel, were used to generate a standard curve and used to calculate the surface concentration of SI-polyP (Figure 2.4C). The surface concentration of SI-polyP was 300 nmol/m^2, and could be decreased to 60 nmol/m^2 by diluting with biotin-PEG. To test the ability of patterned polyP to induce clotting, platelet-poor human plasma was flowed through the chambers. Based on the simulation data, we tested the lowest shear (1 s^{-1}) as it was predicted to have the largest effect on thrombin generation and therefor clotting. A range of shear rates are explored in later experiments. The plasma clotted selectively on areas with immobilized $polyP_{400}$ (300 nmol/m^2) in 50-70 min at a shear rate of 1 s^{-1}. No clotting was observed over 5 hr in channels without $polyP_{400}$ (Figure 2.4C and 2.4D). All polyP concentrations are reported in terms of phosphate monomer.

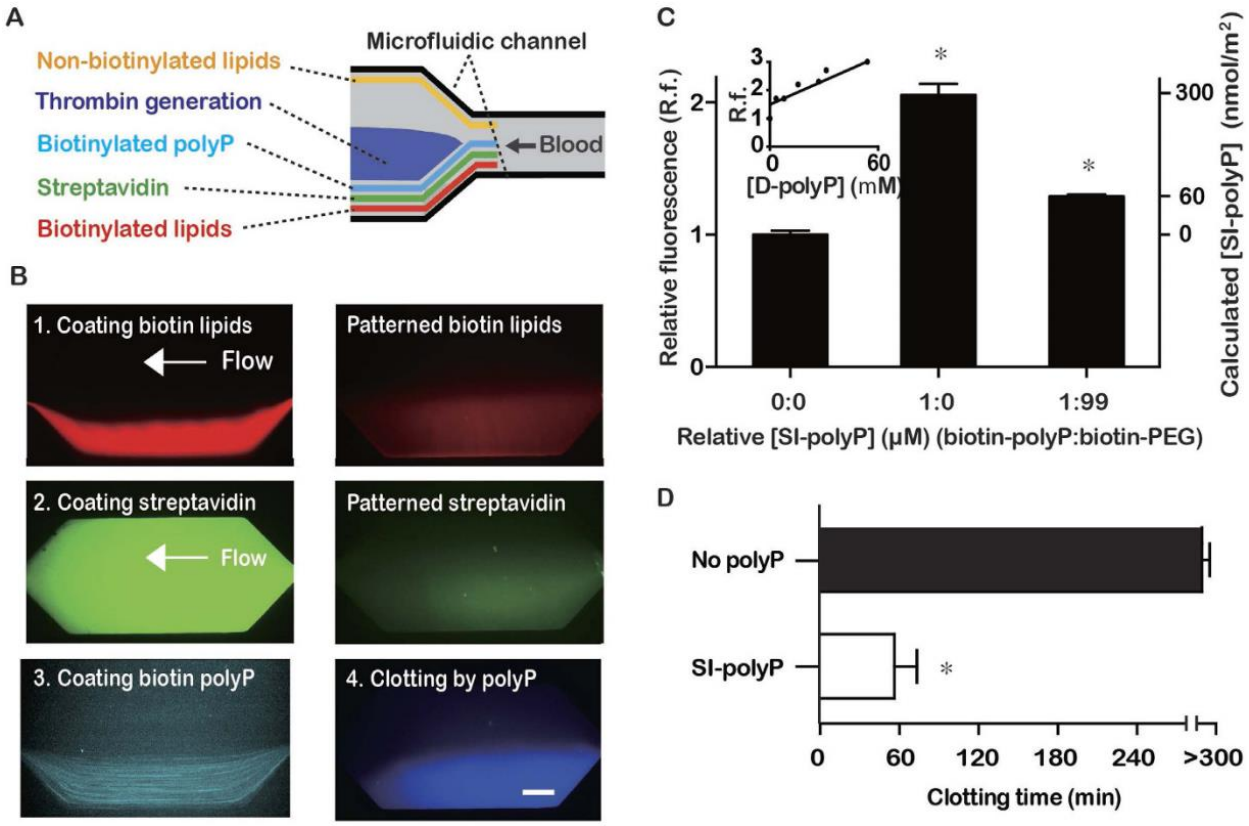

Figure 2.4. PolyP induces clotting of flowing blood plasma when localized on a surface at sub-physiological shear. (A) Schematic of biotinylated synthetic polyP (cyan) patterned onto the surface of half of a microfluidic channel, which induces production of thrombin and clotting (blue) of flowing blood plasma (grey). (B) Images of fluorescent-labeled agents flowing and patterned along one side of a microfluidic channel. Biotinylated lipids (tagged red) self-assembled on the channel wall. Non-biotinylated lipids (not tagged in these images) were simultaneously flowed and patterned on the other side of the chamber using laminar flow patterning. Then, streptavidin (tagged green) was flowed through and bound to the biotinylated lipids, followed by flowing biotinylated polyP labeled with DAPI (cyan), which bound streptavidin. A substrate (blue) for thrombin was activated, indicating initiation of clotting, selectively on patterned $polyP_{400}$ (300 nmol/m^2). Scale bar is 250 μm. (C) Quantifying of the amount of SI-polyP by measuring the fluorescence of DAPI bound to it. Channels with SI-polyP

were compared to channels without polyP and to channels treated with polyP diluted with biotinylated PEG. Inset is a standard curve of known concentrations of solubilized D-polyP, which was used to calculate the surface concentration of SI-polyP in coated channels. (D) The clotting times of normal human plasma flowing through channels coated with $polyP_{400}$ at a shear rate of 1 s^{-1}. *p = < 0.01 compared to controls without polyP. Data indicate mean ± SEM, n = 3.

2.4.3 Measuring clot times simultaneously at various shear rates

A microfluidic system containing six regions with varying shear rates was used to measure clot times of flowing blood plasma (Figure 2.5A). The range of shear rates was 1-110 s^{-1}, which encompasses physiological shear rates which occur in the inferior vena cava, venous valves, and large veins; as well as, sub-physiological shear rates (< ~10 s^{-1}) that occur in pathological contexts [295-298, 311]. These calculated shear rates were within 3-8% of the values obtained by measuring the flow velocity of micro particles by florescence microscopy. Clotting was monitored by visualizing the movement of fluorescent tracer beads specifically in the shear chambers, which became immobilized in clotted regions, and by a fluorogenic peptide substrate, which fluoresced when cleaved by thrombin during clotting (Figure 2.5B). To characterize and determine the range of clot times of flowing blood plasma in the microfluidic system, coagulation factor VIIa (FVIIa) was used, and added to plasma at a range of concentrations (Figure 2.5C). FVIIa does not circulate in plasma in appreciable amounts physiologically (~1% of total FVII circulates as FVIIa) [312], but is administered during severe hemorrhage in some cases to aid in hemostasis at doses of 90 to 270 μg/kg, which roughly corresponds to 1 to 4 μg/mL in plasma [313, 314]. In the device, plasma containing 16 μg/mL of FVIIa clotted in approximately 20-40 min, plasma containing 4 μg/mL of FVIIa clotted in

approximately 60 min, and plasma containing 4 ng/mL did not clot within 6 hr. Intermediate clotting times occurred with concentrations of 400 ng/mL and 40 ng/mL and were dependent on shear rate. Clot formation always occurred from the channel wall, crudely mimicking how physiological thrombus formation occurs from the walls of blood vessels and is shear-dependent [315].

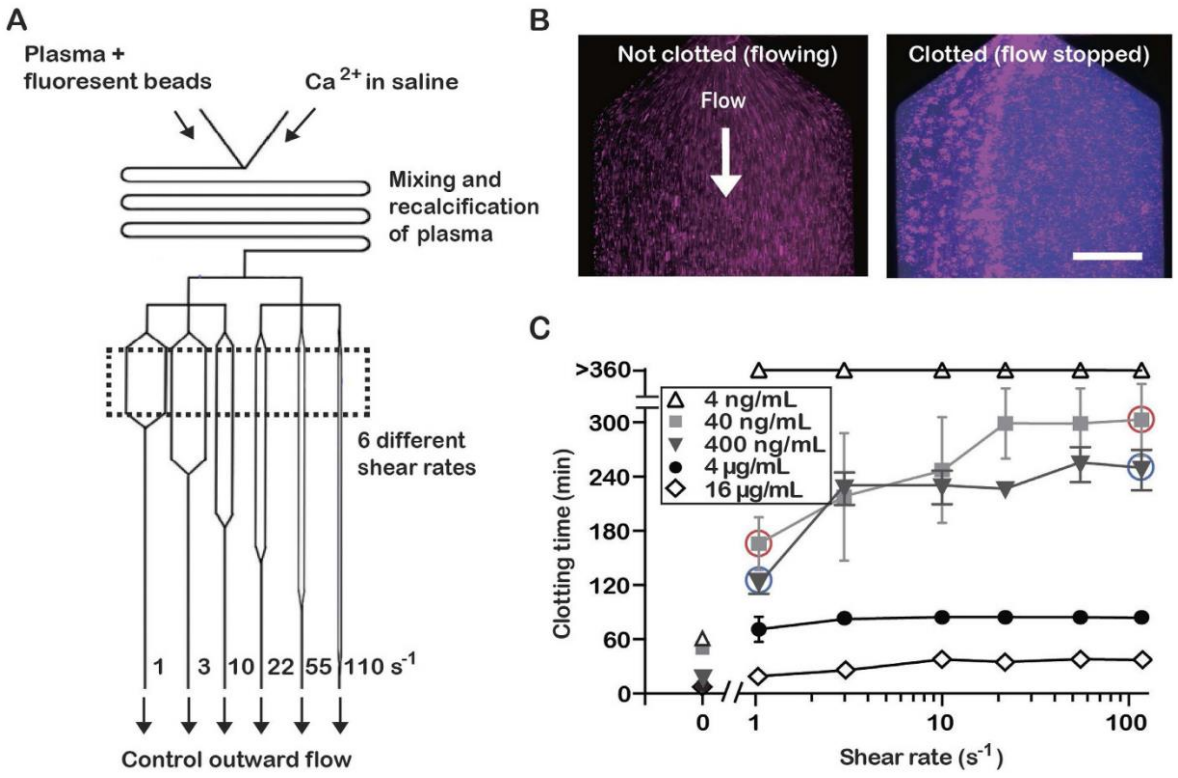

Figure 2.5. The microfluidic system used to measure clotting over a range of shear rates. (A) Schematic of the microfluidic system. Box (dashed lines) indicates the region where shear rates were varied and clot times were measured. (B) Fluorescence images showing that clotting was detected by the cessation of flow of tracer beads (pink) and by the cleavage of a substrate for thrombin (blue). Scale bar is 250 µm. (C) Assessing the range of clotting times in this flow system by adding various concentrations of FVIIa to the plasma. Data points indicate mean ±

SEM, n = 3-4. Red circles indicate p = < 0.05 between the data points, and blue circles indicate p = < 0.01 between the data points.

2.4.4 Short-chain polyP accelerates clot formation faster when surface-localized than when dispersed in nanoparticles or in solution

PolyP$_{160}$ was previously demonstrated to be a weak initiator of the contact pathway, but we examined the hypothesis that spatially localizing polyP$_{160}$ onto a surface (SI-polyP$_{160}$) would enhance its ability to contribute to clot formation compared to polyP$_{160}$ dispersed as nanoparticles (NP-polyP$_{160}$) or in solution (D-polyP$_{160}$, Figure 2.6A). With NP-polyP$_{160}$ (1 μM, 250 nm diameter, Figure 2.7), clotting occurred in approximately 170 min and 200 min at a shear rate of 1 s^{-1} and 22 s^{-1} respectively. When a similar amount of polyP$_{160}$ was localized onto the channel surface, clotting occurred significantly faster than both NP-polyP$_{160}$ and D-polyP$_{160}$. Clotting initiated from the parallel channel shear chamber walls, or in areas where the channel expanded from high to very low shear, and progressively grew outwards (Figure 2.6B). Clotting with D-polyP$_{160}$ (1 μM) was 4- to 2.8-fold slower than SI-polyP$_{160}$ and 1.6- to 0-fold slower than NP-polyP$_{160}$ at all shear rates. Overall, clotting occurred fastest with SI-polyP$_{160}$ than dispersed polyP$_{160}$ in either soluble or NP forms, even with 6-43 fold less SI-polyP$_{160}$ in the channels.

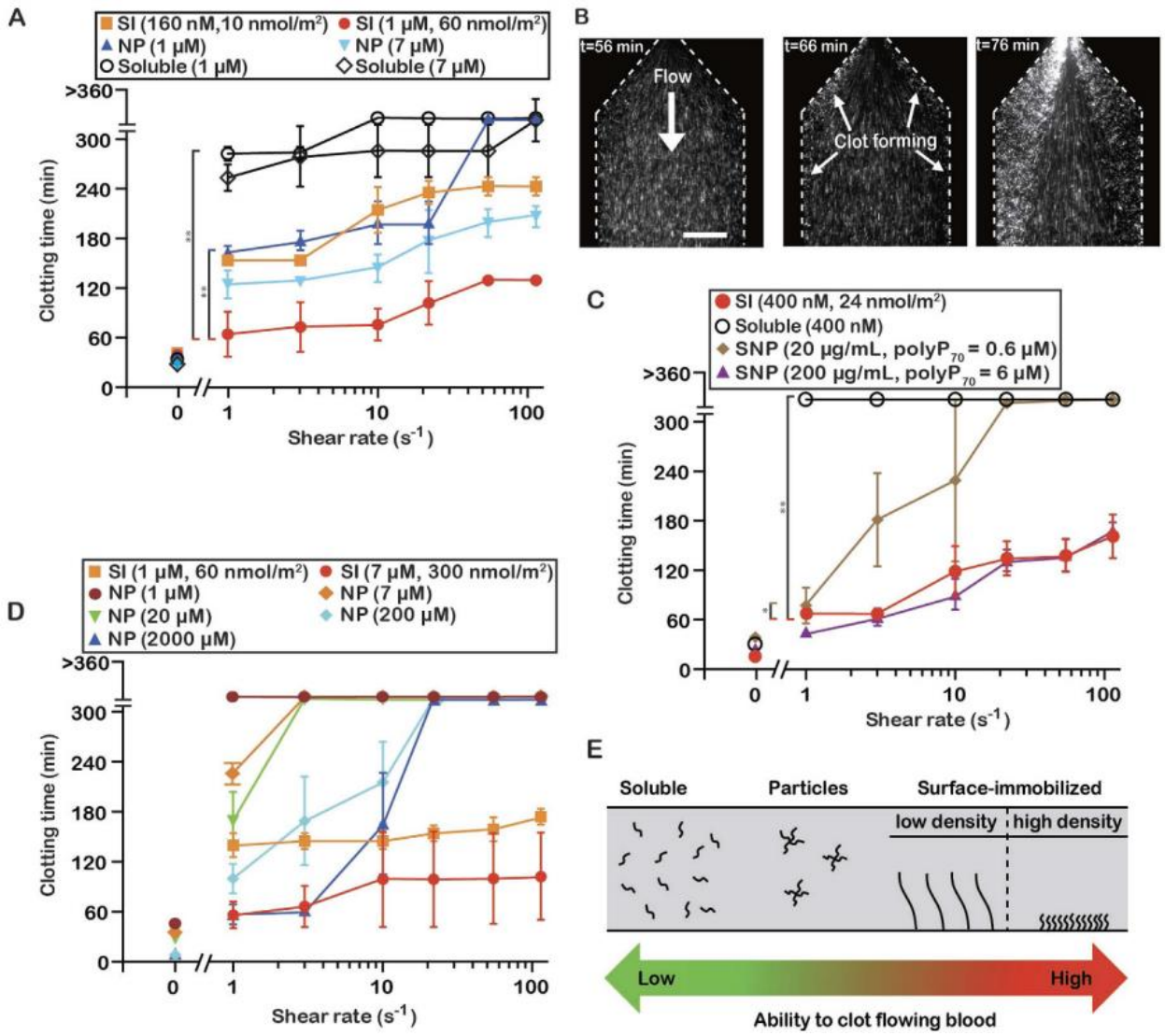

Figure 2.6. PolyP accelerates clotting best when spatially localized onto surfaces, compared to soluble polyP and nanoparticles of polyP. (A) Clotting times of plasma by $polyP_{160}$ at varying shear rates, comparing three states of $polyP_{160}$: solubilized, self-assembled nanoparticles, and surface-immobilized. (B) Time-lapse images showing SI-$polyP_{160}$ initiating clotting (detected by non-flowing beads) from the channel wall (dashed lines). Scale bar is 250 µm. (C) Comparing three states of $polyP_{70}$: solubilized, surface-immobilized onto the microfluidic channels, and immobilized onto silica nanoparticles. Clotting tendencies of plasma containing silica nanoparticles coated with $polyP_{70}$ (SNP-$polyP_{70}$) compared to soluble and surface-

immobilized polyP$_{70}$ under shear in the microfluidic device. (D) Comparing two states of long-chain polyP: surface immobilized polyP$_{400}$ and nanoparticles of self-assembled polyP$_{>1000}$. (E) Schematic summarizing the relationship between spatial distribution of polyP and the acceleration of clotting in the above experiments. Data points indicate mean ± SEM, *p < 0.001, **p < 0.0001, *n* = 3-4. Statistical analysis represents comparisons between whole curves.

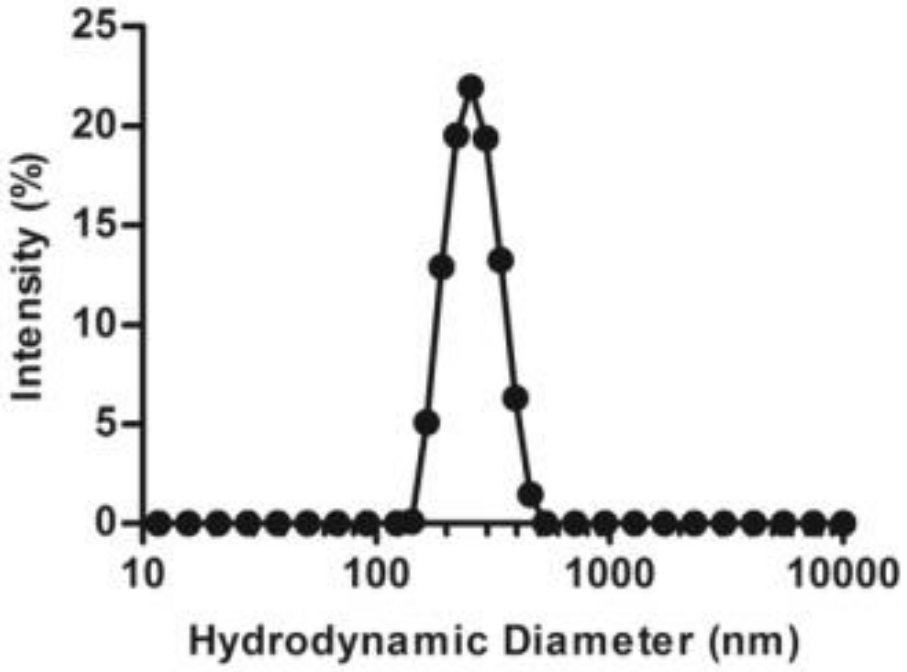

Figure 2.7. Size distribution of NP-polyP160. Representative DLS data demonstrating NP-polyP160 consisting of particles with an average hydrodynamic diameter of 250 ± 65 nm.

2.4.5 Platelet-length polyP can accelerate clotting when surface-localized

The concentration of polyP is approximately 1.1 mM in platelets, where it is stored in platelet dense granules, and can reach up to 2-7 μM in blood upon platelet activation [137, 144]. To test whether synthetic polyP similar in length to those found in human platelets can clot

flowing blood at physiological concentrations, polyP$_{70}$ was tested (Fig. 2.4C). Soluble polyP$_{70}$ (D-polyP$_{70}$) at 400 nM did not accelerate clotting of flowing blood plasma at the shear rates tested. In contrast, an equivalent amount of SI-polyP$_{70}$ substantially accelerated clotting, to 70 min and 160 min at shear rates of 1 s^{-1} and 110 s^{-1} respectively. The amount of SI-polyP$_{70}$ used corresponded to a surface concentration of 24 nmol/m^2 and a total concentration of around 400 nM in the volume of the channel. Initiation time of clotting by SI-polyP$_{70}$ was dependent on FXII (Figure 2.8).

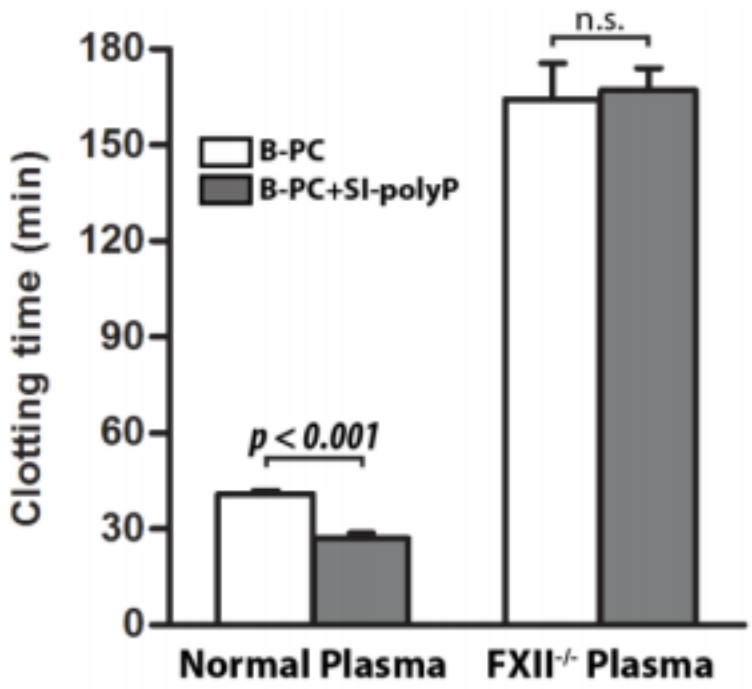

Figure 2.8. PolyP facilitates clotting through activation of Factor XII. Clotting times of normal plasma and FXII-deficient plasma at zero-shear with SIpolyP70 or without (biotinylated-PC alone). Data indicate mean ± SEM, n=3.

SI-polyP$_{70}$ and D-polyP$_{70}$ could not be directly compared to self-assembled nanoparticles of polyP$_{70}$ (NP-polyP$_{70}$), because the solubility of polyP$_{70}$ is greater than longer chain polyP, and NP-polyP$_{70}$ was not stable. Alternatively, we tested a second formulation of polyP nanoparticles, where polyP$_{70}$ was coated on silica nanoparticles (SNP-polyP$_{70}$) [146]. When SNP-polyP$_{70}$ was added to plasma at varying shear, clotting occurred in approximately 70 min to 160 min at 200 µg/mL and 80 min to >360 min at 20 µg/mL. These masses of SNP-polyP$_{70}$ corresponded to concentrations of polyP$_{70}$ of 6 µM and 0.6 µM, respectively, but include both polyP$_{70}$ and silica. Silica is also an activator of factor XII, so an equal comparison between SI-polyP$_{70}$ and SNP-polyP$_{70}$ cannot be made. Nevertheless, the clotting times of SI-polyP$_{70}$ (400 nM) were significantly faster than 20 µg/mL of a SNP-polyP$_{70}$, and were nearly identical to 200 µg/mL of a SNP-polyP$_{70}$ even though there was a 15-fold lower concentration of polyP$_{70}$.

2.4.6 Clotting by long-chain polyP is also enhanced by surface localization

To understand if the effect of surface localization extends to long-chain polyP, we tested a range of concentrations of long-chain polyP either surface localized (SI-polyP$_{400}$) or dispersed as nanoparticles (NP-polyP$_{>1000}$). PolyP$_{>1000}$ naturally self-assembles, localizing into nanoparticles of 150 ± 30 nm in diameter in solutions containing Ca^{2+} at low millimolar concentrations [282]. It is a known activator of clotting under static conditions when dispersed throughout plasma [11]. We compared NP-polyP$_{>1000}$ to SI-polyP$_{400}$, rather than SI-polyP$_{>1000}$, because surface patterning of polyP requires biotinylation of the polyP chains, and the biotinylation procedure caused degradation of long chain-lengths of polyP. When plasma was flowed over SI-polyP$_{400}$, clotting occurred in approximately 60 min to 100 min at 7 µM and 140 min to 170 min at 1 µM at the shear rates examined (Figure 2.6D). The clot times using NP-polyP$_{>1000}$ demonstrated robust shear- and concentration-dependence at 2000, 200, 20, 7 and 1

μM. NP-PolyP$_{>1000}$ was most potent at 2000 μM, initiating clotting at 60 min at 1 and 3 s^{-1}, although requiring 285-fold more phosphate to match the propensity of SI-polyP$_{400}$ to clot flowing plasma under the same conditions.

2.5 Discussion

Together, these data show that the spatial localization of synthetic polyP onto surfaces affects its ability to activate clotting under flow (Figure 2.6E). Short-chain polyP polymers (polyP$_{160}$ and polyP$_{70}$) greatly accelerated clotting of flowing blood plasma at low to sub-physiological shear when surface-localized onto the walls of microfluidic chambers compared to when they are dispersed (nanoparticle or soluble forms). Soluble short-chain polyP only clotted stagnant blood (near-zero flow) in our experiments, and clotting did not occur within a span of hours even at sub-physiological shear rates. Localization of polyP onto the surface of channels showed the greatest activity overall. The concentration at which SI-polyP$_{70}$ accelerated clotting *in vitro* is well-within the range of amounts of polyP released into plasma following platelet activation. Although it is not known if polyP localizes to cell surfaces or thrombi, or to the extent polyP contributes to physiological or pathophysiological coagulation, it is important to identify scenarios in which polyP could potentially elicit a role. These results propose that if polyP can surface-localize it may contribute to clotting at sub-physiological shear following platelet activation, but further *in vitro* and *in vivo* experiments are necessary to verify that this is a potential mechanism.

Remarkably, comparing SI-polyP$_{70}$, SI-polyP$_{160}$, and SI-polyP$_{400}$, to each other shows that short-chain polyP could match the propensity of longer chain polyP to accelerate clotting under flow. SI-polyP$_{70}$ accelerated clotting to a similar extent as SI-polyP$_{160}$ and SI-polyP$_{400}$ with a lower concentration of phosphate. Although clotting times were similar between them with

respect to surface coverage of full-length polymers. This is likely because shorter chains have high surface coverage relative to the amount of monomer. Thus, clotting occurred faster with both increasing surface concentration of phosphate and increasing surface coverage.

The simulations predicted the trend observed *in vitro*. Localization creates high local concentrations of polyP, and in the numerical simulations this led to larger thrombin bursts due to increased positive feedback from the coagulation cascade. The simulations included polyP binding and inhibiting TFPI and accelerating activation of factors V and XI, which all occur in plasma. The mechanism is likely contact system mediated as under stagnant conditions FXII contributed to initiation of clotting by polyP, but we did not test this further in flow experiments. It was recently shown that short-chain polyP could complex with FXII *in vitro* to allostericly induce its activation at high polyP concentrations of 70-130 μM [153]. This polyP-induced activation of FXII was enhanced in the presence of zinc ions, which is known to bind robustly to both FXII and PolyP [11, 153]. Short-chain polyP can also contribute to clotting independently of FXII when TF is present [283]. The results here, without TF, indicate that localization can further increase the propensity of short-chain polyP to clot blood plasma.

There are several other proteins than FXII that could potentially bind the polyP surface and contribute the mechanism of enhanced clotting. PolyP can bind kallikrein, thrombin, and FXIa [306]. The binding of polyP to various coagulation factors serves as a template to localize these proteins to a surface, thereby increasing their effective local concentration and increasing the rate of amplification of clotting [136]. As a result, polyP can bind and accelerate the activation of FXI by thrombin, and accelerate activation of FV by both thrombin and FXIa [316]. Furthermore, polyP can bind to fibrin(ogen), which renders a more stable clot structure and increases resistance to fibrinolysis [316]. As such, a polyP surface may serve as a scaffold for

fibrin(ogen) binding, which can potentially enhance deposition and accelerate clotting through localization of not only fibrin(ogen), but also fibrin(ogen) bound proteins such as FXIII.

In these microfluidic experiments, shear rate and concentrations of either FVIIa or polyP influenced the clotting times over several hours. The shear rates mimicked the shear rates that are typical in large veins and valves; as well as, pathological shear which occurs it the context of thrombosis. The reported clotting times appear very long compared to clotting times in most *in vitro*, stagnant clotting assays, which occur in seconds to minutes. However, residence time of plasma in the microfluidic chambers was only ~10 sec, with plasma being continuously transported into and out of the chamber, and thus the rate of clotting cannot be directly compared to stagnant clotting assays. Long clot times were possible in this device, compared to most other flow systems, because platelet-poor plasma was recalcified on the device and because TF was not included [317]. The observed clotting times were much slower than what is typical in acute hemostasis and at high concentrations of TF, but they were within the time-frame that formation and growth of thrombi occurs inside veins and regions of low shear [301-303]. Thrombosis, in contrast to hemostasis, can involve progressive and gradual clot growth, where there is much less TF but increased contribution of factors XI and XII [154, 318]. The clotting times measured in this microfluidic system are more representative of clotting times that would occur during thrombosis inside intact veins, rather than punctured vessels or stagnant clotting assays. In addition, the shear rates used in our microfluidic model include the rates which occur in large veins. Though platelets appear to contribute more to arterial thrombi than venous thrombi, they also contribute to venous thrombosis [150, 319]. For example, antiplatelet drugs have also been beneficial in treating venous thrombosis [319-321].

For several concentrations and chain-lengths of polyP, it was not possible to make equivalent comparisons between SI-polyP, NP-polyP, SNP-polyP, and D-polyP, because the chain-length and concentration are important determinants of whether polyP self-assembles into particles or remains soluble. The solubility of short-chain polyP is greater than long-chain polyP, but solubility also depends on the concentration of polyP and Ca^{2+}. For example, $polyP_{160}$ can be formulated to be soluble or to form NP-polyP by varying the concentration of polyP and Ca^{2+} [282]. We used concentrations of $polyP_{160}$ well below its limit of solubility. $PolyP_{160}$ was first dissolved into water and then diluted into plasma. When added to citrated plasma, soluble polyP likely remained dissolved, as plasma has insufficient free divalent cations to facilitate nanoparticle formation [282]. Once plasma is recalcified, polyP likely remains protein-bound even in the presence of low millimolar amounts of ionic calcium, at least for the 35 sec that it is present in the microfluidic devices (Figure 2.9) [282, 306]. In contrast, NP-polyP were formed by precipitating $polyP_{160}$ in 5 mM Ca^{2+}, generating nanoparticles that were stable for over 6 hr, as measured by dynamic light scattering. NP-polyP was diluted in the calcium-saline solution that mixed with blood plasma inside the microfluidic devices to keep the nanoparticles intact. The stability of NP-polyP in plasma is unknown; however, NP-polyP was initially prepared under supersaturated conditions, and the solubility of NP-polyP displays hysteretic behavior [282]. Thus, a large portion of NP-polyP, once formed, likely remained as NPs in the microfluidic devices. Although synthetic polyP was used in these experiments, natural polyP is also typically bound to calcium [322].

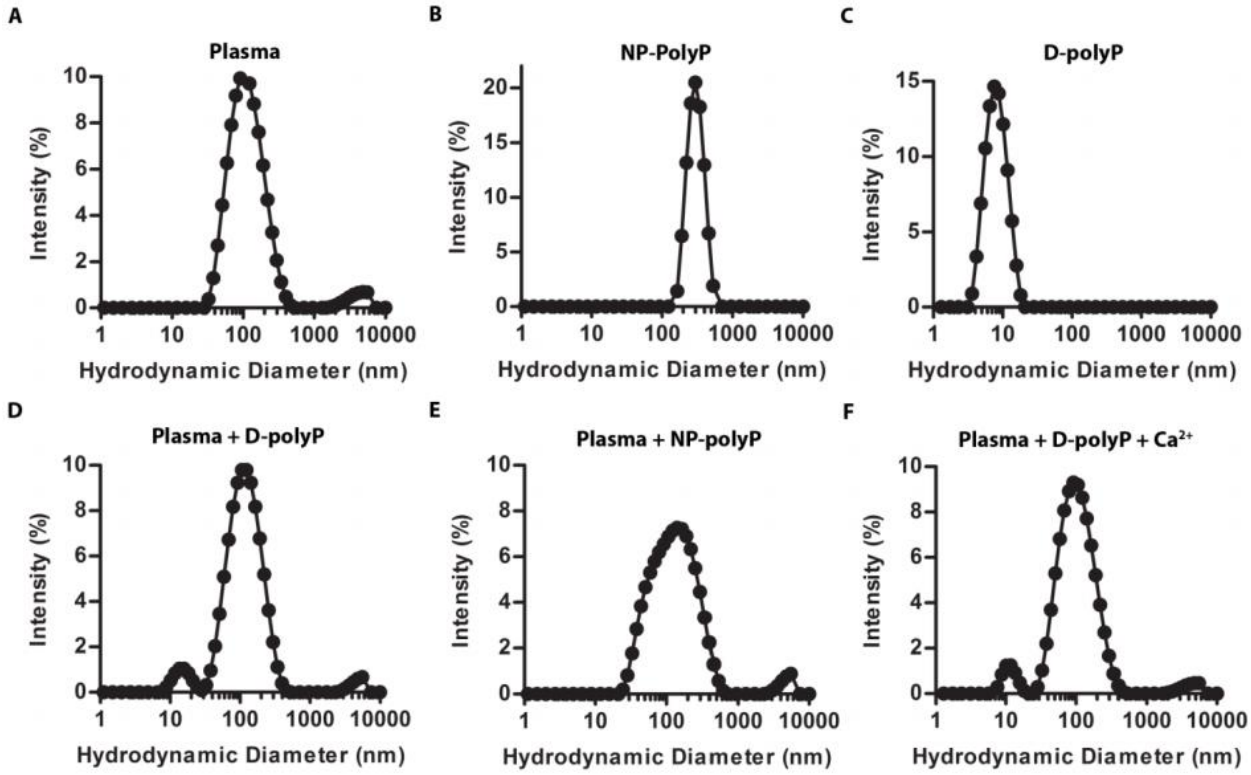

Figure 2.9. DLS size distribution of soluble D-polyP160 and NPpolyP160 in buffer and plasma. (A) Normal citrated plasma without polyP, which contains background intensity from components normally in plasma. (B-C) Aggregated and soluble polyP160 respectively in HEPES buffered saline. (D) Soluble polyP160 added to citrated plasma. (E) Preformed NP-polyP160 added to citrated plasma. (F) Soluble polyP160 was added to citrated plasma and recalcified; the graph of panel F resembles panel D (D-polyP) rather than panel E (NP-polyP).

In summary, this work shows that spatial localization of synthetic polyP, including short-chain polyP, increases its propensity to accelerate clotting of blood plasma at low to sub-physiological shear. The observed clotting times were much slower than what is typical in hemostasis, but they were within the time-frame that thrombosis occurs inside veins, particularly post-operative deep vein thrombi, which form over a period of days [302, 303, 323]. The

experiments were designed solely to test if surface-localization of short-chain polyP accelerates clot formation under flow, at venous and sub-physiological shear rates. An important observation from this was that when localized, short-chain polyP could match the ability of long-chain polyP to accelerate clotting. The concentration required to accelerate clotting is markedly reduced when polyP is spatially localized onto surfaces, and to a lesser extent, into particles, even under flow and without TF. These biophysical insights provide a potential biophysical mechanism by which platelet-length polyP could contribute to thrombosis in regions of low shear, but further work is required to validate if this mechanism could indeed extend to *in vivo* scenarios. This effect of localization may potentially contribute to clotting at higher shear when TF is present [283]. Although these *in vitro* results, in an artificial flow system, support the notion that platelet-derived polyP could contribute to coagulation *in vivo*, the flow system used here does not include many factors that normally regulate clotting, such as platelets, platelet-derived polyP, red blood cells, immune cells, endothelium and other soluble factors. For these reasons, appropriate *in vivo* models are necessary to verify whether platelet-derived polyP and its spatial localization contributes to clot formation and thrombosis.

Chapter 3: Coagulation factor XIIIa is inactivated by plasmin

3.1 Contribution

This research was a collaborative project published in *Blood*. W.S.H. conceived the idea, designed experiments and performed experiments, analyzed and interpreted data and wrote the paper. W.S.H. performed experiments to collect data specifically for Figures 3.1, 3.2A-E, 3.3, 3.4, 3.5, 3.7, 3.8, 3.9, 3.10, 3.10A-B and 3.11. N.M. designed and performed experiments for Figure 3.2F, 3.6A-D, 3.10C-E, analyzed and interpreted data, and wrote the paper. I contributed to 20% of this paper. C.J.K. helped design experiments, interpret data and write the paper. Collaborators and undergraduate thesis students contributed to different aspects of the paper, such as methods development (J.R.B.), performing preliminary experiments (X.J.L and H.M.B.) and data analysis (A.S.W.).

3.2 Introduction

The coagulation system controls a polymerization process that is required to seal vascular damage. Fibrin is quickly generated and cross-linked into a mesh of insoluble fibers by the transglutaminase factor XIIIa (FXIIIa). Mechanisms of synthesis and activation of FXIIIa are known [12], however the physiological mechanism of inactivation remains unclear.

Plasma FXIII (pFXIII-A_2B_2) consists of two catalytic A subunits and two regulatory B subunits arranged as a heterotetramer, whereas platelets and monocytes express intracellular FXIII-A_2 without the B subunits (cFXIII-A_2) [12]. During clotting, thrombin cleaves a 37-residue activation peptide from the A subunit of pFXIII-A_2B_2. Then, in the presence of calcium, the A subunits disassociate from the B subunits and undergo a conformational change to become catalytically active. The active FXIIIa, also referred to as FXIII-A_2*, catalyzes the formation of a pseudo-peptide bond between a glutamine residue of one protein and a lysine residue of another

protein, releasing ammonia [12]. Fibrin is the major substrate of FXIIIa. Self-assembled fibrin becomes stabilized when it is covalently cross-linked to itself, the vessel wall, and to anti-fibrinolytic proteins by FXIIIa. In plasma, pFXIII-A_2B_2 circulates bound to fibrinogen [324]. Although most FXIIIa remains bound to fibrin during clot formation [325], active FXIIIa released from the clot, such as during clot lysis, would presumably circulate systemically. While it has been reported that FXIIIa can be inactivated by thrombin [326] or proteolytic enzymes released by granulocytes [327], it remains unclear whether these mechanisms extend to all the intracellular, intravascular and extravascular FXIIIa. These reports have led to the question: Are there other mechanisms of inactivation of FXIIIa?

A long-standing hypothesis is that FXIIIa is inactivated by the fibrinolytic system, which normally degrades the fibrin clot and associated proteins [15]. The fibrinolytic enzyme plasmin is generated from plasminogen by activators such as tissue plasminogen activator (tPA). Previous reports found that cFXIII-A_2, cFXIII-A_2*, and pFXIII-A_2B_2 were resistant to plasmin degradation [16]. Here, we show that zymogen FXIII is resistant to degradation by fibrinolytic enzymes at physiological concentrations. However, contrary to previous reports, the enzymatically active FXIII-A_2* (FXIIIa) is readily degraded by endogenous plasmin during clot lysis.

3.3 Methods

3.3.1 Activating and degrading FXIII A and B subunits in purified systems and in blood

To generate FXIIIa, human pFXIII-A_2B_2 (Haematologic Technologies Inc.) was incubated with bovine thrombin (Sigma, 400 nM, 2 U/mL) and calcium chloride (4 mM) for 30 min in HEPES-buffered saline (HBS) (10 mM HEPES, 140 mM NaCl, pH 7). Thrombin was then inhibited by hirudin (EMD Millipore, 400 ATU/mL), and plasmin (Haematologic

Technologies Inc.) was added to pFXIII-A_2B_2 or pFXIIIa (30 nM, 0.6 U/mL). For platelet experiments, platelets (1×10^{11}/L) were activated with bovine thrombin (400 nM, 2 U/mL) before incubation with plasmin or tPA (Genentech). For plasma-based experiments, citrated plasma was recalcified (10 mM $CaCl_2$) and then activated with diluted Innovin (Dade Behring, 1 pM) for 30 min. Fibrinogen-deficient plasma was activated with thrombin (200 nM, 1 U/mL) to fully activate FXIII. In control samples that were not activated, hirudin (100 ATU/mL) was added to inhibit endogenous thrombin and thus FXIIIa generation. Tranexamic acid (TXA) (Sigma, 7.5 mM), an inhibitor of plasmin and tPA [328], was added to specified samples before plasmin or tPA was added. All samples were incubated at 37 °C. Each experiment was repeated at least three times. All *p* values were calculated by two-tailed Student's *t*-test.

3.3.2 Preparing platelets

This study was approved by the research ethics boards of the University of British Columbia, and informed consent was obtained from all healthy volunteers before whole blood donation. Whole blood was collected into tubes containing sodium citrate (12 mM) and was centrifuged at 100 × g for 20 min. The top 75% of the PRP fraction was collected. Platelets were pelleted by centrifugation at 250 × g for 10 min, and washed in CGS buffer (120 mM NaCl, 30 mM D-glucose, 11 mM trisodium citrate, pH 6.5) and then in Tyrode's buffer (1.8 mM $CaCl_2$,137 mM NaCl, 2.7 mM KCl, 0.4 mM NaH_2PO_4, 10 mM HEPES, 5.6 mM monohydrate D-glucose, 1.1 mM $MgCl_2$, pH 6.5). Platelets were then resuspended in Tyrode's buffer at a final concentration of 2×10^{11} platelets/L.

3.3.3 Western blotting

Samples were prepared as described previously [51]. All samples were reduced and boiled prior to electrophoresis on 4-15% Mini-PROTEAN TGX gel (Bio-Rad) and transferred to a

nitrocellulose membrane (Pall Life Sciences). Boiling the samples did not induce auto-degradation of FXIIIa (Figure 3.1). After blocking with Odyssey Blocking Buffer (Li-Cor), the membrane was incubated overnight at 4 °C with the primary antibody; sheep or rabbit anti-human FXIII A (Affinity Biologicals or Thermo, respectively, diluted 1:1000), rabbit anti-human FXIII B (Sigma, diluted 1:1000) or rabbit anti-human fibrinogen (Dako, diluted 1:50 000). The membrane was washed with phosphate buffered saline with Tween 20 (8 mM Na_2HPO_4, 150 mM NaCl, 2 mM KH_2PO_4, 3 mM KCl, 0.05% Tween 20, pH 7.4). After incubation with the pre-adsorbed secondary antibody (Abcam, diluted 1:10,000), the membrane was washed and antibody detected with ECL substrates (Bio-Rad). Membranes were stripped with a solution of 62.5 mM Tris pH 6.8, 2% SDS, and 0.7% beta-mercaptoethanol for 1 hr at 60 °C with occasional agitation and then reprobed. The statistical significance was calculated using a two-tailed Student's *t* test. The statistical analysis was not adjusted for multiple comparisons and there is a chance for a type I error. The current work is early experimental research and further work needs to be done with a sample size and appropriate statistical analysis such as ANOVA and post-hoc analysis. In addition to larger sample sizes, the work requires confirmation from plasma analysis from different human donors, different animal species and different sexes.

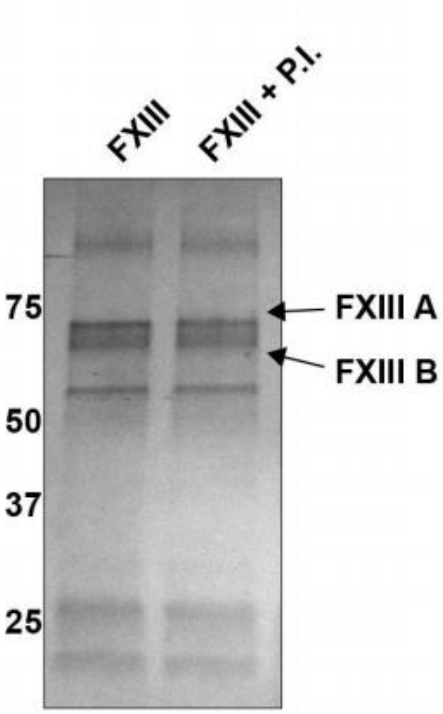

Figure 3.1. FXIII did not degrade when heat-inactivated at 95°C. FXIII was incubated with or without a protease inhibitor cocktail (P.I.) and heated for 5 min at 95°C.

3.3.4 Identifying the plasmin-mediated cleavage site of FXIIIa

FXIIIa (10 μM) was incubated with plasmin (2.7 μM) at 37°C for 2 hr. The reaction was stopped by heat-inactivating the sample at 95°C for 5 minutes. The samples were labeled on the newly exposed N-termini using reductive methylation, trypsin-digested and cleaned [329-331]. Peptide samples were purified by solid phase extraction and analyzed using a linear-trapping quadrupole-Orbitrap mass spectrometer on-line coupled to an Agilent 1290 Series HPLC using a nanospray ionization source. Centroided fragment peak lists were processed with Proteome Discoverer v.1.2 and searched with Mascot algorithm. The peptides identified as cleavage products were those that had IonScores over the 99% confidence limit. This experiment was repeated twice with similar results.

3.3.5 Measuring the kinetics of inactivation of FXIIIa by plasmin

Plasmin-mediated inactivation of FXIIIa was evaluated using steady-state kinetics at 37°C. The rate of inactivation of FXIIIa was determined by measuring the transglutaminase activity of FXIIIa via the production of ammonia. First, a calibration curve was generated that related the concentrations of ammonia to A_{570} using a colorimetric detection assay for ammonia (BioVision Inc.), monitored with a Tecan M200 plate reader. A second calibration curve was generated that related the concentration of FXIIIa (1.6 to 78.1 nM) to the velocity of ammonia generation. This transglutaminase assay was performed by mixing FXIIIa with an amine donor (glycine ethyl ester, GOE, 2.5 mM), a glutamine-containing peptide (NQEQVSPLTLLK, 1 mM), DTT (40 μM), and $CaCl_2$ (3 mM). Aliquots from the transglutaminase reaction mixture were removed and quenched every 15 min with EDTA (15 mM). Plasma FXIII-A_2B_2 (7.8 to 62.5 nM) was converted to FXIIIa by pretreating it with thrombin (4 U/mL) and $CaCl_2$ (3 mM) for 1 hr to distinguish the rate of degradation by plasmin from the rate of activation by thrombin. Thrombin was then inhibited with excess hirudin (13 ATU/mL). To this mixture, plasmin (300 nM) was added. At various time-points, aliquots were removed and plasmin activity was quenched with a cocktail of protease inhibitors (Sigma). The velocity of inactivation of FXIIIa was determined by measuring the residual amount of FXIIIa activity at each time point using the transglutaminase assay with the two calibration curves. Kinetic parameters were calculated using graphing software (OriginPro 9.1). This full experiment was repeated three times with similar results.

3.3.6 Measuring elastic moduli by thromboelastography (TEG)

Studies were performed using normal, plasminogen-deficient, α2-antiplasmin-deficient or fibrinogen-deficient plasma (Haematologic Technologies Inc.) and shear elastic moduli were

evaluated at 37°C using a TEG Hemostasis Analyzer System 5000 (Haemoscope Corporation). Inactivation of FXIIIa was evaluated during clot formation by combining 230 μL of plasma with $CaCl_2$ (10 mM), Innovin (2 pM), and tPA (200 pM), with or without T101 (0.8 mM). FXIIIa inactivation was evaluated during clot lysis by initiating clotting of plasma with $CaCl_2$ (10 mM) and bovine thrombin (400 nM, 2 U/mL), allowing the clot to form for 30 min and then adding tPA (800 nM). Fibrinolysis was inhibited by TXA (10 mM) at either 1 or 3 hr after addition of tPA and the resulting plasma was added to a TEG cup containing fibrinogen (FXIII-free 1.4 mg/mL, Enzyme Research Laboratories), thrombin (2 U/mL), and either HBS, T101 (0.8 mM), or FXIII (200 nM), upon which the TEG analysis began. FXIIIa inactivation was evaluated during clot formation under conditions mimicking thrombolysis by combining $CaCl_2$ (10 mM), Innovin (2 pM), and each plasma containing either 5 nM tPA (α_2-antiplasmin-deficient plasma) or 50 nM tPA (normal and plasminogen-deficient plasma). Activation of clotting progressed for 4 minutes before adding TXA (10 mM), followed by adding HBS, T101 (0.8 mM), or FXIII (200 nM), then fibrinogen (1.4 mg/mL, Haematologic Technologies Inc.), before commencing TEG analysis.

3.4 Results

3.4.1 Activated FXIIIa, but not zymogen pFXIII-A_2B_2, is proteolytically inactivated by plasmin

To evaluate the degradation of plasma-derived FXIII by plasmin, pFXIII-A_2B_2 and FXIIIa were each treated with varying concentrations (100 pM to 100 nM) of plasmin for 3 hr, and analyzed by Western blot. During the 3 hr, FXIIIa was cleaved by concentrations as low as 1 nM of plasmin (Figure 3.2A). Cleavage products of ~50 and 25 kDa were visible, but were transient. However, the A subunit of pFXIII-A_2B_2 was more resistant to cleavage (Figure 3.2B,

Figure 3.3). Degradation of the B subunit from both activated and unactivated pFXIII-A_2B_2 also occurred (Figure 3.2C, 3.2D). Activation of FXIII by plasmin was not observed. Cleavage products of the B subunit, and possibly other cleavage products of the A subunit, may not have been detected due to a faster rate of degradation relative to that of intact FXIII, or a low abundance or absence of antigens identified by the antibody (Figure 3.4). To evaluate if the cleavage products were enzymatically active, the cleavage and activity of FXIIIa were monitored over time. Degradation of FXIIIa by plasmin (90 nM) was evident within 5 min and the transglutaminase activity of FXIIIa decreased rapidly over 30 minutes (Figure 3.2E, 3.2F). The loss of FXIIIa activity correlated with the loss of fully intact FXIIIa, indicating that cleavage products of FXIIIa were enzymatically inactive.

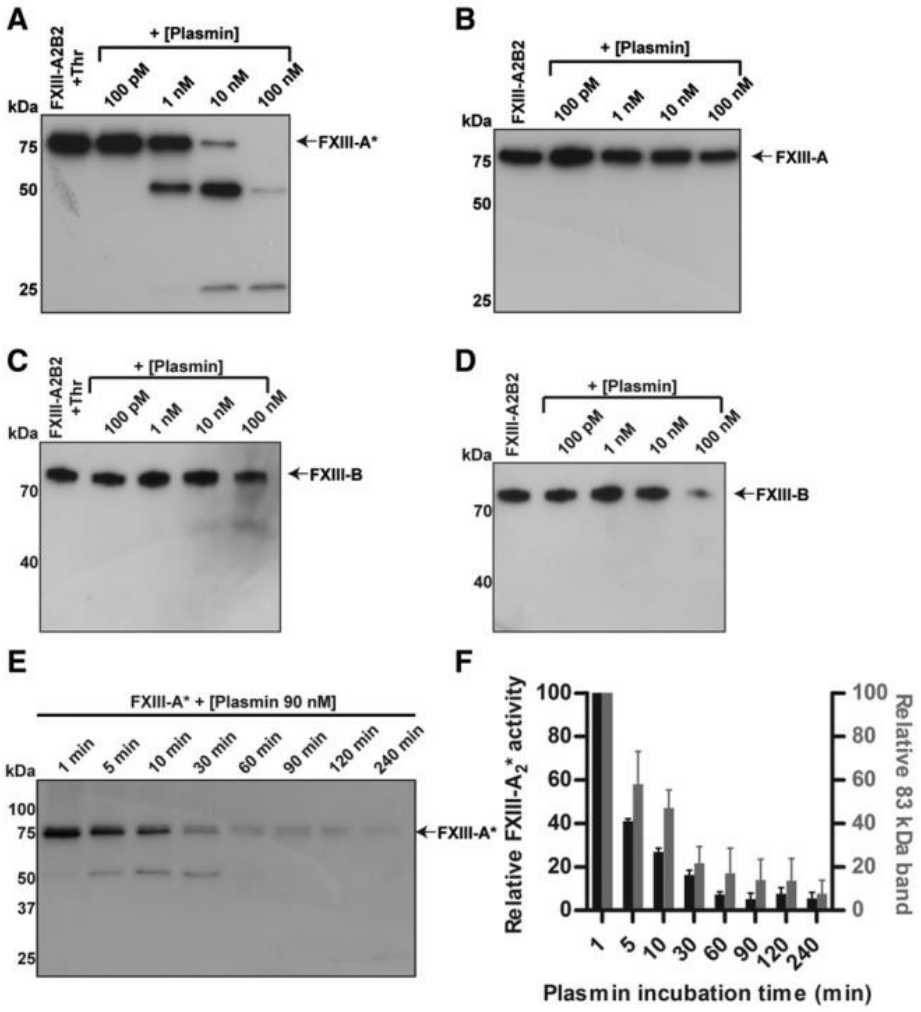

Figure 3.2. FXIIIa is cleaved and inactivated by plasmin. FXIII (100 nM), with or without prior activation by thrombin (400 nM), was mixed with varying concentrations of plasmin (100 pM to 100 nM) for 3 hr, and analyzed by Western blot against FXIII A and B subunits. (A) Blot against the A subunit of pFXIIIa, with thrombin activation. (B) Blot against the A subunit of pFXIII-A_2B_2. (C) Blot against the B subunit of pFXIIIa, with thrombin activation. (D) Blot against the B subunit of pFXIII-A_2B_2. (E) Time course of cleavage of FXIIIa by plasmin (90 nM). (F) Transglutaminase activity (left axis) of FXIII-A_2* (FXIIIa) after incubation with plasmin (90 nM) and the relative amount of intact FXIIIa (right axis), determined by quantifying

the intensity of the band at 83 kDa. FXIIIa was calculated as % of total signal in the lane using densitometry. The error bars represent S.E.M. n = 3 for all experiments.

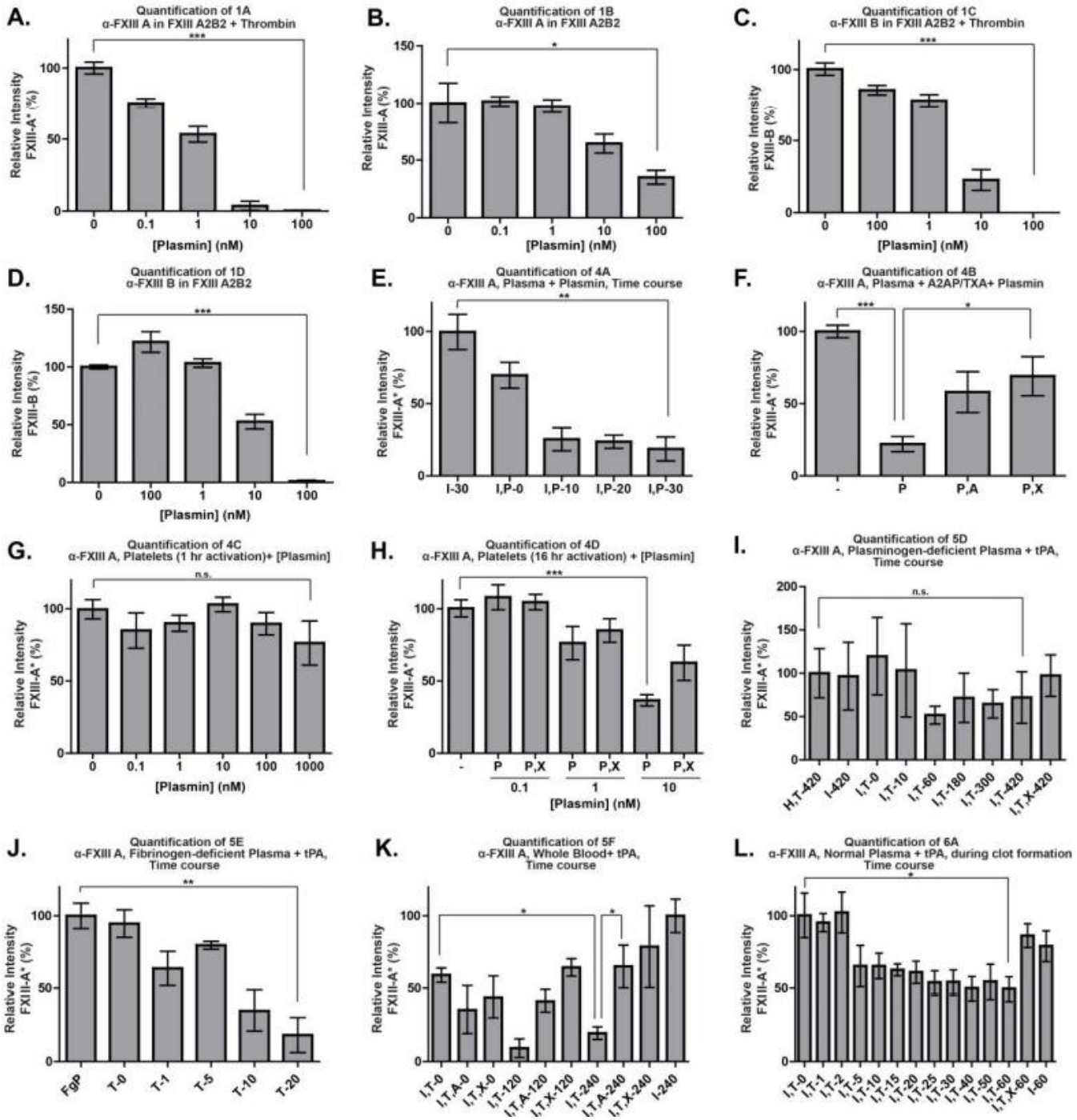

Figure 3.3. Quantification of Western Blots from figures in the main text. FXIIIa was calculated as % of total signal in the lane using densitometry. *P < 0.05, **P < 0.01, ***P < 0.001; n.s, not significant. The error bars represent SEM.

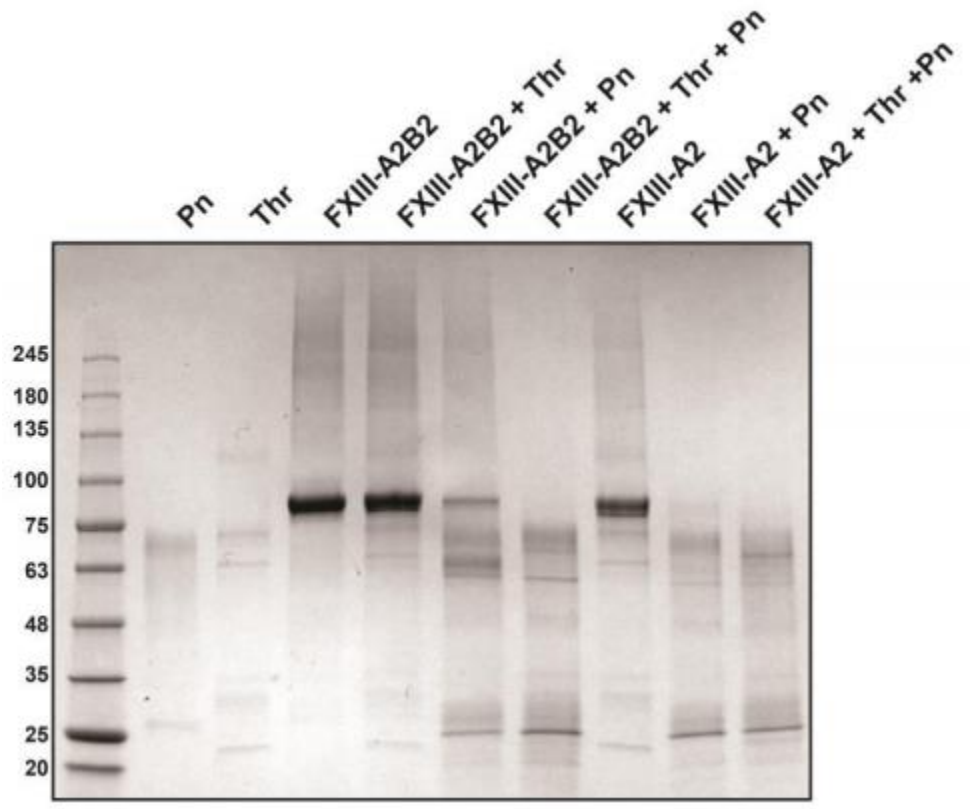

Figure 3.4. Blue-silver stained gel of FXIII(a) treated with plasmin. Blue-silver stained gel containing FXIII-A2B2 (600 nM), FXIII-A2 (600 nM), and thrombin (Thr, 400nM), incubated with plasmin (Pn, 600 nM) for 3 hr.

3.4.2 FXIIIa is cleaved by plasmin at multiple sites

To identify which sites of FXIIIa were cleaved by plasmin, purified FXIIIa was incubated with plasmin and analyzed by mass spectrometry. Nineteen cleavage sites were identified, 8 at

arginines and 11 at lysines, out of the 43 arginines and 34 lysines found in FXIII-A, with detection frequencies between 0.3 – 26 % (Figure 3.5A). The most prominent cut-site was between K468 and Q469, the product of which corresponds in size to the 25 and 50 kDa cleavage products observed in figure 3.2A. To determine the spatial location of cleavage, the site was mapped onto 3-dimensional structures of FXIIIa and FXIII-A_2 [332, 333]. In the FXIII-a structure, the K468-Q469 cleavage site is near the surface, consistent with accessibility to plasmin-mediated cleavage (Figure 3.5B). Interestingly, this K468-Q469 bond also appears surface-accessible in the FXIII-A_2 (unactivated) structure (Figure 3.5C). Because FXIII-A_2 is not readily cleaved by plasmin, as shown in Figure 3.1B, this bond may be protected in the zymogen conformation by the B subunit, which has not been co-crystalized with the A subunit. Five other surface-exposed cleavage sites were identified, but detected eightfold to 38-fold less frequently.

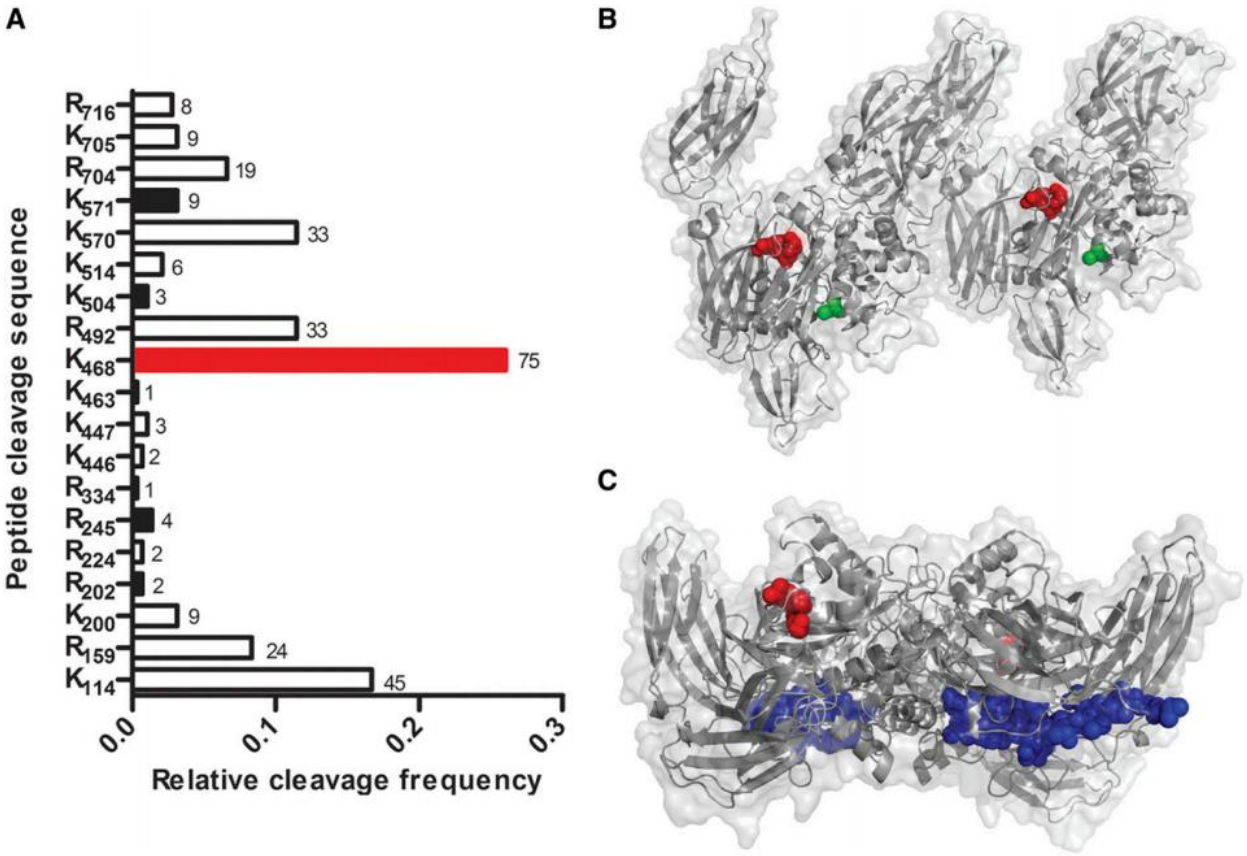

Figure 3.5. Plasmin cleaves FXIIIa at multiple sites. (A) FXIIIa cleavage sites were identified by MALDI/TOF mass spectrometry after purified FXIIIa (10 μM) was incubated with plasmin (2.7 μM) for 2 hr. Surface exposed sites are represented with black bars, and the primary cleavage site with a red bar. The frequency of detection of cut sites is indicated beside the respective bars (n = 2). (B) A reported structure of FXIIIa [333], showing the surface-exposed K468-Q469 cleavage site (red) and the catalytic cysteine (green). The distance between the cleavage site and the catalytic cysteine is 18 Å. (C) A reported structure of FXIII-A_2 [332], showing K468-Q469 (red), and the activation peptide (blue).

3.4.3 The rate of inactivation of FXIIIa can occur on a physiologically-relevant timescale

To determine the kinetic parameters of plasmin-mediated inactivation of purified FXIII-a, the loss of FXIIIa activity with plasmin treatment was measured. Plasmin-mediated inactivation of FXIIIa had an apparent K_m of 0.49 ± 0.02 μM and k_{cat} of 4.2 ± 1.1 × 10^{-3} s^{-1}, resulting in a catalytic efficiency of 8.3 ± 1.7 × 10^3 $M^{-1}s^{-1}$. The K_m was ~10-fold higher and the k_{cat} was ~10-fold lower than reported parameters for fibrin [334]. The half-life of FXIIIa degradation by plasmin, in the absence of fibrin, is estimated to be 34 sec, using these experimentally-determined kinetic parameters and the physiological concentrations of the zymogens (200 nM for plasma- and platelet-derived FXIII[a], and 2.4 μM for plasmin[204]) in circulating blood. V_{max} and K_m were calculated by nonlinear fitting of the measured initial velocities to the Michaelis-Menten equation, which produced similar values to those obtained from a Lineweaver-Burke plot (Figure 3.6A, 3.6B). The rate of inactivation was calculated from the loss of FXIIIa activity, determined using an ammonia production assay (Figure 3.6C). The activity of FXIIIa decreased as it was cleaved by plasmin, resulting in a lower rate of ammonia generation

(Figure 3.6D). These data indicate that the rate of FXIIIa degradation can occur on a physiologically-relevant timescale.

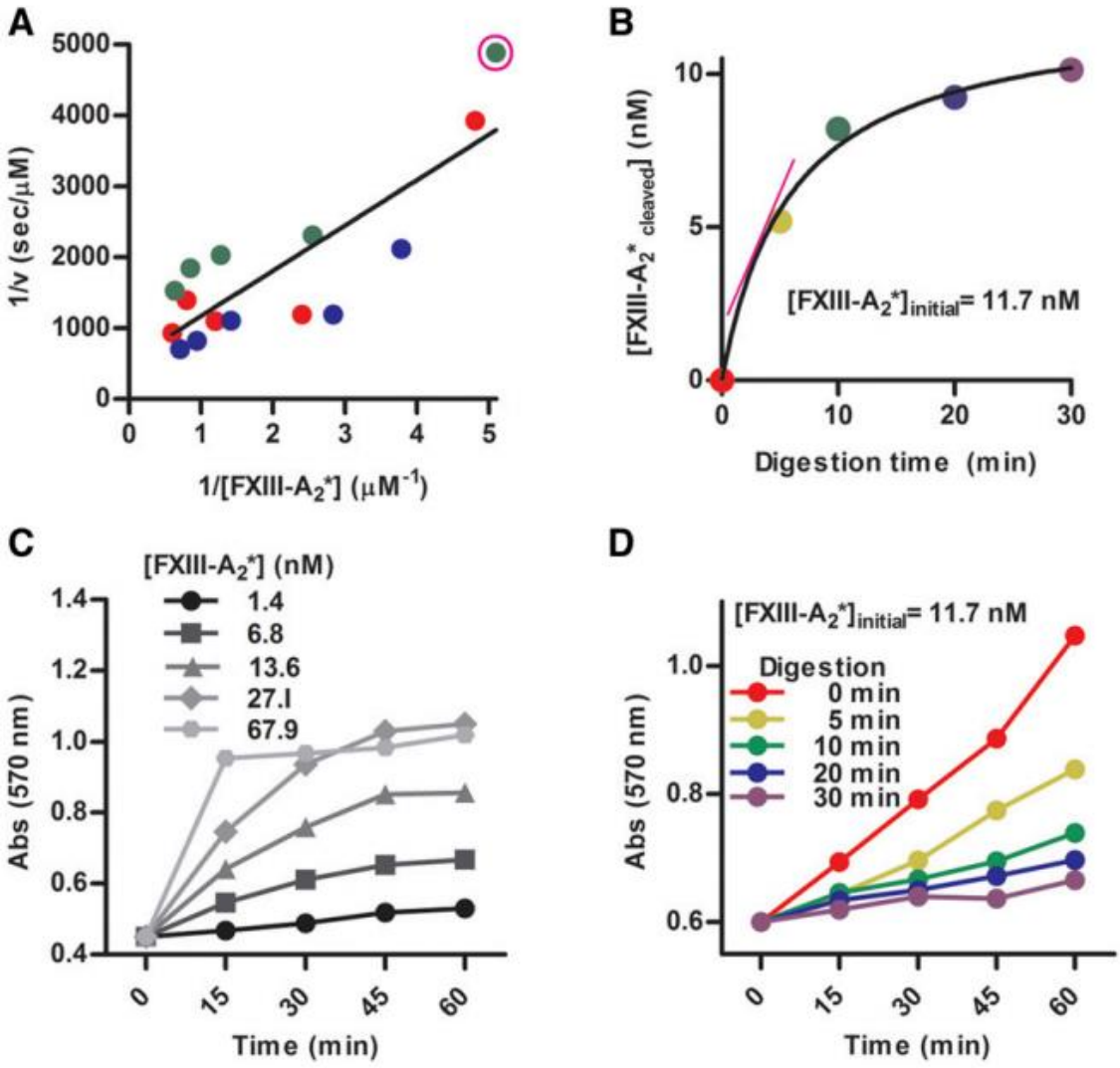

Figure 3.6. The rate of inactivation of FXIII-A$_2$* can occur on a physiologically-relevant timescale. (A) Lineweaver-Burk plot used to generate kinetic parameters for FXIII-A$_2$* (FXIIIa), with data sets represented by different colors. The data point circled in pink is derived from the slope of the initial velocity in panel B (pink line). (B) The generation of FXIII-A$_2$* (FXIIIa) cleavage products by plasmin (300 nM) at a representative FXIII-A$_2$* (FXIIIa)

concentration, determined using an ammonia release assay. (C) Standard curves of ammonia generation over time using various [FXIII-A_2*] (FXIIIa). (D) Ammonia generation over time, with varying times of FXIII-A_2* (FXIIIa) digestion with plasmin. n = 3 for all experiments.

3.4.4 Plasmin inactivates both plasma-derived and platelet-derived FXIIIa

To test if FXIIIa is sensitive to degradation by plasmin in plasma, plasmin was added to fibrin clots in platelet-poor plasma. FXIIIa was mostly degraded within 30 min by plasmin (3 μM, Figure 3.7A). Degradation of FXIIIa was inhibited when exogenous α2-antiplasmin or TXA was added (Figure 3.7B). These data show that plasma-derived FXIIIa can be degraded by plasmin in the presence of fibrin. To test if cFXIII-A_2 (from platelets) was sensitive to degradation by plasmin, platelets were initially activated by thrombin, followed by the addition of plasmin (1 nM to 1 μM). Platelet cFXIII-A_2 was degraded, and transient degradation products were observed when concentrations of plasmin as low as 10 nM were added 16 hr after platelet activation, but not when plasmin was added 1 hr after platelet activation (Figure 3.7C, 3.7D). The degradation products were also observed in the presence of TXA, likely because reduced plasmin activity slowed their rate of cleavage. It is known that cFXIII-A_2 translocates from the cytoplasm to the membrane upon platelet activation [180]; however, the results here suggest that cFXIII-A_2 was not exposed to plasmin and thus not degraded shortly after platelet activation. To test if cFXIII-A_2 was shielded from extracellular proteases, trypsin, which can cleave zymogen FXIII-A_2B_2 [335], was added to platelets at 1 and 16 hr after activation. Platelet cFXIII-A_2 was not degraded by trypsin at 1 hr, but was degraded by trypsin at 16 hr (Figure 3.8), indicating that exposure of cFXIII-A_2 to extracellular proteases was delayed relative to platelet activation. Thus, platelet-derived FXIIIa can be degraded by plasmin following platelet activation.

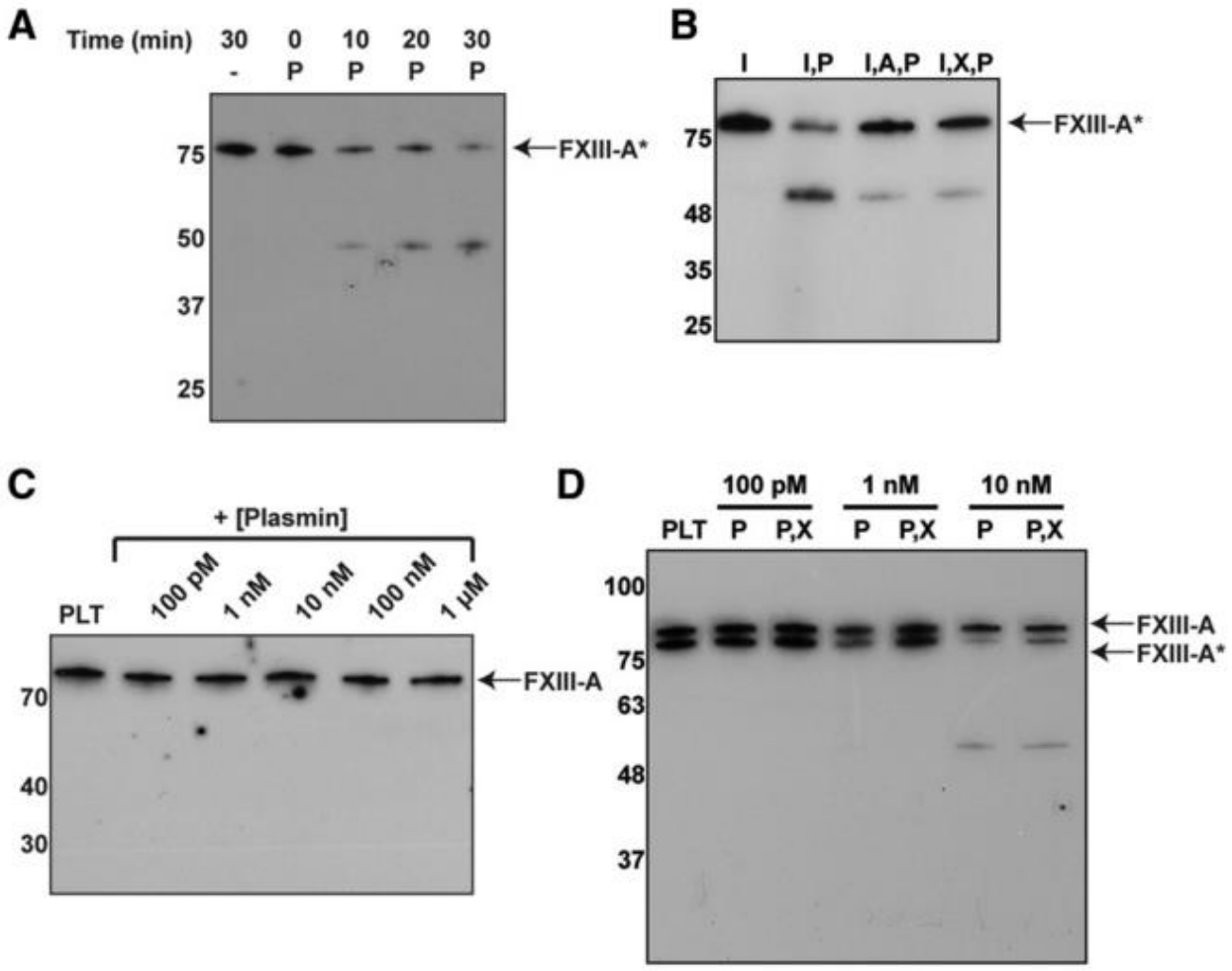

Figure 3.7. Plasmin degrades plasma- and platelet-derived FXIIIa. Western blots against the FXIII A subunit. (A) Endogenous FXIII-A_2* (FXIIIa) from human plasma after adding plasmin (3 µM) for various times. (B) FXIII-A_2* (FXIIIa) from plasma with plasmin (3 µM) and α2-antiplasmin (5 µM) or TXA (7.5 mM). (C-D) Endogenous FXIII-A_2/FXIII-A_2* (FXIIIa) from platelets (PLT) 1 hr (C) and 16 hr (D) after exposure to thrombin, and incubating with various concentrations of plasmin. Samples contain combinations of Innovin (I), plasmin (P), α2-antiplasmin (A), and TXA (X). n = 3 for all experiments.

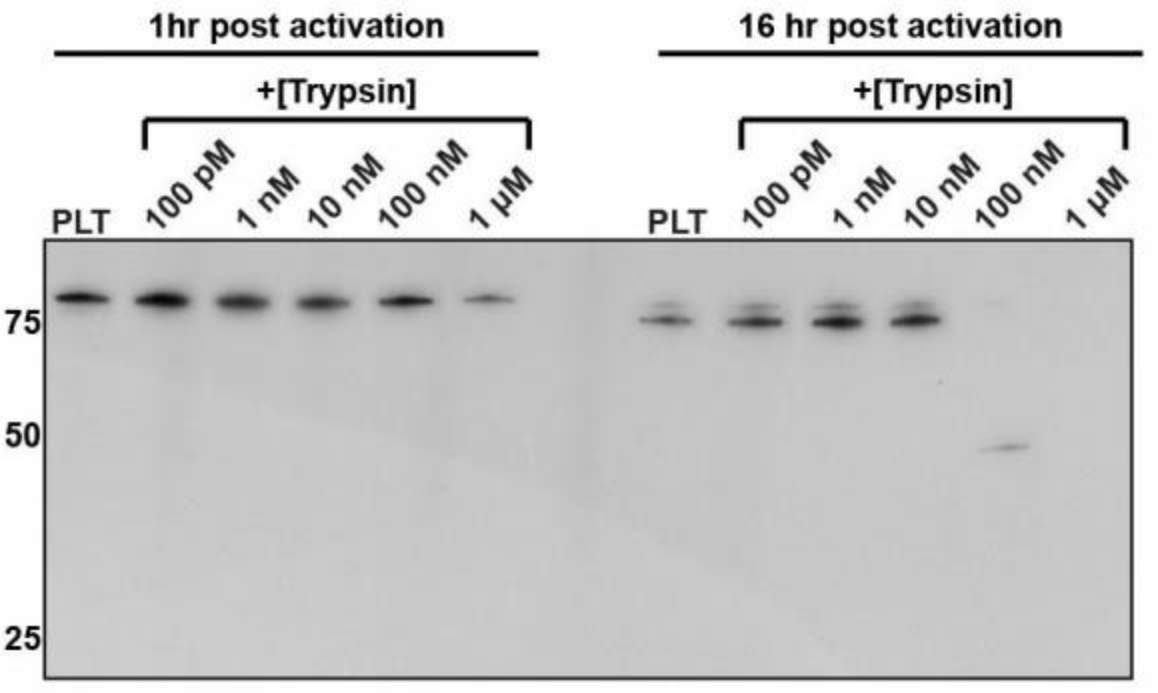

Figure 3.8. Trypsin degrades platelet-derived FXIIIa. Endogenous FXIIIa from platelets (PLT) 1 hr and 16 hr after exposure to thrombin, incubated with various concentrations of trypsin.

3.4.5 Addition of tPA to plasma leads to degradation of pFXIIIa by endogenous plasmin

Addition of tPA (2 µM) to clotted normal plasma led to the degradation of FXIIIa and fibrin within 3 hr (Figure 3.9A-C). Degradation was inhibited by TXA. The degradation of pFXIIIa and fibrin occurred within a similar time-frame, beginning within 10 min, and continuing to 180 min. To determine whether tPA degraded FXIIIa directly or by generating plasmin, plasminogen-deficient plasma was treated with tPA. Degradation of FXIIIa did not occur in plasminogen-deficient plasma, indicating that FXIIIa was degraded by tPA-mediated plasmin activity (Figure 3.9D). In fibrinogen-deficient plasma, FXIIIa was degraded more rapidly than in normal plasma when treated with tPA (comparing Figure 3.9E with Figure 3.9A),

and degraded almost completely within 10-20 min. In whole blood, FXIIIa was degraded when tPA was added, except in the presence of α2-antiplasmin or TXA (Figure 3.9F). Together, these data demonstrate that pFXIIIa degradation can occur by endogenous plasmin.

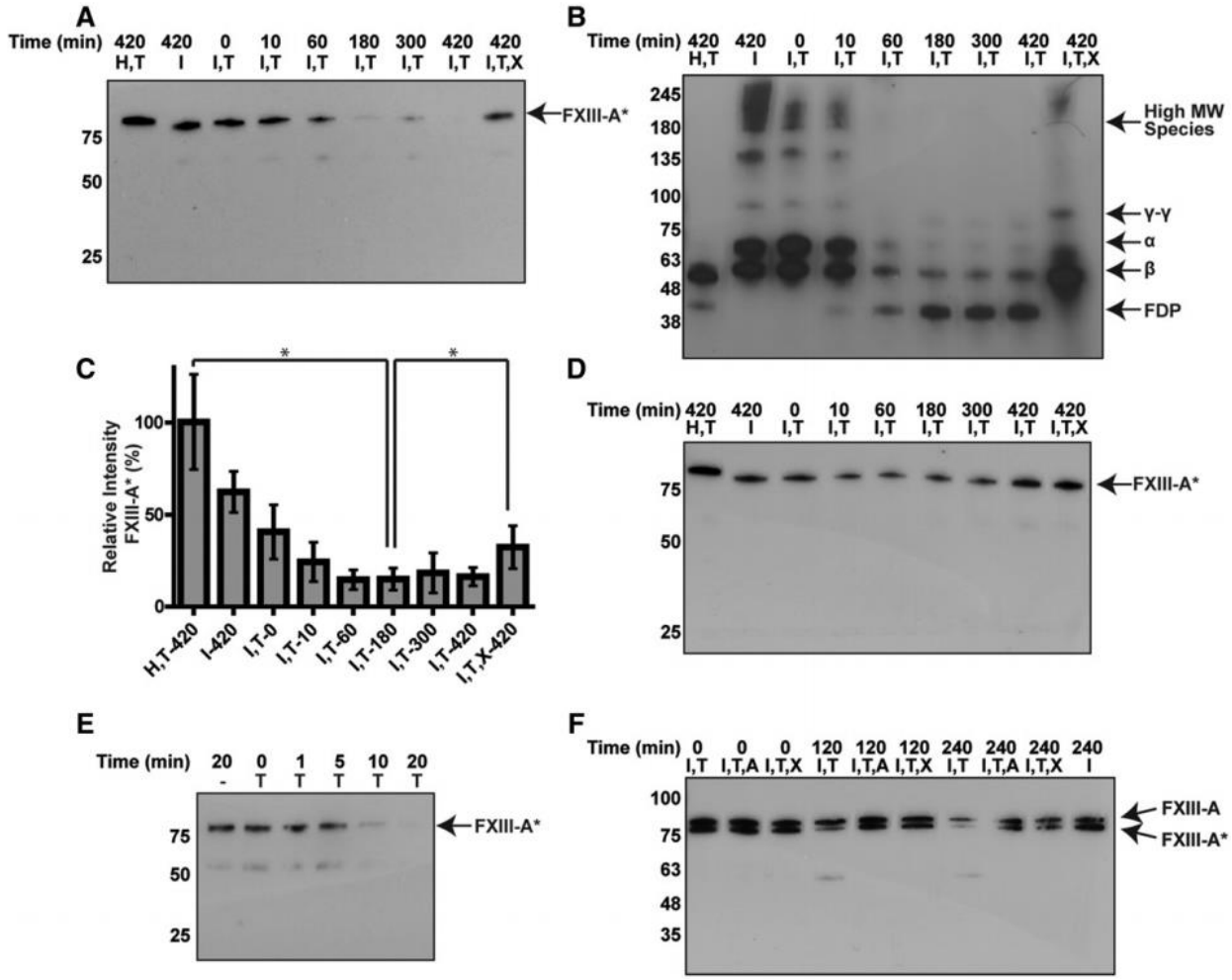

Figure 3.9. Endogenous plasminogen is activated by tPA to degrade endogenous FXIIIa. Plasma was analyzed by Western blot against FXIII-A, after addition of tPA and TXA. (A-B) Time-dependent degradation of endogenous (A) FXIIIa and (B) fibrin(ogen) in normal plasma. (C) The relative amount of intact FXIII-A* (FXIIIa) from panel A using densitometry, calculated as % of total signal in the lane. *$p < 0.05$ (n = 3). (D) Time-course for plasminogen-deficient

plasma (n = 3). (E) Time-dependent degradation of FXIIIa in fibrinogen-deficient plasma following addition of tPA (n = 3). (F) Degradation of endogenous FXIII-A_2* (FXIIIa), but not FXIII-A_2, in whole blood clots with tPA (n = 3). Samples contain combinations of hirudin (H), Innovin (I), tPA (2 μM) (T), TXA (7.5 mM) (X), and α2-antiplasmin (4 μM) (A).

3.4.6 Plasmin-mediated FXIIIa inactivation occurs following fibrinolysis

To further characterize the pFXIIIa degradation by plasmin we examined if degradation occurred during or after clot formation, and if there were downstream effects on fibrin cross-linking. We first used Western blotting to monitor pFXIIIa and fibrin during clot formation. TPA (200 pM) was added to plasma, and clotting was immediately initiated. Only a portion of pFXIIIa was degraded during fibrin formation and cross-linking, indicating that pFXIIIa remained active during clot formation in normal plasma (Figure 3.10A, 3.10B). We then evaluated pFXIIIa activity and its downstream effects using TEG because the mechanical strength (shear elastic modulus, G) of fibrin is closely tied to the activity of pFXIIIa. For these experiments, we utilized plasminogen-deficient plasma (reduced plasmin activity), normal plasma, and α_2-antiplasmin-deficient plasma (increased plasmin activity), all containing tPA (200 pM). No differences in the moduli were observed between clots from the three types of plasma prior to fibrinolysis (Figure 3.10C). The moduli were all ~3-fold higher compared to samples containing an inhibitor of FXIIIa (T101), which does not inhibit the plasmin-mediated degradation of FXIIIa (Figure 3.11). These data indicate that pFXIIIa was not inactivated prior to fibrinolysis.

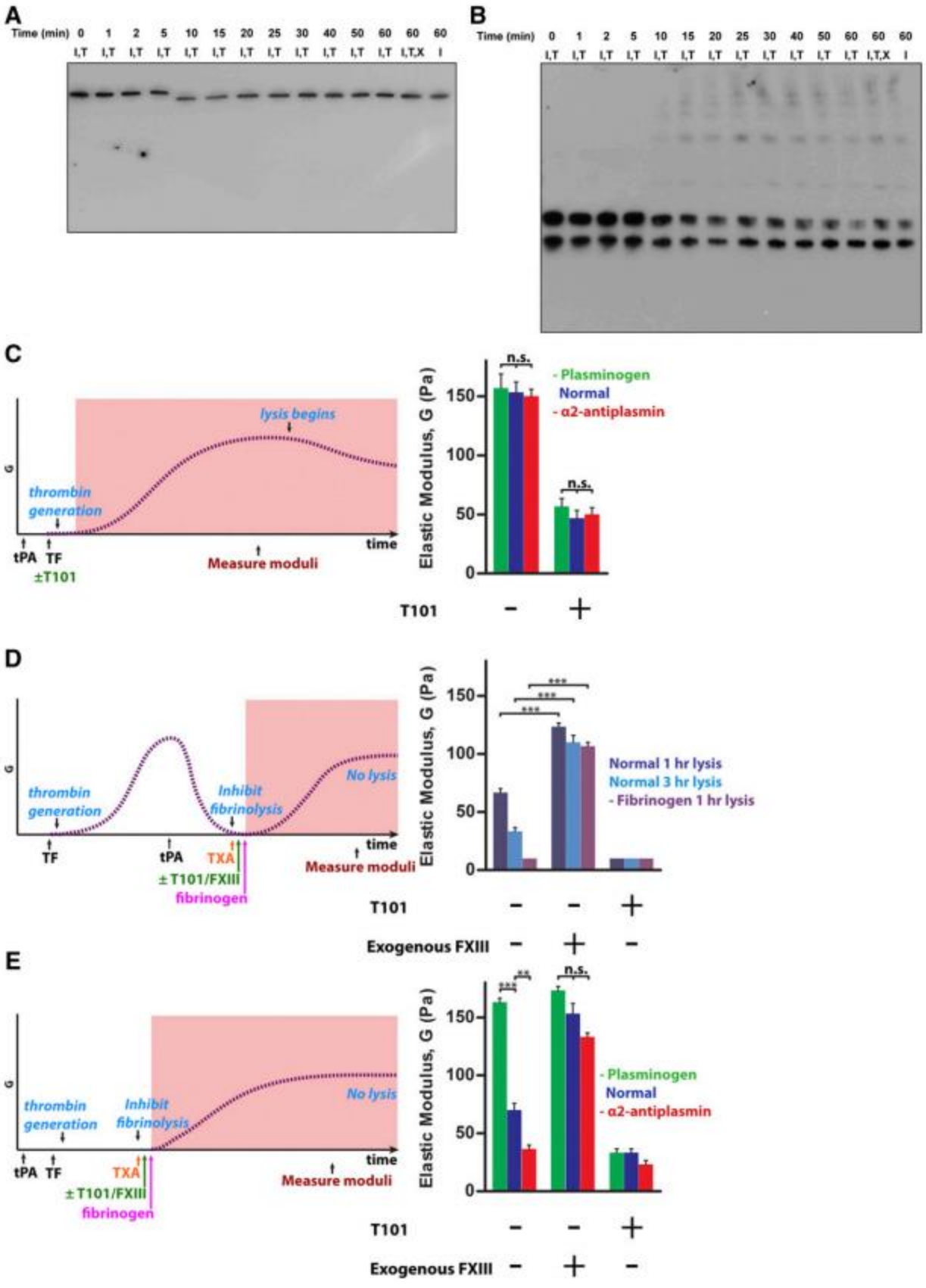
A
Time (min) 0 1 2 5 10 15 20 25 30 40 50 60 60 60
I,T I,T I,T I,T I,T I,T I,T I,T I,T I,T I,T I,T I,T,X I
B
Time (min) 0 1 2 5 10 15 20 25 30 40 50 60 60 60
I,T I,T I,T I,T I,T I,T I,T I,T I,T I,T I,T I,T I,T,X I
C
lysis begins
thrombin generation
G
time
tPA TF
±T101
Measure moduli
n.s.
- Plasminogen
Normal
- α2-antiplasmin
Elastic Modulus, G (Pa)
150
100
50
0
n.s.
T101 - +
D
thrombin generation
Inhibit fibrinolysis
No lysis
G
time
TF
tPA
TXA
±T101/FXIII
fibrinogen
Measure moduli
***
***
***
Normal 1 hr lysis
Normal 3 hr lysis
- Fibrinogen 1 hr lysis
Elastic Modulus, G (Pa)
150
100
50
0
T101 - - +
Exogenous FXIII - + -
E
thrombin generation
Inhibit fibrinolysis
No lysis
G
time
tPA TF
TXA
±T101/FXIII
fibrinogen
Measure moduli
***
**
n.s.
- Plasminogen
Normal
- α2-antiplasmin
Elastic Modulus, G (Pa)
150
100
50
0
T101 - - +
Exogenous FXIII - + -

Figure 3.10. Plasmin-mediated inactivation of FXIIIa does not occur during normal clot formation, but does occur during fibrinolysis and thrombolytic conditions. (A-B) Clot formation in normal plasma with tPA (200 pM) and, in some cases, TXA (7.5 mM). Western blots against (A) FXIII-A and (B) fibrin(ogen) (n = 3). (C-E) TEG analyses of clot formation and cross-linking of exogenous (purified) fibrin. Schematics on the left show timelines of the procedures and characteristic shear elastic moduli (G, dashed lines), with shaded areas indicating time-periods analyzed with TEG. Charts on the right side show measured moduli of fibrin clots, a direct indicator of FXIIIa activity and fibrin structure. Control samples contain exogenous FXIIIa or T101. (C) Moduli of clots from plasminogen deficient, normal, and α2-antiplasmin deficient plasma formed in the presence of tPA (200 pM). (D) Moduli of exogenous fibrin (indicator of residual FXIIIa activity), added following clot lysis. Exogenous fibrinogen (1.4 mg/mL) and TXA were added 1 or 3 hr after clot lysis by tPA (800 nM). (E) Moduli of exogenous fibrin that was added during clot formation under thrombolytic conditions. TXA and then fibrinogen were added 4 min after clotting was initiated in the presence of tPA (50 nM or 5 nM for α2-antiplasmin deficient plasma). Samples contain combinations of Innovin (I), tPA (T), and TXA (X). $^{**}p < 0.01$ $^{***}p < 0.001$, n = 3 for all experiments.

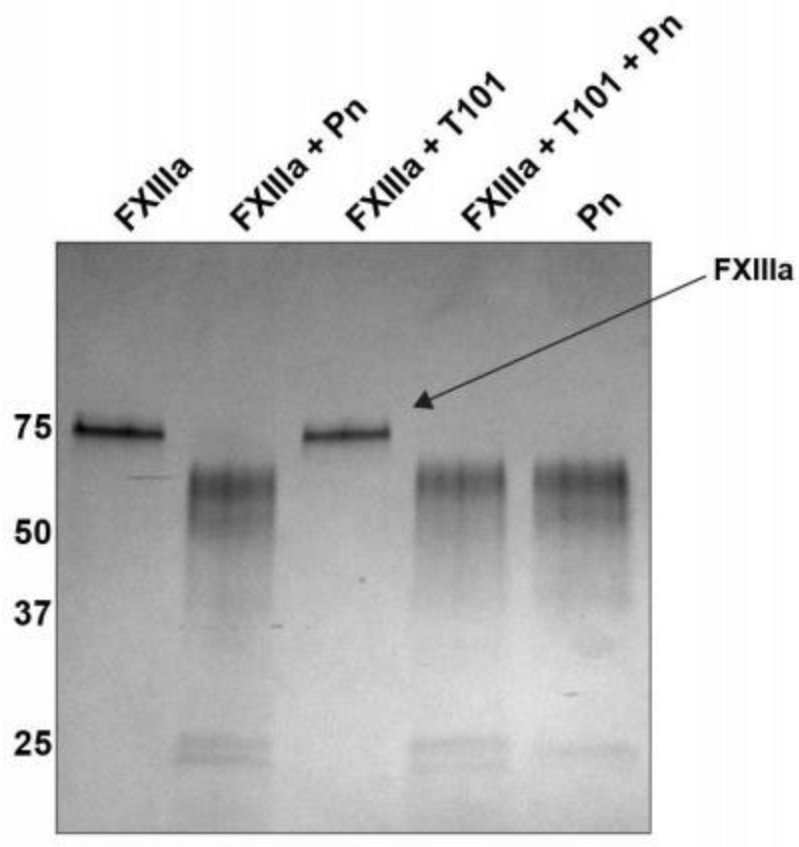

Figure 3.11. T101 does not affect FXIIIa stability. Blue-silver stained gel containing FXIIIa (1.6 μM) and T101 (5 μM), incubated with plasmin (Pn, 1 μM) for 3 hr.

To determine if inactivation occurred during fibrinolysis, normal plasma clots were fully formed and tPA (800 nM) was added to facilitate rapid lysis. The fibrinolytic system was inhibited by TXA at either 1 or 3 hr after addition of tPA and the contribution of residual pFXIII-a to the modulus of exogenous (purified) fibrin was determined. There was 42% and 60% decrease in the moduli at 1 hr and 3 hr, respectively, compared to control samples where fibrin was fully cross-linked with exogenous pFXIIIa (Figure 3.10D). These decreases in moduli indicate that FXIIIa became inactivated during fibrinolysis, and the downstream effect of this inactivation was reduced cross-linking of fibrin. This result is consistent with the Western blots

of degradation of pFXIIIa and fibrin shown in Figure 3.9A-C. Furthermore, in fibrinogen-deficient plasma, at 1 hr into lysis, the modulus of exogenous fibrin was 90% less than when fibrin was fully cross-linked, consistent with Figure 3.9E. The moduli of normal and fibrinogen-deficient plasma were similar when exogenous pFXIIIa was added; this indicates the moduli were dependent primarily on exogenous fibrin rather than residual endogenous fibrin.

3.4.7 Inactivation of pFXIIIa occurs during clot formation under thrombolytic conditions in plasma

Finally, we probed pFXIIIa activity and its downstream effects on fibrin during clot formation under thrombolytic conditions. Prior to clot initiation, thrombolytic levels of tPA were added to plasma with varying plasmin activities. The fibrinolytic system was inhibited 4 min into clot formation by adding TXA. Exogenous fibrinogen was then added and moduli were measured and compared to samples also containing exogenous pFXIIIa or T101. The resulting elastic modulus was 56% less in normal plasma than in plasminogen-deficient plasma (Figure 3.10E). Exogenous pFXIIIa rescued the modulus of normal plasma (bringing it to a similar value as plasminogen-deficient plasma) while it had little effect on plasminogen-deficient plasma. The loss of FXIIIa activity at 4 min was exacerbated in α_2-antiplasmin-deficient plasma, where the modulus was 43% lower than normal plasma and 75% lower than plasminogen-deficient plasma, but could again be rescued by adding exogenous pFXIIIa. Thus, high fibrinolytic activity rapidly prevented pFXIIIa from cross-linking fibrin.

3.5 Discussion

The results show that FXIIIa can be inactivated by plasmin, and that plasmin is selective for FXIIIa, the active enzyme, over FXIII-A_2B_2, the zymogen. The specificity of plasmin for pFXIIIa over pFXIII-A_2B_2 may have confounded earlier reports, which only analyzed pFXIII-

A_2B_2 and cFXIIIa to conclude that FXIII was resistant to degradation [16]. Importantly, degradation of FXIIIa and resistance of FXIII-A_2B_2 were observed in both purified systems and in plasma. Thus, these findings reveal a newly-recognized mechanism that may regulate cross-linking in physiologically-relevant circumstances.

Degradation of FXIIIa in clots occurred within the same time-period as degradation of fibrin. However, the rate of cleavage of FXIIIa in plasma was slower than the estimated half-life of FXIIIa, likely due to the presence of competing substrates such as fibrin [336] and inhibitors of plasmin such as α_2-antiplasmin [337]. Notably, however, during normal clot formation, FXIIIa appeared to reach its full potential in cross-linking fibrin before it was inactivated, but fibrin was not cross-linked when added to reactions following FXIIIa inactivation. Thus, this mechanism may prevent FXIIIa from aberrantly cross-linking fibrin and other proteins in blood vessels.

Interestingly, degradation of platelet-derived cFXIIIa only occurred when plasmin was added 16 hr after platelet activation, but not 1 hr after activation. The slow availability of degradable cFXIIIa may be due to intracellular localization of cFXIII-A_2 and thus inaccessibility by thrombin and plasmin. The initial resistance of cFXIII-A_2 to degradation is consistent with the degradation of plasma FXIII-A_2, which occurred primarily during fibrinolysis. Likewise, a subpopulation of FXIII-A_2 was not readily activated in whole blood, as seen in the blot of Figure 3.9F and this initially spared a portion of the FXIII-A_2, likely cFXIII-A_2, from degradation.

Overall, these data support the notion that FXIIIa is inactivated during fibrinolysis, but not during clot formation. However, we note that these *in vitro* experiments do not rule out the possibility that plasmin may inactivate FXIIIa during clot formation *in vivo.* Moreover, plasmin may not be the sole inhibitor of FXIIIa *in vivo*. FXIIIa can also be cleaved and inhibited by thrombin and polymorphonuclear granulocyte proteases [326, 327]. In our experiments in

plasma, FXIIIa was only degraded in the presence of plasmin, suggesting cleavage of FXIIIa by thrombin may be secondary to that of plasmin. Questions remain regarding whether plasmin and polymorphonuclear granulocyte proteases work in concert or if they inactivate FXIIIa under distinct circumstances. Future studies may reveal additional points of FXIIIa inactivation in certain circumstances *in vivo*.

FXIIIa is at the interface between coagulation and fibrinolysis, and its ability to inhibit fibrinolysis is well-established. The results presented here indicate fibrinolytic enzymes can, in turn, down-regulate FXIIIa. Thus, our findings reveal cross-talk between these pathways that may provide critical information for managing thrombosis and hemostasis [338, 339]. For example, the therapeutic use of plasminogen activators to treat embolic stroke [340] and heart attack [341] may be complicated by the novel discovery of plasmin-mediated inhibition of FXIIIa. Physiologically, tPA is present in the blood at ~70 pM, however; therapeutic tPA is typically administered either intravenously, leading to systemic blood concentrations of ~50 nM [342], or locally into clots from intravascular catheters at ~400 nM [337]. In our experiments, FXIIIa was degraded during clot formation under thrombolytic conditions, at 50 nM of tPA. This mechanism may contribute to hemorrhaging associated with thrombolytic therapy [340]. Notably, side effects of tPA administration resemble the phenotype of patients with FXIII deficiency, where in both cases there is a higher incidence of intracranial hemorrhage than would be expected when compared to other types of hemorrhage [338, 340]. Further research into the relevance of this mechanism in thrombolytic therapy is warranted.

Inhibition of FXIIIa by plasmin may also have implications in diseases where plasmin activity is abnormal, although this still needs to be verified *in vivo.* For example, patients with Quebec Platelet Disorder have elevated urokinase activity and thus are hyperfibrinolytic [343],

suggesting that there may be less FXIIIa activity. In plasminogen deficiency, there may be higher FXIIIa activity, and increased aberrant cross-linking of proteins. In fibrinogen deficiency, degradation of FXIIIa could be enhanced since fibrin is a competing substrate for plasmin [336], or the degradation could be slower since fibrin is a cofactor for fibrinolytic enzymes [344]. We observed the former in both Western blots and TEG, and this rapid inactivation may have implications in congenital fibrinogen deficiency. Thus, these results provide insight into several physiological and pathophysiological scenarios that warrant further investigation.

In conclusion, the experiments show that plasmin preferentially inactivates FXIIIa over FXIII-A_2B_2, and that this mechanism occurs in a wide range of experimental conditions. The downstream effect of fibrinolytic inactivation of FXIIIa is that FXIIIa is no longer able to contribute to cross-linking and retaining the mechanical strength of fibrin. However, to confirm that plasmin-mediated inactivation of FXIIIa plays a major role in thrombosis or hemostasis, additional data from human samples are necessary.

Chapter 4: Coagulation factor XIIIa cross-links amyloid β into dimers and oligomers and to blood proteins

4.1 Contributions

This publication was a collaborative work and published in the *Journal of Biological Chemistry*. W.S.H. designed, performed experiments, analyzed and interpreted the data and wrote the paper. W.S.H. performed experiments to collect data for Figure 4.1A-B, 4.2C-D, 4.3, 4.4, 4.5A, 4.7A and 4.7C-D. N.M. performed experiments for Figure 4.1C, 4.5B-C, 4.6A-C and 4.7B and wrote the paper. I contributed to 40% of this paper. J.B. performed experiments for Figure 4.2A-B. C.J.K. helped design and analyze experiments and write the paper. Collaborators and undergraduate thesis students contributed to other aspects of the paper such as preliminary data collection (D.L., L.S.Y., L.H., J.H.Y, S.F.), and data analysis and editing of the paper (A.S.W. and W.A.J.).

4.2 Introduction

Amyloid-beta (Aβ) is a 4 kDa intrinsically disordered protein that accumulates along the cerebral vasculature during cerebral amyloid angiopathy (CAA). The accumulation of Aβ leads to the degeneration of surrounding cells, and is associated with microhemorrhages [345]. Although CAA is present in over 90% of patients with Alzheimer's disease (AD) [346], the mechanisms underlying Aβ deposition on blood vessels remains unclear.

There are many links between hemostasis and cerebrovascular pathology in AD. Aβ can activate platelets, induce microhemorrhages in the brain, and interact with several coagulation factors [18, 27, 347, 348]. Aggregates of Aβ can activate coagulation factor XII (FXII) to initiate blood clotting, and can increase fibrin density and resistance to fibrinolysis [348, 349]. CAA deposits contain several coagulation factors, and antiplatelet therapy reduces accumulation of

CAA deposits and improves cognitive function in mice [350]. Currently, the biochemical mechanisms that connect intravascular CAA deposition and hemostasis are not clear.

Aβ is formed from the amyloid beta precursor protein (APP), which is expressed by several cells, including platelets, neurons, glial cells and astrocytes. Platelets account for 95% of circulating APP [21]. APP can be cleaved to generate Aβ peptides of typically 40 or 42 residues long, Aβ40 and Aβ42, respectively. Platelets cleave APP and release both Aβ40 and Aβ42 when they are activated [19]. In both blood and CAA deposits, Aβ40 is more abundant than Aβ42, whereas Aβ42 is more abundant in senile plaques within the brain parenchyma, which is a hallmark of AD [351]. Mutations within the Aβ sequence can alter the pathogenicity of the peptide; for example, patients with the Flemish or Italian mutation (A21G and E22K, respectively) have increased CAA deposits, while patients with the Arctic mutation (E22G) have more plaque burden [352-356]. Aβ40 and Aβ42 can spontaneously aggregate into small, non-covalent oligomers and subsequently large aggregates, both of which are toxic to surrounding cells [357].

The formation of protein aggregates in CAA and AD may be regulated in part by transglutaminases (TG). TGs are a family of enzymes that form ε-(γ-glutamyl) lysyl isopeptide bonds between their substrates, creating irreversible bonds. TG activity co-localizes with plaques in brains in AD [18]. Tissue transglutaminase 2 (TG2) can induce Aβ oligomerization and aggregation *in vitro* and reduce its clearance [358]. However, it is unknown if activated coagulation factor XIIIa (FXIIIa), a transglutaminase in blood plasma and on platelets, can cross-link Aβ in blood. FXIIIa is formed from coagulation factor XIII (FXIII), a protransglutaminase, when it is activated by thrombin in the presence of calcium during blood clotting [12]. The primary function of FXIIIa is cross-linking fibrin to itself and to other proteins to stabilize blood

clots from premature fibrinolysis. FXIIIa also increases clot stiffness and platelet adhesion to further reduce blood loss.

Aβ forms stable complexes with FXIIIa and co-localizes with FXIIIa and fibrin in CAA deposits of AD patients [18]. Because Aβ is a substrate for TG2 and influences hemostasis in several ways [358], we tested if Aβ is a substrate for FXIIIa, and found that it is.

4.3 Methods

4.3.1 Platelet preparation

This study was approved by the research ethics board of the University of British Columbia (H12-01516), and written informed consent was obtained from all healthy volunteers in accordance with the Declaration of Helsinki. Platelets and PRP were isolated as previously described [359]. Platelets were resuspended in Tyrode's buffer (119 mM NaCl, 5 mM KCl, 25 mM HEPES, 2 mM $CaCl_2$, 2 mM $MgCl_2$, 6 g/L glucose, pH 6.5) or in plasma at a final concentration of 2 x 10^9 platelets/mL or as otherwise specified.

4.3.2 Cross-linking of Aβ

Aβ peptides (Anaspec, California, USA) were initially dissolved in dimethylsulphoxide at 20 mg/ml and diluted with 25 mM HEPES buffer to 1 mg/ml. To test if Aβ is cross-linked by purified FXIIIa, Aβ (25 μM) was incubated with purified FXIIIa (200 nM, Haematologic Technologies, Vermont, USA), $CaCl_2$ (4 mM), dithiothreitol (DDT, 200 μM), human thrombin (70 nM, Haematologic Technologies Vermont, USA) and T101 (2.5 mM, Zedira GambH, Germany) or Z006 (2.5 mM, Zedira GambH, Germany) at 37°C for 16 hr. To test if Aβ is cross-linked to other proteins, human normal plasma (Affinity Biologicals, Ontario, Canada) or purified fibrinogen (6 mM, Haematologic Technologies, Vermont, USA) was incubated with Aβ (25 μM), $CaCl_2$ (4 mM) and tissue factor (TF, 1 pM, Dade Behring, Illinois, USA) or human

thrombin (70 nM) at 37°C. The samples were treated with a reaction-quenching buffer (8 M Urea, 50 mM DTT, 12.5 EDTA) for at least 1 hr at 60°C to dissolve the clot. To test if Aβ was cross-linked to platelet proteins, platelets were incubated with Aβ40 (25 μM), $CaCl_2$ (4 mM), and human thrombin (70 nM), ADP (50 μM), rat tail collagen (10 nM, Sigma, Germany), EDTA (12.5 mM) or T101 (2.5 mM).

4.3.3 Western blotting

Samples were reduced, boiled, and separated on 10% or 4-15% Tris-glycine gradient gels (Bio-Rad, California, USA). After electrophoresis, the samples were transferred to a nitrocellulose membrane (GE Healthcare, Illinois, USA) and blocked with Odyssey Blocking Buffer (Li-Cor, Nebraska, USA). The membranes were treated with a primary antibody against Aβ (1:1000; 6E10, Covance, New Jersey, USA), FXIII-A (1:1000; SAF13A-AP, Affinity Biologicals, Ontario, Canada) or fibrin (1:50 000; A0080, Dako, California, USA), washed, and treated with HRP-labeled anti-host secondary antibody (1:15 000; Abcam, Cambridge, UK).

4.3.4 Kinetic assay

The rate of cross-linking of Aβ was determined by measuring the rate at which ammonia was produced during the TG reaction, using steady state kinetics at 37°C. A calibration curve of ammonia concentration and absorbance at 570 nm was determined with a Tecan M200 plate reader (BioVision Inc., California, USA). FXIIIa was mixed with Aβ peptides or GOE (5 – 50 μM) as amine donors, a glutamine-containing peptide (NQEQVSPLTLLK, 1 mM), DTT (40 μM), and $CaCl_2$ (3 mM). Aliquots from the transglutaminase reaction mixture were removed and quenched every 15 min with EDTA (15 mM). Kinetic parameters were calculated using graphing software (OriginPro 9.1).

4.3.5 Microfluidic analysis

Microfluidic devices were prepared from polydimethylsiloxane (PDMS) as previously described [360]. The channels were coated with lipid vesicles containing TF, phosphatidylserine (PS) and phosphatidylcholine (PC), while the rest of the device was coated with inert PC vesicles. The vesicles were prepared and devices were coated as previously described [361]. Citrated PRP containing fluorescent Aβ40-TAMRA (100 μg/mL, Anaspec) and fluorescent α-CD42b-FITC antibodies (1:100, eBioscience, California, USA) with or without T101 (500 μM) was flowed into the device at 1 μL/min along with a calcium-saline solution (40 mM $CaCl_2$, 90 mM NaCl) at a rate of 0.33 μL/min, which corresponds to venous shear rates (20 s^{-1}). Clotting was monitored using an epifluorescence microscope (Leica DMI6000B). The clots were then washed with calcium-saline solution (40 mM $CaCl_2$, 90 mM NaCl) at a rate of 5 μL/min for 10 min and imaged. For statistical analysis, fluorescence intensities were measured at five equally distributed locations along the length of the channel.

4.3.6 Thromboelastography

The shear elastic moduli were evaluated at 37°C using a TEG Hemostasis Analyzer System 5000 (Haemoscope Corporation, Massachusetts, USA). Citrated whole blood, PRP, or PPP (Affinity Biologicals, Ontario, Canada) was combined with $CaCl_2$ (10 mM) and thrombin (200 nM), with or without Aβ40 (15 μM), T101 (800 μM), or eptifibatide (1.4 mM, Sigma, Germany) over 3 hr.

4.3.7 Statistical evaluation

Statistical analyses were performed using GraphPad Prism 7.0. All results presented in graphs are the mean ± standard error of the mean (SEM). N indicates number of independent

experiments, performed on separate days. A 2-tailed unpaired Student's t test was used for all analyses. Significance was designated at p values <0.05.

4.4 Results

4.4.1 Aβ40 is a substrate of FXIIIa

To test if Aβ could be covalently cross-linked by FXIIIa, Aβ was incubated with FXIIIa and changes in molecular weights were detected using Western blot. FXIIIa cross-linked monomeric Aβ40 into dimers and oligomers, and to FXIIIa itself (Figure 4.1A). Cross-linked Aβ oligomers did not form when FXIIIa was inhibited by chelating calcium ions with EDTA or with T101, an irreversible inhibitor of FXIIIa transglutaminase activity. However, with T101, there was a distinct band near 85 kDa, corresponding to the molecular weight of FXIIIa attached to Aβ40, which has been previously reported [18]. Similar trends were observed with Aβ42, although low concentrations of SDS-resistant oligomers formed without FXIIIa. When the only glutamine of Aβ40 was mutated to asparagine (Aβ40 Q15N), FXIIIa did not generate Aβ oligomers, indicating that the oligomerization was dependent on the glutamine residue of Aβ40.

To determine the kinetic constants of FXIIIa-mediated Aβ cross-linking, the release of ammonia, a product of the transglutaminase reaction (Figure 4.1B), was measured using a photometric assay. FXIIIa-mediated cross-linking of Aβ40 had K_m of 8.5 ±1.2 μM and k_{cat} of 1.3 ± 0.5 s^{-1}, resulting in a catalytic efficiency of 1.5 ± 0.5 x10^5 $M^{-1}s^{-1}$. A small molecule substrate of FXIIIa, glycine ethyl ester (GOE), had a similar catalytic efficiency of 2.0 ± 0.7 x10^5 $M^{-1}s^{-1}$ (Figure 4.1C). The catalytic efficiency of a peptide with the Aβ40 residues scrambled had 10-fold lower catalytic efficiency, indicating that the sequence of Aβ40 is important for FXIIIa activity. We were not able to calculate the catalytic efficiency of Aβ42 because Aβ42 precipitated at the concentrations necessary to perform the assay.

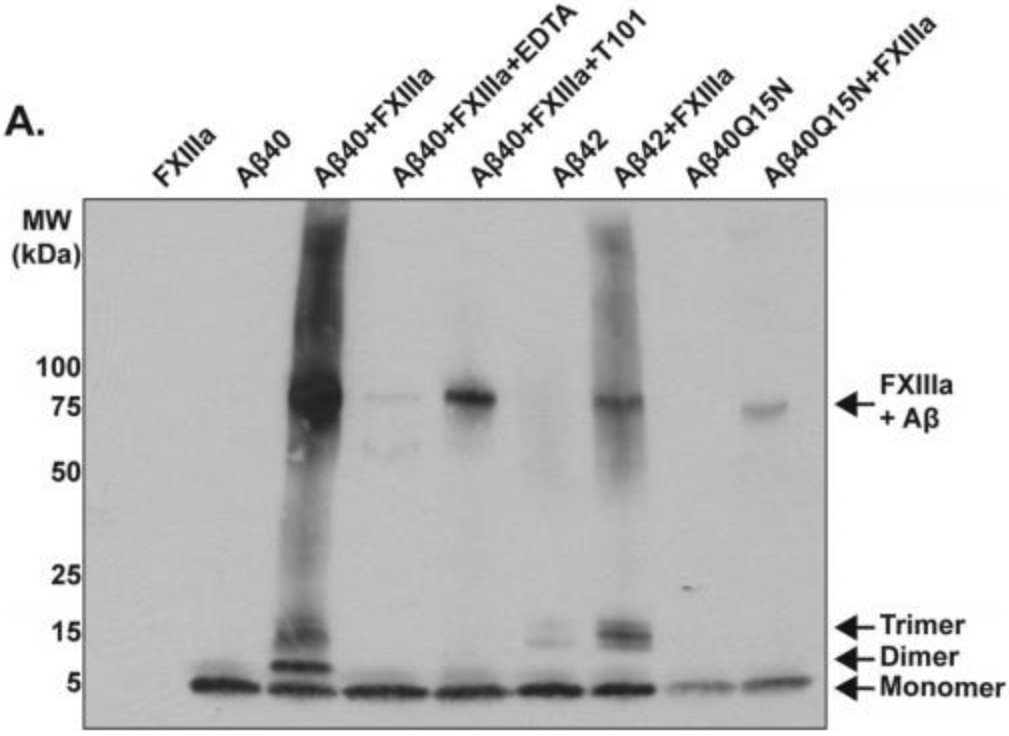

B.

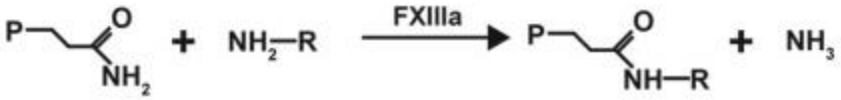

C.

Substrate	K_m (μM)	k_{cat} (s^{-1})	k_{cat}/K_m ($M^{-1}s^{-1}$)
GOE	4.3±2.4	0.8±0.2	2.0±0.7 x 10^5
Aβ40	8.5±1.2	1.3±0.5	1.5±0.5 x 10^5
Aβ40 Scrambled	10.9±0.3	0.23±0.1	2.1±0.1 x 10^4
Aβ42	N.D.	N.D.	N.D.

Figure 4.1. Factor XIIIa can covalently cross-link Aβ. (A) Western Blot against Aβ, after Aβ40, 42 or Q15N with or without EDTA or T101 were incubated with FXIIIa. (B) The transglutaminase reaction by FXIIIa. P indicates a protein or peptide containing a glutamine residue. R indicates a small molecule, peptide or protein with a primary amine, such as a lysine. (C) Table of kinetic parameters for FXIIIa cross-linking Aβ40 and 42. GOE: glycyl ethyl ester. N.D.: Not determined. n = 3.

4.4.2 FXIIIa covalently cross-linked Aβ40 to fibrin

Aβ can bind to many proteins in blood, such as FXII, FXIII, and fibrinogen [347-349]. To test if Aβ40 could be covalently cross-linked to other blood proteins, plasma containing Aβ40 was clotted, separated by SDS-PAGE, and immunoblotted against Aβ. Within 10 min, distinct Aβ bands were visible around 50 kDa, 70 kDa, and 100k kDa, and much higher molecular weights (Figure 4.2A). The molecular weights of these bands were similar to those of the α and γ chains of fibrin, the main substrates of FXIIIa. Bands with similar molecular weights as fibrin were visible after the γ-γ dimers were formed (Figure 4.2B). Aβ was still cross-linked when an inhibitor of TG2 (Z006) [186] was added to plasma, but not when T101 was added, indicating that FXIIIa, not TG2, cross-linked Aβ (Figure 4.3). To confirm that Aβ40 was cross-linked directly to fibrin, Aβ40 was incubated with purified fibrinogen, FXIIIa, and thrombin. Bands of Aβ were visible around 50 kDa, 70 kDa and 100 kDa, correlating to the molecular weights of the α and γ chains of fibrin and cross-linked γ-γ dimers (Figure 4.2C and 4.2D). Aβ40 was cross-linked to fibrin chains faster than to itself. Aβ40 was not cross-linked to fibrin chains when FXIIIa was inhibited with T101. Lower concentrations of Aβ40 (1 μM) also cross-linked to both purified and plasmatic fibrin by FXIIIa (Figure 4.4).

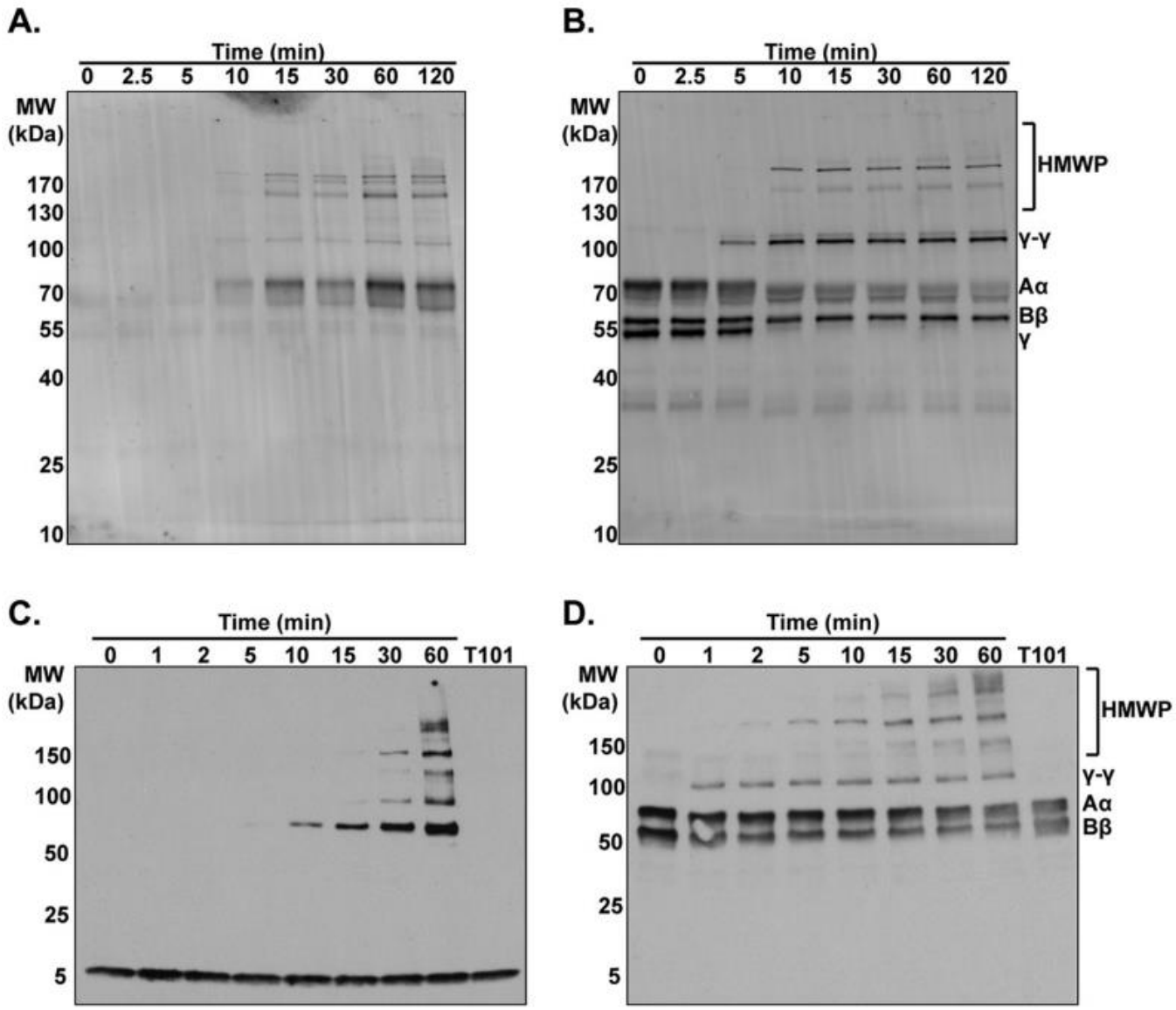

Figure 4.2. Aβ40 is cross-linked to fibrin during clotting. (A-B) Western blot against Aβ (A) and fibrin(ogen) (B) after Aβ40 and tissue factor were added to recalcified plasma. (C-D) Western blot against Aβ40 (C) and fibrin(ogen) (D) after Aβ40 were incubated with fibrinogen, FXIIIa, thrombin, and $CaCl_2$. HMWP: High molecular weight polymers. Aα: α-chain of fibrinogen. Bβ: β-chain of fibrinogen, γ: γ-chain of fibrinogen, γ-γ: γ-dimers of fibrinogen.

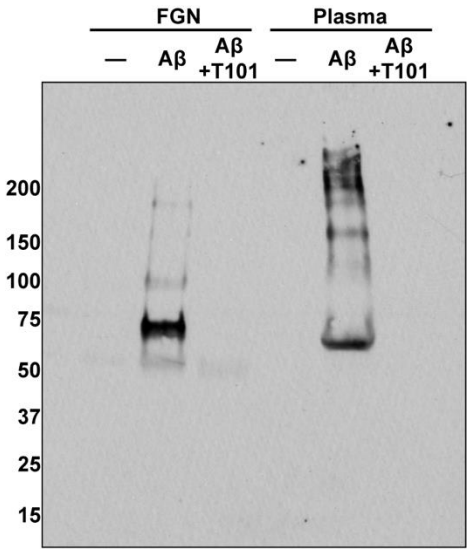

Figure 4.3. Aβ40 is cross-linked in plasma. (A-B) Western blot against Aβ (A) and fibrin(ogen) (B) after Aβ40 and tissue factor were added to plasma containing T101 (inhibitor of FXIIIa and TG2) or Z006 (inhibitor of TG2). HMWP: High molecular weight polymers; FGN, fibrinogen.

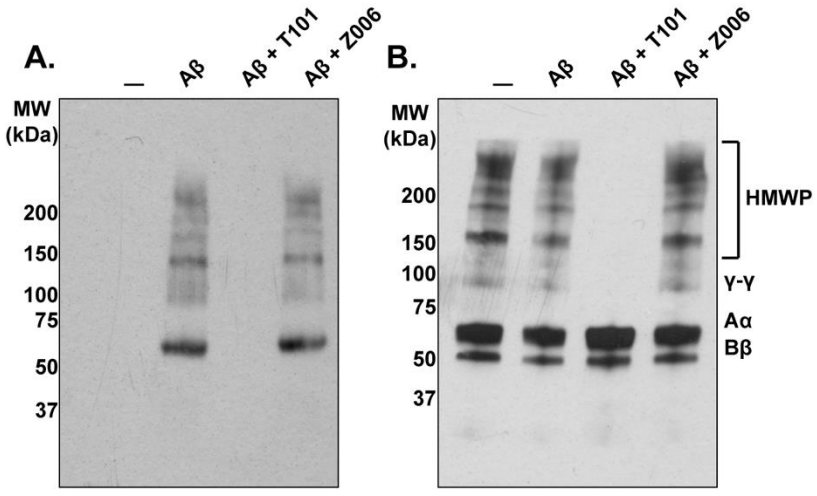

Figure 4.4. Aβ40 is cross-linked to fibrin. Western blot against Aβ after 1 μM of Aβ40 was incubated with fibrinogen, FXIIIa, thrombin, and $CaCl_2$, or in plasma activated with tissue factor.

4.4.3 FXIIIa cross-linked Aβ40 to platelet proteins under flow

Since platelets contain the FXIII-A subunits, which can be activated by high concentrations of Ca^{2+}, Aβ40 was incubated with platelets to test if platelet-derived FXIIIa could cross-link Aβ40 to itself or to other proteins. When platelets were activated with adenosine diphosphate (ADP), collagen, or thrombin, different patterns of Aβ cross-linking were detected compared to when platelets were not activated (Figure 4.5A). The Aβ bands formed with platelets had higher molecular weights than Aβ dimers and trimers, suggesting Aβ was cross-linked to platelet proteins. Both EDTA, which chelates the Ca^{2+} required for FXIIIa activity and platelet activation, and T101 prevented Aβ oligomers from forming. In contrast, Z006 did not prevent Aβ oligomers from forming, indicating that FXIIIa, not TG2, is responsible for cross-linking Aβ in platelets.

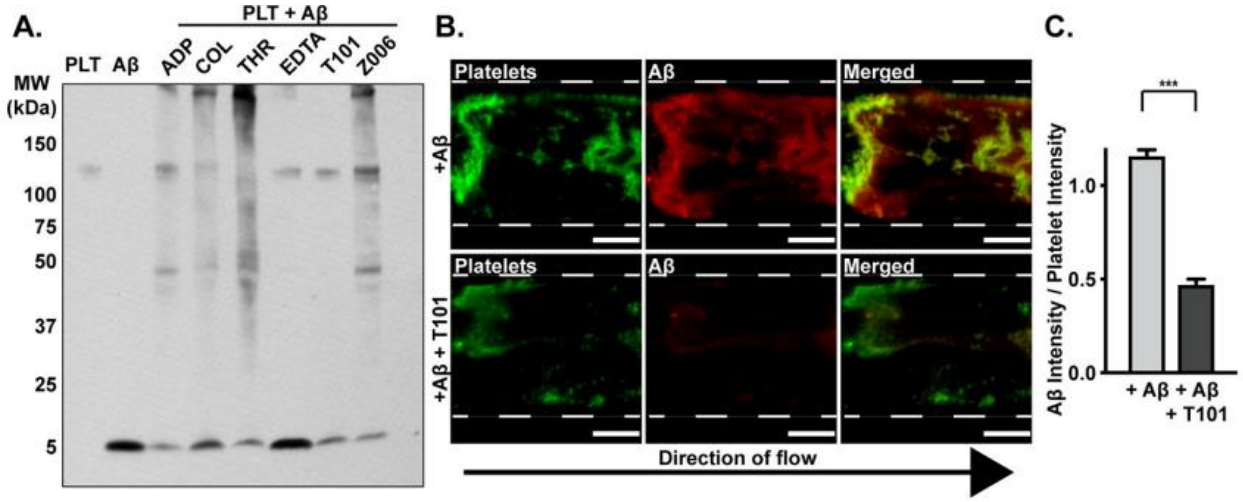

Figure 4.5. Platelet FXIIIa cross-links Aβ40 to platelet proteins and localizes Aβ to blood clots under flow. (A) Western blot against Aβ, after Aβ40 was incubated with platelets. PLT: platelets, ADP: adenosine diphosphate, COL: collagen, THR: thrombin. (B) Platelet-rich plasma (platelets stained green with α-CD42b-FITC antibody) containing Aβ40-TAMRA (red) with or

without T101 was flowed through a channel containing a tissue factor-coated region. Scale bar: 200 μm. (C) Graph quantifying Figure 3the co-localization of Aβ40 and platelets in images in panel B. ****P < 0.001*. Error bars indicate ± SEM. n = 3.

To test whether FXIIIa cross-links Aβ40 to blood clots formed under flow, plasma containing platelets and fluorescently-tagged Aβ40 were flowed through a microfluidic device. Aβ40 accumulated on the clot, and co-localized directly on platelet aggregates and fibrin fibers. The co-localization of Aβ40 with platelets, measured by the ratio of Aβ40 fluorescence to platelet fluorescence, was significantly decreased when T101 was added, indicating that FXIIIa can cross-link Aβ40 to blood clots under flow (Figure 4.5B and 4.5C).

4.4.4 Aβ40 increases clot stiffness of PRP and PPP via FXIIIa

Since cross-linking increases fibrin stiffness [12], we tested the effect of Aβ40 on fibrin clot stiffness using thromboelastography (TEG). When whole blood was clotted in the presence of Aβ40, no significant difference in clot stiffness was observed (Fig. 4A). Since the contribution of red blood cells may have masked subtle differences of Aβ on clot stiffness, we tested if the influence of Aβ40 on fibrin could be detected when red blood cells were removed [362]. Aβ40 increased the stiffness of clots formed in platelet-rich plasma (PRP) and platelet-poor plasma (PPP) by 27% and 39%, respectively (Fig. 4B and 4C). The increase in clot stiffness was dependent on both cross-linking by FXIIIa and platelet-platelet interactions, since inhibitors of FXIIIa (T101) or integrin $\alpha II_b\beta_3$ (eptifibatide) abrogated the increase of clot stiffness induced by Aβ40.

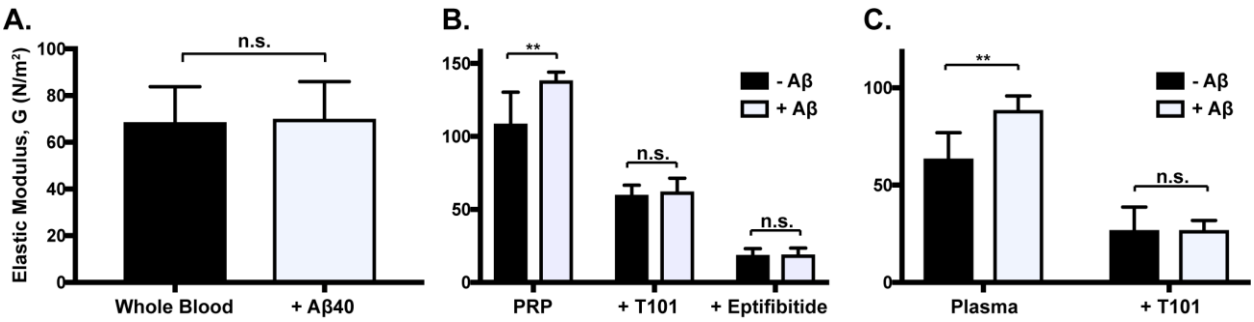

Figure 4.6. Aβ40 increases stiffness of platelet-rich plasma clots and platelet-poor plasma clots in a FXIIIa-dependent manner. Thromboelastography analysis of blood and blood fractions with and without Aβ40 is shown. (A) Moduli of whole blood clots. (B) Moduli of platelet-rich plasma clots with or without T101 or eptifibatide (platelet aggregation inhibitor). (C) Moduli of platelet-poor plasma clots with and without T101. ***P < 0.01*. n.s. indicates no significance. Error bars indicate ± SEM. PRP: platelet-rich plasma. n = 5-9 for all experiments.

4.4.5 Aβ40 mutants are differentially cross-linked by FXIIIa

Certain point mutations of Aβ increase the probability of developing CAA [352-356]. To test whether FXIIIa cross-links mutants of Aβ40, FXIIIa was incubated with Aβ40 containing Arctic (E22G), Italian (E22K), Iowa (D23N), Dutch (E22Q), Flemish (A21G) or Iowa/Dutch (E22Q/D23N) mutations. Oligomerization occurred in some mutants even in the absence of FXIIIa, which is consistent with the high propensity of these mutants to aggregate. However, when the mutants were incubated with FXIIIa, different species of Aβ oligomers were formed in varying concentrations. For example, the Flemish mutation (A21G) was cross-linked to a greater extent than WT, while the Iowa/Dutch mutation (E22Q/D23N) was cross-linked to a lesser extent (Figure 4.7A). The catalytic efficiencies of these mutant Aβ40 sequences were lower than, or comparable to, the catalytic efficiency of WT Aβ40 (Figure 4.7B). The Flemish mutation was cross-linked to fibrin to a greater extent than WT (Figure 4.7C and 4.7D).

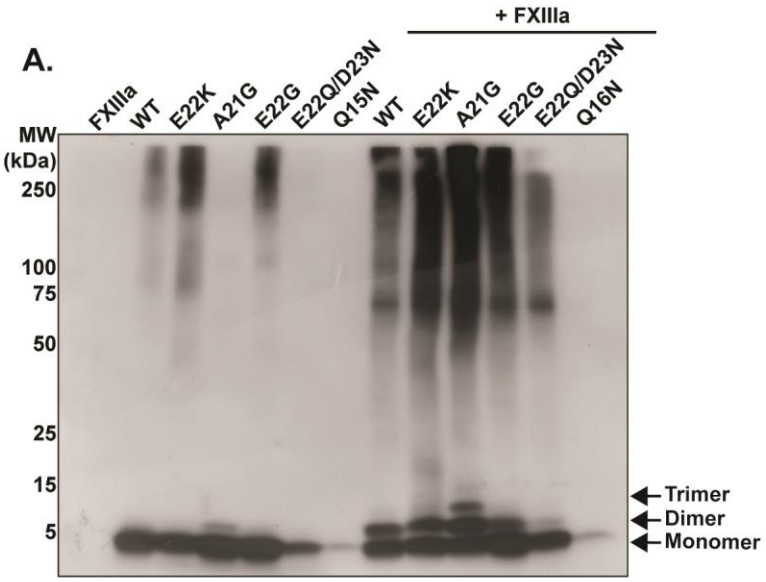

B.

Substrate	Mutation	K_m (μM)	k_{cat} (s^{-1})	k_{cat}/K_m ($M^{-1}s^{-1}$)
WT	-	8.5±1.2	1.3±0.5	1.5±0.5 x 10^5
Artic	E22G	5.4±1.0	0.52±0.03	1.0±2.4 x 10^5
Italian	E22K	13.3±2.8	0.84±0.03	6.5±1.1 x 10^4
Iowa	D23N	20.4	0.58	2.9 x 10^5
Dutch	E22Q	21.4±14.3	0.23±0.3	2.1±1.6 x 10^5
Flemish	A21G	25.6±2.6	0.43±0.05	1.7±0.1 x 10^5
Iowa/Dutch	E22Q/D23N	B.D.	B.D.	B.D.

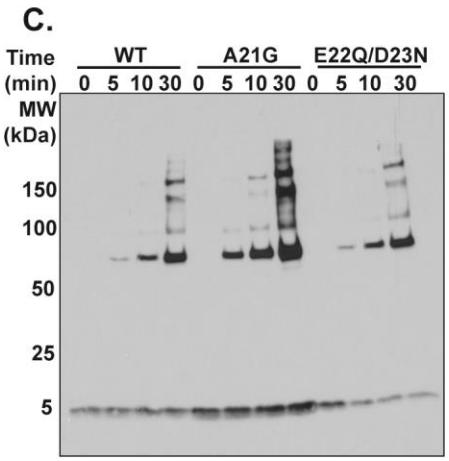

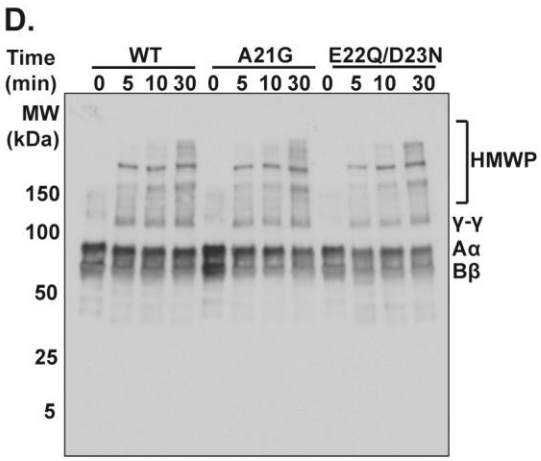

Figure 4.7. FXIIIa differentially cross-links mutant Aβ40 peptides. (A) Western blot against Aβ, after Aβ40 and mutants of Aβ40 were incubated with FXIIIa. (B) Table of kinetic parameters for FXIIIa cross-linking Aβ40 mutants, measured by the rate of ammonia release. WT: Wild type, B.D.: Below detection n = 3. (C-D) Western blot against Aβ40 (C) and fibrin(ogen) (D) after Aβ40 WT, Aβ40 A21G (Flemish) or Aβ40 E22Q/D23N (Iowa/Dutch) were incubated with fibrinogen, FXIIIa, thrombin, and $CaCl_2$. HMWP: High molecular weight polymers. Aα: α-chain of fibrinogen. Bβ: β-chain of fibrinogen, γ: γ-chain of fibrinogen, γ-γ: γ-dimers of fibrinogen.

4.5 Discussion

The results show that Aβ40 is covalently cross-linked by FXIIIa, both to itself to form dimers and oligomers, and also to other blood proteins in plasma, such as fibrin. FXIIIa also cross-linked Aβ40 to clots under flow, and the cross-linking of Aβ40 increased clot stiffnesses in PRP and PPP, but not in whole blood. Although the reaction occurs *in vitro*, the physiological relevance and significance of these reactions *in vivo* must be further investigated.

The cross-linking of Aβ40 to fibrin chains was visible only after the γ-γ dimers were formed. This is consistent with the kinetic data, where the catalytic efficiency of FXIIIa and Aβ ($k_{cat}/K_m = 1.5 \pm 0.5 \times 10^5\ M^{-1}s^{-1}$) was lower than that of fibrin γ-chains ($5.1 \times 10^7\ M^{-1}s^{-1}$) [363]. Aβ was cross-linked to fibrin at an Aβ concentration of 1 μM, which is a concentration that may occur at sites of cerebrovascular damage [364].

The cross-linking of Aβ may potentially be influenced by Aβ-albumin interactions. Albumin sequesters approximately 90% of Aβ in plasma and preferentially binds oligomeric Aβ to monomeric Aβ [365, 366]. FXIIIa cross-linked Aβ to fibrin both in buffer and in plasma at

similar rates, suggesting that albumin does not play a significant role in influencing the rate of cross-linking in these conditions. However, how albumin affects the clearance of cross-linked oligmeric Aβ requires further examination.

Aβ and FXIIIa can form stable complexes *in vitro*, and FXIIIa is catalytically active in vessels with CAA [18]. Although isopeptide bonds formed by transglutaminases have been discovered in CAA, covalent cross-linking of Aβ by FXIIIa was not previously detected *ex vivo* [18]. The discrepancy with the data here may be due to the higher, though physiological, FXIIIa concentrations and longer reaction times used here, and potentially higher specific activity of FXIIIa. Although the cross-linking of Aβ to itself was visible only after 3 hr, cross-linking to fibrin occurred within minutes.

Cross-linking of Aβ may have implications in at least two scenarios. First, Aβ may modify clot structure at sites of damage in the cerebral vasculature or at platelet aggregates. It remains to be determined what the effect on clotting might be, but it may contribute to fibrinolysis since non-crosslinked aggregates of Aβ increase resistance to fibrinolysis and activate the coagulation cascade through FXII [348, 367]. Cross-linking Aβ to fibrin could enhance clotting by localizing the platelet activating sequence (Aβ25-35) to fibrin [27]. Cross-linking of Aβ may have a greater significance in arteries than veins, as arterial clots have fewer red blood cells, since Aβ increased the stiffness of PRP, but not whole blood clots.

Second, FXIIIa-mediated activity may contribute to CAA and AD pathology. Given that blocking the binding between Aβ and fibrin with a small molecule can improve cognitive impairment in mouse models of AD, covalent cross-linking of Aβ and fibrin may exacerbate CAA pathology [367]. In patients with AD, there is a higher frequency of a FXIII allele (Val-34-Leu) that undergoes faster activation, suggesting that accelerated cross-linking can aggravate AD

development [368]. The differences in cross-linking between the Aβ variants and mutants provides further insight to the potential significance of the interaction between FXIIIa and Aβ. FXIIIa cross-linked Aβ40 to a higher extent than Aβ42, providing a potential explanation as to why Aβ40 is the more prominent form of Aβ within CAA. AD patients with the Flemish mutation (Aβ40 A21G) have increased CAA phenotype and Aβ40 with the Flemish mutation was cross-linked to a higher extent compared to wild type Aβ40 [357]. An alternative hypothesis is that cross-linking of Aβ by FXIIIa is a physiological process that is separate from aggregation and amyloid accumulation.

In conclusion, synthetic Aβ40 can be covalently cross-linked to itself, and to fibrin and platelet proteins by FXIIIa under flow. Given that Aβ and FXIIIa co-localize within CAA, these results provide motivation to test if FXIIIa contributes to the accumulation of intravascular deposits of Aβ in CAA.

Chapter 5: Post-translational modifications of platelet-derived amyloid precursor protein regulated by transglutaminase coagulation factor XIIIa

5.1 Contributions

This research was a collaborative project with the manuscript currently being prepared to submit to *Journal of Biological Chemistry*. W.S.H. designed, performed experiments, analyzed and interpreted the data and wrote the paper. W.S.H. performed experiments to collect data for Figure 5.1A-C, 5.2A, 5.2C-F, and 5.4A-C. N.M. performed experiments for Figure 5.2B and 5.3A-D and edited the paper. L.J.J. is assisted in performing experiments to supplement Figure 5.4A-C I contributed to 40% of this paper. C.J.K. and W.A.J. helped design and analyze experiments and write the paper.

5.2 Introduction

The amyloid beta precursor protein (APP) is a type 1 transmembrane protein that can be proteolytically processed to generate several metabolites including amyloid beta peptides (Aβ) [20]. Aβ contributes to the pathology of Alzheimer's disease through the formation of protein aggregates and insoluble deposits in the brain and in the cerebrovasculature [27]. APP is expressed in a variety of cells, including platelets, astrocytes, glial cells and neurons [20]. Over 90% of circulating APP and Aβ originates from platelets, but the contribution of blood-derived APP and Aβ to cerebral amyloid angiopathy and Alzheimer's disease remains unclear. Understanding the function and regulation of blood-derived APP and Aβ may provide insight into these conditions.

APP is highly expressed in platelets, with over 9300 molecules of APP per platelet [21]. Platelets store APP and its metabolites both on the cell surface and in α granules. Upon platelet activation, APP can be proteolytically cleaved by secretases expressed in platelets and secreted

as various proteolytic metabolites, including soluble forms of APP (sAPPα and sAPPβ) and Aβ [22]. In the brain, the function of APP is associated with cell adhesion, cell communication and synaptic plasticity, but the function is less clear in platelets [369, 370]. Since platelets are integral to hemostasis, the contribution of APP to hemostasis has been investigated. APP knockout mice do not exhibit spontaneous bleeding or thrombosis. Platelets from APP KO mice exhibit normal aggregation, secretion and αIIbβ3 signalling [30]. Thus, platelet-derived APP does not appear to be a major contributor to physiological hemostasis, and its physiological function in platelets remains elusive. However, APP and its metabolites can elicit both pro- and anti-coagulant effects by interacting with several coagulation factors, including coagulation factors VII, IX, X, XI, XII and XIII (FXIII) and fibrin(ogen) [18, 347-349]. Aβ promotes thrombin generation via FXII activation, and can directly induce platelet activation, aggregation and thrombus formation *in vitro*. Fibrillar Aβ stabilizes clots by preventing the binding of fibrinolytic proteins to fibrin. In contrast, APP in platelets can reduce the size of venous thromboemboli in mice through its Kunitz-type proteinase inhibitor domain [30].

Plasma FXIII is a heterotetrameric proenzyme, containing both a dimer of the zymogen A subunits (FXIII-A) and a dimer of the regulatory B subunits (FXIII-B), while platelet FXIII only consists of the catalytic A subunit dimer [12]. When thrombin cleaves plasma FXIII, or when platelets are activated, the A subunit undergoes a conformational change to be catalytically active (FXIIIa). Although the role of platelet FXIII in hemostasis is less clear than plasma FXIII, platelet FXIII contributes to platelet motility, clot retraction and to fibrinolysis [371, 372]. FXIII-A in resting platelets is localized in the cytoplasm, but upon platelet activation translocates to the cell surface where it is catalytically active [372]. The exposure of FXIIIa on the activated platelet surface contributes to post-translational modifications of platelet proteins, including covalent

attachment of serotonin to secreted and membrane proteins [186]. However, it is not known if FXIIIa modifies APP. Because FXIIIa binds to and crosslinks Aβ to itself and to fibrin [18, 23], we tested if FXIIIa binds to and crosslinks APP.

5.3 Methods

5.3.1 Platelet preparation

This study was approved by the Human, Biosafety and Animal research ethics board of the University of British Columbia (H12-01516 and A16-0176). Written informed consent was obtained from all healthy volunteers in accordance with the Declaration of Helsinki. Platelets and PRP were isolated as previously described [359]. Platelets were resuspended in Tyrode's buffer (119 mM NaCl, 5 mM KCl, 25 mM HEPES, 2 mM $CaCl_2$, 2 mM $MgCl_2$, 6 g/L glucose, pH 6.5) or in plasma at a final concentration of 2 x 10^9 platelets/mL. Whole blood from C57BL/6J or APPKO mice (The Jackson Laboratory, Maine, USA) was collected in Acid Citrate Dextrose (ACD, 38 mM citric acid, 107 mM sodium citrate, 136 mM dextrose) via cardiac puncture. After whole blood was centrifuged at 600 × g for 3 min, PRP was collected. The PRP was centrifuged at 400 × g for 2 min to remove remaining red blood cells. Platelet-poor plasma was isolated by centrifuging whole blood at 1000 × g for 10 min twice. Prostaglandin E1 (10 μg/ml Sigma, Missouri, USA) was added to minimize platelet activation during isolation.

5.3.2 Western blotting

Samples were reduced, boiled, and separated on 10% or 4-15% Tris-glycine gradient gels (Bio-Rad, California, USA). After electrophoresis, the samples were transferred to a nitrocellulose membrane (GE Healthcare, Illinois, USA) and blocked with Odyssey Blocking Buffer (Li-Cor, Nebraska, USA). The membranes were treated with a primary antibody against APP (1:1000; 6E10, Covance, New Jersey, USA or ab15272, Abcam, Cambridge, UK, or 1:500;

22C11, ThermoFisher, Massachusetts, USA), FXIII-A (1:1000; SAF13A-AP, Affinity Biologicals, Ontario, Canada) or fibrin (1:50 000; A0080, Dako, California, USA), washed, and treated with HRP-labeled anti-host secondary antibody (1:10 000 ab7090, 1:15 000 ab97040 Abcam).

5.3.3 Co-immunoprecipitation assay

After washed platelets were activated by 70 nM of thrombin (Haematological technologies, Essex Junction, VT) for 5 min or 1 hr in the presence of exogenous FXIII-A (300 nM, Haematological technologies) or an irreversible inhibitor of FXIII-A, D004 (2.5 mM, Zedira GmbH, Darmstadt, Germany), platelets were lysed with lysis buffer (87787, ThermoFisher, Massachusetts, USA). Platelets were then centrifuged at 14 000 × g for 10 min to isolate the lysates. The lysates were incubated with beads crosslinked with an antibody against APP (6E10 or ab15272, Abcam) or against serotonin (S5545, Sigma) and eluted according to the co-immunoprecipitation kit (PI-26147, Sigma). The eluates were either submitted for mass spectrometry or prepared for Western blotting.

5.3.4 Mass spectrometry

The samples were reduced with dithiothreitol, alkylated with iodoacetamide and then digested with trypsin at 1:50 protein:enzyme ratio [330]. The peptides from different samples were reductively demethylated with differing isotopologues of formaldehyde. This imparts a light, medium, or heavy mass tag on the peptides from different samples, which can then be mixed and analyzed concurrently in the mass spectrometer [373]. The resuspended samples were loaded onto a capillary-LC-MS/MS system (Agilent 6550 Q-ToF, with Agilent 1200 HPLC system, featuring a 2.1mm × 250mm POROShell C18 column) and run with 70 min H_2O:CAN gradients. The QToF was run in AutoMS/MS mode, at 2 spectra/sec for MS and 3 sepctra/sec for

MS/MS scans. LC MS/MS data files were searched and quantified using MaxQuant software [374] using tryptic digestion specificity, default values from Agilent QToF data (including 1% FDR), and the triplex demethylation quantification mode, against the Uniprot human database.

5.3.5 Examining the effect of APP on platelet FXIII

To examine the role of APP on FXIII release, isolated platelets from C57BL/6J or APPKO mice were activated with 70 nM of human thrombin (Haematological technologies) for 1 hr and the platelets were pelleted by centrifugation at 1 000 × g for 10 min. The supernatant was then centrifuged again at 21 000 × g for 1 hr to separate the microparticles, which was resuspended in Tyrode's buffer. The rate of fibrin crosslinking by platelet FXIII was tested by activating platelets with 70 nM of human thrombin and adding quench buffer (5M urea, 50 mM DTT, 12.5 mM EDTA).

5.3.6 Modification of APP processing by FXIIIa

For whole cell platelet APP processing, platelets were activated with 70 nM of thrombin for 1 hr with either 40 nM of FXIIIa (Haematological technologies) or 2.5 mM of D004 (Zedira GmbH). To isolate platelet APP releasates, purified platelets were activated with 1 U/mL thrombin in the presence or absence of 2.5 mM D004 for 5 min, followed by spinning the samples at 2000 g for 2 min. The releasates were then incubated with either 40 nM of FXIIIa or 2.5 mM of D004. To examine if FXIIIa could covalently crosslink APP metabolites, 10 μg/mL sAPPβ (S4316, Sigma) was incubated with 200 nM DTT, 100 nM of FXIII and 70 nM of thrombin (Haematological technologies) for up to 1 hr and analyzed by Western blotting.

5.3.7 Clot retraction assay

Clot retraction tubes were pretreated with 1% Tween 20 solution for 1 hr, before removing the solution. Clotting was by adding PRP to the clot retraction solution, which

consisted of HEPES buffered saline (HBS; 20 mM HEPES, pH 7.4, 150 mM NaCl, 3 mM $CaCl_2$), 2 U/mL thrombin, with or without 1 mM eptifibatide. Samples were incubated at 37°C for 120 min and imaged at regular intervals. Images were analyzed as area of clot remaining to determine clot retraction percentage over time.

5.3.8 Statistical analyses

Statistical analyses were performed using GraphPad Prism. All results presented in graphs are in mean ± SEM. n indicates the number of independent experiments, performed on separate days. A two-tailed unpaired Student's *t* test was used for all analyses. Significance was designated at p values < 0.05.

5.4 Results

5.4.1 APP binds to platelet FXIII after human platelets were activated

Proteins that interact with APP after platelet activation were isolated by co-immunoprecipitation against the C-terminus of APP and identified by quantitative LC-MS/MS analysis. Many platelet proteins binding to APP were identified, including fibrin, FXIII-A, platelet factor 4 (PF4) and GAPDH. After platelets were activated with thrombin for 1 hr, the binding of APP to fibrin (α, β and γ chains averaged), FXIII-A and PF4, increased by 11-fold and 7-fold and 26-fold, respectively (Figure 5.1A). Since thrombin catalyzes the generation of insoluble fibrin fibers, which may compromise the immunoprecipitation process, the experiment was repeated by activating the platelets in the presence of GPRP peptides that inhibit fibrin polymerization [375]. In the presence of GPRP peptides, the binding of fibrin(ogen) and FXIII-A to APP increased by 19-fold and 7-fold, respectively. Since Aβ, a metabolite of APP, is a substrate for FXIII-A [23], the binding of FXIII-A to APP was confirmed by Western blotting. FXIII-A binding to APP was undetectable in resting platelets, but rapidly increased within

minutes of activation (Figure 5.1B). The binding of FXIII-A to APP increased by over 31-fold after 5 min activation and 77-fold after 60 min activation (Figure 5.1C). FXIII-A was detected by immunoprecipitation from both the N-terminus and the C-terminus of APP, indicating FXIII-A can bind to the full-length APP, not just its individual fragments.

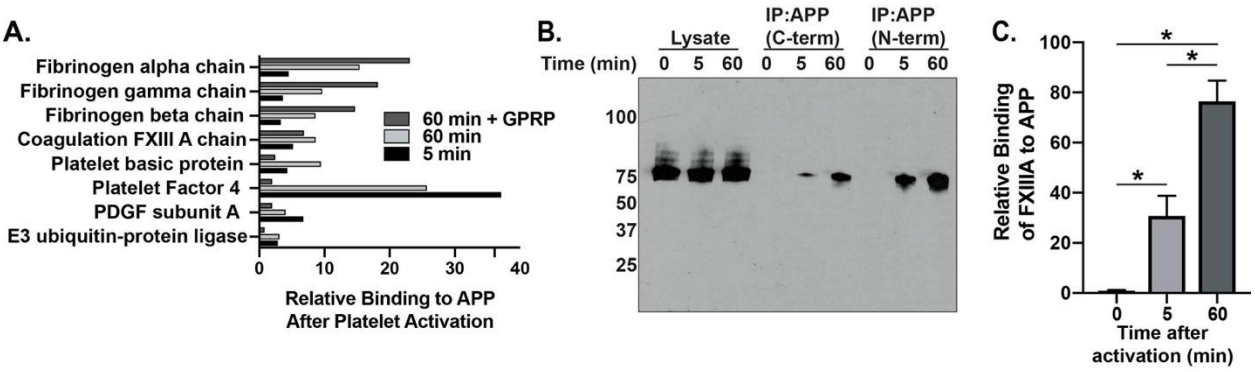

Figure 5.1. Binding of human platelet FXIII-A to APP following platelet activation. (A) The relative binding of proteins to APP after washed platelets were activated with thrombin, identified by immunoprecipitation against the C-terminal of APP followed by mass spectrometry. (B) Western blot against FXIII-A after lysates of thrombin-activated washed platelets were immunoprecipitated against the C-terminal or the N-terminal of APP. (C) Quantification of panel B; the relative binding of FXIII-A to APP C-terminal after platelet activation. n = 3. *, $p < 0.01$

5.4.2 APP did not influence FXIII-A release, activity or degradation in mouse platelets

Since APP binds with FXIII-A upon platelet activation, the potential role of APP on FXIII-A function was investigated. To determine whether APP influences the localization or the release of FXIII-A, platelets from wild type (WT) and APP knockout (APPKO) mice were separated into the pellet, releasate and microparticles fractions following activation with thrombin. FXIII-A remained in the pellet and the microparticle fraction in both WT and APPKO

mice and did not differ in the amount released, indicating that APP does not influence the amount of FXIII-A released from platelets (Figure 5.2A). To test if APP influences the activity of platelet FXIII on clot retraction, the rate and extent of clot retraction was examined in platelet rich plasma (PRP) collected from WT and APPKO mice. PRP clots from WT and APPKO mice both retracted comparably by 80% within 3 hrs, indicating that APP does not influence the contribution of FXIIIa to clot retraction (Figure 5.2B). To test for subtle changes of APP on FXIII-A function in clot retraction, we inhibited clot retraction using eptifibatide, an antagonist of platelet receptor glycoprotein IIa/IIIb [376]. In the presence of eptifibatide, the rate and the extent of clot retraction in WT and APPKO samples were similarly decreased to 60% over 3 hrs. To determine whether APP influences the activity of FXIIIa in crosslinking fibrin, another identified binding partner of APP, the rate of formation of fibrin γ-γ dimers was compared between platelets from WT and APPKO mice following activation with thrombin. The γ-γ dimers were detected 2 min after platelets were activated and increased in intensity over 15 min. The relative intensities of γ-γ dimers formed did not differ significantly between platelets from WT and APPKO mice, indicating that APP does not influence the crosslinking of fibrin by FXIII-A (Figures 5.2C and 5.2D). Platelet FXIII-A can be degraded by plasmin when externalized to the platelet surface [359], so we tested the effect of APP on FXIII-A stability. When activated platelets from WT and APPKO mice were incubated with plasmin, FXIII-A from both WT and APPKO platelets were similarly degraded by plasmin by 70% after 1 hr, indicating that APP does not influence plasmin-mediated degradation of FXIII-A (Figure 5.2E and 5.2F).

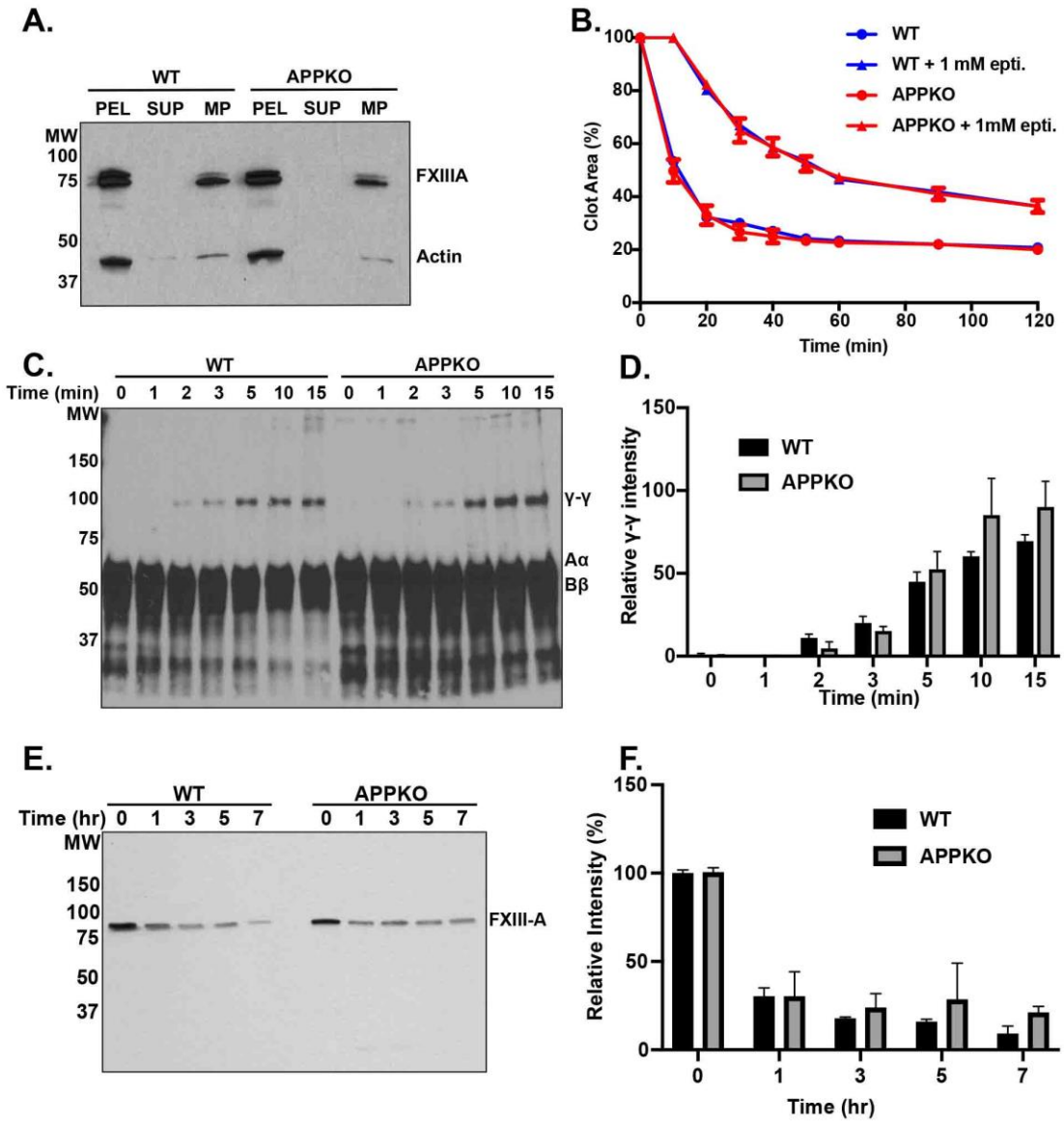

Figure 5.2. APP does not influence FXIII-A activity, degradation, or amount released from mouse platelets. (A) Western blot against FXIII-A after activated platelets were separated into pellet, microparticles, and supernatant in WT and APPKO mice. (B) The retraction of PRP clots from WT and APPKO with and without eptifibatide (1 mM). (C) Western blot against fibrinogen after platelets from WT and APPKO mice were activated with thrombin. (D) Quantification of the intensity of the γ-γ dimers in panel C. (E) Western blot against FXIII-A after activated platelets from WT and APPKO mice were incubated with plasmin (500 nM). (F) Quantification

of the relative intensity of FXIII-A in panel D. n = 3. PEL: pellet, SUP: supernatant, MP: microparticle, WT: wild type, APPKO: APP knockout, epti: eptifibatide.

5.4.3 FXIIIa activity prevented APP processing

Upon platelet activation, APP is processed by proteases on the platelet membrane and released as various metabolites [377]. Since we found that FXIII-A bound with APP at the membrane upon platelet activation, we tested whether FXIIIa affects the processing of APP (Figure 5.3A and 5.3B). When platelets were activated with thrombin, 57% of the full-length APP was cleaved over 1 hr. When exogenous FXIIIa was added, only 32% of the full-length APP was cleaved, suggesting that FXIIIa inhibits the processing of APP. Conversely, when the activity of FXIIIa was inhibited by adding an irreversible inhibitor, D004, the processing was increased to 89% and the initial lower molecular weight cleavage products were not detected, presumably because they were also cleaved (Figure 5.3A and 5.3B). Various forms of soluble APP (sAPPα/β) are released upon platelet activation [20], and the effect of FXIIIa activity on the processing of sAPP was examined (Figure 5.3C and 5.3D). First, platelets were activated by thrombin to generate and release sAPP. The presence of D004 reduced the amount of sAPP released from platelets by approximately 90%. Next, platelet releasates were incubated with either FXIIIa or D004 for 3 hr to evaluate how FXIIIa activity influences the metabolism of released sAPP. sAPP was degraded in the releasate by 47% over 3 hr, and there were no statistically significant differences in the degradation of sAPP when FXIIIa or D004 was added to the releasate. Together, this shows that FXIIIa inhibits the processing of APP within or on platelets, inhibits release of sAPP, but does inhibit cleavage of sAPP after it is secreted.

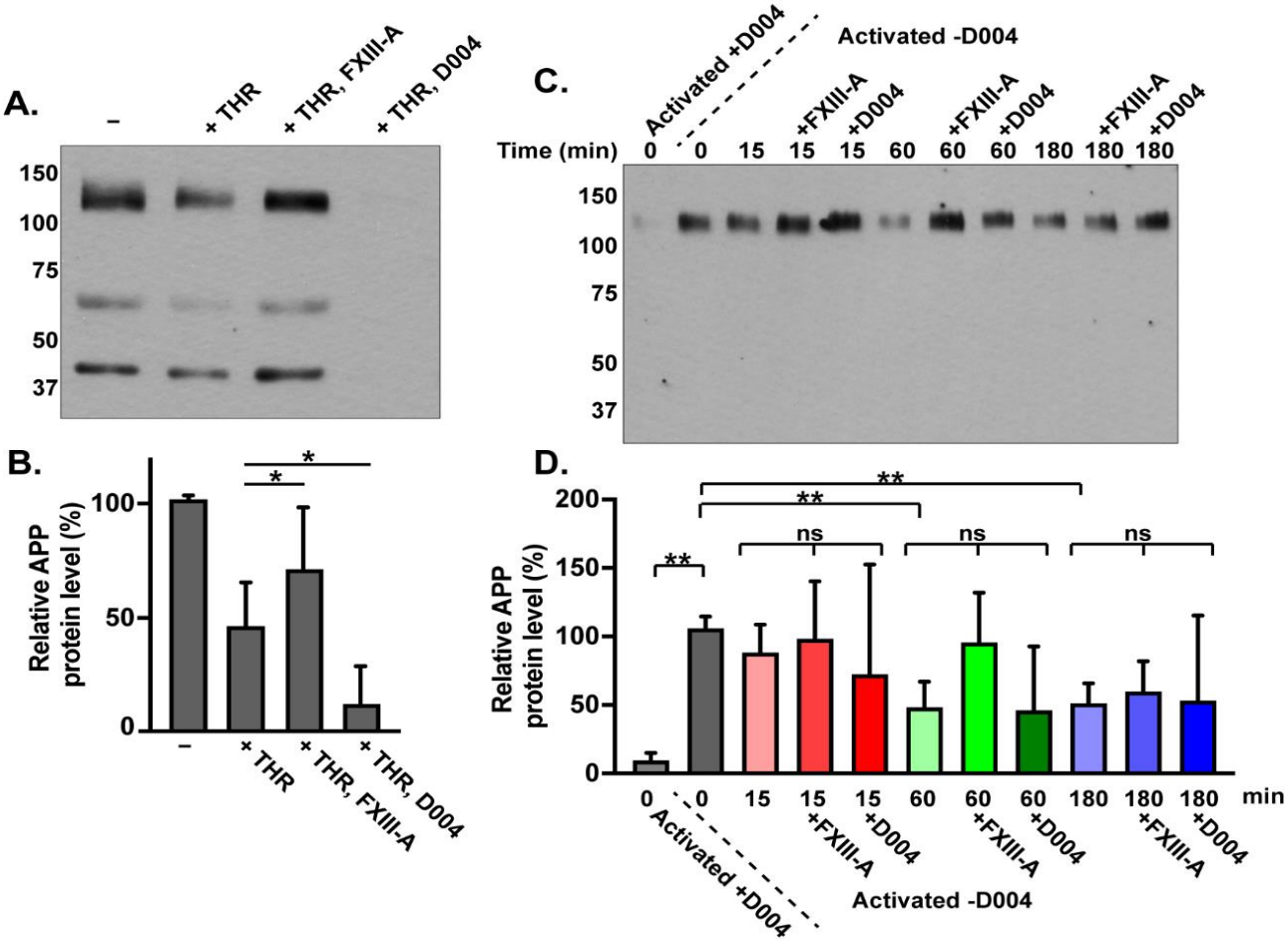

Figure 5.3. FXIIIa activity slows APP processing. (A) Western blot against APP after platelets were incubated with thrombin and either exogenous FXIII-A or D004 for 1 hr. These samples included platelets and platelet releasates. (B) Quantification of panel A. (C) Western blot against sAPP in platelet releasates after platelets were activated in the presence or absence of D004. Releasates, including soluble components and microparticles without intact platelets, were collected and then incubated with FXIII-A or D004 for up to 3 hrs. One of the groups contained D004 during platelet activation. (D) Quantification of panel C. n = 5. ns = not significant. *, $p < 0.05$. **, $p < 0.01$.

5.4.4 FXIIIa cross-links APP

FXIIIa delays the clearance of fibrin by covalently crosslinking fibrin to itself and to other proteins [12]. To determine if APP is a substrate of FXIIIa, purified soluble APPβ (sAPPβ), the extracellular fragment of sAPP, was incubated with FXIII-A and thrombin. The appearance of higher molecular weight products indicated sAPPβ was covalently crosslinked by FXIIIa (Figure 5.4A). When platelets are activated, FXIIIa crosslinks serotonin to pro-coagulant proteins, such as fibrinogen, from the α-granule to retain them on the platelet surface [186]. We tested to determine if serotonylation by FXIIIa influenced APP processing. Platelets were activated in the presence of exogenous FXIIIa or D004, and the lysates of platelets were immunoprecipitated against serotonin, and immunostained against APP. After platelet activation, the relative amount of APP in the eluate increased by 5.7-fold (Figure 5.4B and 5.4C). When exogenous FXIIIa was added, the relative amount of APP in the eluate did not increase significantly. However, when D004 was added, the relative amount of APP in the eluate decreased 3-fold.

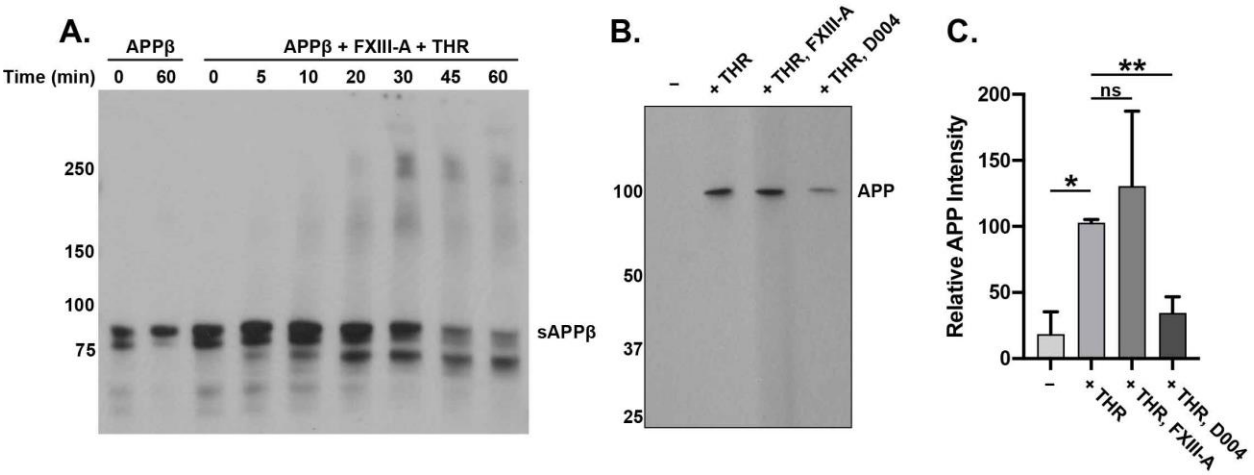

Figure 5.4. Platelet FXIIIa crosslinks APP. (A) Western blot against APP, where purified sAPPβ was incubated with or without FXIII and thrombin (B) Western blot against platelet-APP, where lysates of unactivated or activated platelets were co-immunoprecipitated with antibodies against serotonin. Platelets were activated for 60 min in the presence or absence of FXIII-A or D004. (C) Quantification of the intensity of the APP in panel A. n = 3. ns = not significant. *, $p < 0.05$. **, $p < 0.01$. THR: thrombin

---

5.5 Discussion

Here we demonstrate that platelet APP binds to platelet FXIII-A and fibrinogen upon platelet activation. Although APP did not alter the release, activity or degradation of FXIIIa, the activity of FXIIIa influenced the processing and cleavage of APP. Additionally, the extracellular portion of APP, sAPPβ, was covalently crosslinked by FXIIIa.

The most prominent binding partners of platelet APP following platelet activation were fibrin(ogen), FXIII-A and PF4, which are key proteins in hemostasis. Since APPKO mice do not appear to have a severe bleeding phenotype, APP may contribute to the non-hemostatic processes to which fibrinogen and FXIII-A also contribute, including those in inflammation and wound healing [12]. Intracellular FXIII-A modulates the cytoskeletal proteins of platelets, such as vinculin and actin, to modulate the platelet morphology [371]. Platelet FXIII also crosslinks antiplasmin to fibrin during platelet activation to stabilize the blood clot [372]. The functional significance of the interaction between APP, fibrin(ogen) and FXIII-A remains unclear and requires further investigation.

Platelets generate and release Aβ upon platelet activation, contributing to the deposition of Aβ along the cerebrovasculature [350, 364]. The deposition of Aβ is a hallmark of cerebral

amyloid angiopathy and Alzheimer's disease (AD). Currently, BACE-1 and γ-secretases, which cleave APP to generate Aβ, are considered drug targets; inhibitors of these proteases have been attempted in clinical trials, though no secretase inhibitors have yet approved for AD [378]. The data here shows that increased FXIIIa activity prevents APP processing, potentially through serotonylation of APP. It has been previously proposed that the serotonylation of APP at Gln-686, near the α-secretase cleavage site, would prevent metabolism of APP by α-secretase and stabilize APP [379]. Although the impact of FXIIIa on Aβ deposition and subsequent AD development remains to be tested, this is a potential mechanism that should be further explored.

In conclusion, APP binds with fibrin(ogen) and FXIII-A upon platelet activation. Exogenous FXIIIa activity inhibited the processing of APP after platelet activation, and FXIIIa crosslinked serotonin to APP fragments. These results are significant since platelets contribute to the aggregation of Aβ in the cerebrovasculature, a process involved in cerebral amyloid angiopathy and AD.

Chapter 6: The absence of amyloid precursor protein in an animal model measurably increases bleeding

6.1 Contributions

This publication was a collaborative work and a manuscript has been published in *Research and Practice in Thrombosis and Haemostasis*. N.M. designed, performed experiments, analyzed and interpreted the data and wrote the paper. N.M. performed experiments to collect data for Figure 6.1, 6.2 and 6.3. I contributed to 75% of this paper. A.W.S. performed experiments to collect data for Figure 6.4A-C. J.R.B. performed experiments to collect data for part of Figure 6.1 and 6.3. C.J.K. and W.A.J. helped design and analyze experiments and write the paper. W.S.H. analyzed data and edited the paper.

6.2 Introduction

Amyloid beta precursor protein (APP) is a type 1 transmembrane glycoprotein that is expressed in platelets [267]. On average there are approximately 9000 molecules of APP per platelet, making APP one of the most abundant platelet proteins [268]. In humans, platelet-derived APP (platelet-APP) is the primary source of APP in the blood, accounting for more than 90% of circulating APP [380]. Platelet-APP and its metabolites, particularly Aβ peptides, have several activities, involving both anticoagulant and procoagulant properties, but it is unclear whether APP contributes to physiological hemostasis.

Brain-derived APP (brain-APP) and platelet-APP are metabolic precursors of Aβ peptides. The accumulation of Aβ in brain parenchyma and cerebral vessel walls is correlated with the onset of Alzheimer's disease (AD) [381]. Membrane APP can be proteolytically processed by secretases in both amyloidogenic and non-amyloidogenic pathways, which release soluble Aβ and soluble APPβ (sAPPβ), or peptide P3 and soluble APPα (sAPPα) [257]. Platelets

express the necessary proteases to cleave APP into these metabolites [382]. In platelets, APP, sAPPα, and Aβ are stored in alpha granules and released upon platelet activation and degranulation [382, 383].

Platelet-APP and brain-APP differentially affect reactions of the coagulation cascade. Due to differential splicing, platelet-APP, but not brain-APP, contains a Kunitz-type protease inhibitor (KPI) domain that inhibits multiple proteases, including chymotrypsin, trypsin, blood coagulation factors IXa, Xa, XIa, and the complex of factor VIIa with tissue factor [24, 384]. Platelet-APP has previously been described as a cerebral anticoagulant [24]. Overexpression of platelet-APP, or intravenous administration of its KPI domain, has decreased cerebral thrombosis in mice [29, 276]. Similarly, transgenic mice lacking the active KPI domain are prothrombotic and have shortened times of occlusion in the carotid artery and brain [385]. Mice deficient in APP (APP KO) have 20% fewer, but larger platelets with normal aggregation, secretion, and integrin αIIbβ3 inside-out activation [30]. APP KO mice also developed larger thrombi following inferior vena cava stenosis [30]. Additionally, these APP KO mice had elevated FXIa, and shorter activated partial thromboplastin times, but not prothrombin times, in the presence of platelets, compared to WT mice. These same APP KO mice had elevated platelet-leukocyte aggregates and neutrophil extracellular traps.

Platelet-APP and its metabolites can also promote coagulation. Aβ increases clot formation *in vitro* through activation of coagulation factor XII [25]. Increased activation of the intrinsic coagulation pathway has also been observed in mouse models of AD and humans with AD [169]. Aβ peptides directly activate platelets, promote aggregation, and trigger thrombus formation [278, 386]. Platelets release Aβ during thrombosis, and platelets can adhere to deposited Aβ [26, 387, 388]. Aβ interacts with fibrin to induce structural changes in the clot,

forming plasmin-resistant blood clots [28]. Aβ is also a substrate for coagulation factor XIIIa [389]. Factor XIIIa can covalently cross-link Aβ to itself and to other platelet and coagulation proteins, and this can increase clot stiffness. Although Aβ can promote and stabilize clot formation in these ways, APP KO mice did not have an obvious bleeding phenotype in previous studies [30]. A significant difference in blood loss from a tail transection model between APP KO and WT mice was not previously detected, however the mean tail bleeding time appeared to be over twice as long in APP KO mice [30]. Thus, it is not clear if APP contributes to hemostasis *in vivo*. Here, we extended these studies by examining hemostasis in multiple mouse models, by selectively inhibiting several aspects of coagulation in these models, and by analyzing coagulation of blood from APP KO mice using thromboelastography (TEG).

6.3 Methods

6.3.1 Mouse experiments

All procedures were approved by the University of British Columbia Animal Care Committee and performed in accordance with the guidelines established by the Canadian Council on Animal Care. WT (C57Bl/6J) and APP KO (B6.129S7-App^{tm1Dbo}/J) mice were purchased from Jackson Laboratories (not littermates). To reduce variability in mouse bleeding models, mice were matched by weight (20-24 g) and sex-matched to ensure equal proportions of males and females in each group.

6.3.2 Liver laceration bleeding model

Mice were anesthetized via isoflurane inhalation and livers were accessed via a 3 cm transverse incision. Two lacerations, each 2 mm long and 2 mm deep, were made on each liver using a 2-mm ophthalmic knife. Blood loss was quantified from each laceration independently. Blood was collected on preweighed filter paper immediately after injury until bleeding stopped.

Filter papers (~2 cm by 2 cm) were arranged to line the site of puncture before incision. Each laceration bled for approximately 30 s. Blood loss was compared by Mann-Whitney U test. To confirm that changes in filter paper mass correlated with the volumes of blood soaked, known volumes of fresh blood were soaked onto preweighed filter papers.

6.3.3 Mouse tail clip bleeding model

Bleeding was monitored using the immersion method [390]. WT and APP KO mice were anesthetized via isoflurane inhalation and were kept at 37 °C using a heating pad temperature probe. Mice then received intraperitoneal injections of apixaban (2 mg/kg, 100 µl, 30 min before injury, Eliquis; Bristol-Myers Squibb, Canada), aspirin+clopidogrel (100 mg/kg and 5 mg/kg respectively, 100 µl, 60 min before; Sigma), recombinant human tissue plasminogen activator (tPA, 9 mg/kg, 150 µl, 5 min before, Tenecteplase; Genentech), tranexamic acid (TXA, 800 mg/kg, 250 µl, 20 min before; Sigma), or saline (50 µl phosphate buffered saline) as a control. Tails were transected 3 mm from the tip and were then immediately immersed in warm isotonic solution (citrated phosphate buffered saline (PBSC)) to collect shed blood and to monitor bleeding for 20 min. To quantify blood loss, the blood-PBSC solutions were treated with a solution that lyses red blood cells (1.5 M NH_4Cl, 0.1 M $NaHCO_3$, 0.01 M EDTA, Millipore Sigma) and incubated at room temperature for 10 min while gently inverting the mixture. The absorbance of each blood solution was measured at 590 nm (Tecan Genios plate reader) and converted to blood loss (µl) using a standard curve with known amounts of mouse blood that was collected via intracardiac puncture. The calculated blood loss was normalized by the mouse body weight (µl/g) to account for the severity of blood loss with respect to the animal size. For all bleeding experiments, when comparing blood loss without correcting for body weight, three of the four comparisons which are significant remain significant. All statistical analyses were

performed using Prism 5 (GraphPad Software, La Jolla, CA). Data sets were normally distributed within groups, and were compared by unpaired t-test. Data sets were also compared using non-parametric Mann-Whitney U test and maintained the same statistical significance. The current work is early experimental research and further work needs to be done with a sample size and appropriate statistical analysis. such as ANOVA and post-hoc analysis. In addition to larger sample sizes, the work requires confirmation from different bleeding models, different animal species and different sexes.

6.3.4 TEG analysis

Using a different group of mice separate from the bleeding experiments, clotting parameters of whole blood were evaluated at 37°C using a TEG Hemostasis Analyzer System 5000 (Haemoscope Corporation). Citrated whole blood (10.9 mM sodium citrate final concentration) was collected by cardiac puncture and combined with $CaCl_2$ (13.6 mM), tissue factor (0.03 nM, MedCorp Brazil), and tPA (3.8 nM). Measurements began immediately after mixing all components together and the experiment was run for 3 hr. Statistical analyses were performed using Prism 5 (GraphPad Software, La Jolla, CA). Data sets were normally distributed within groups, and were compared by unpaired t-test.

6.4 Results and discussion

To extend and validate previous reports evaluating bleeding in APP KO mice under physiological conditions, we conducted liver laceration and tail clip models of hemorrhage. APP KO mice did not bleed significantly more following liver lacerations, but they bled four-fold more than WT mice following tail clips ($P < 0.05$, Figure 6.1). This result extends a previous report in which bleeding times appeared to be increased two-fold, though that study did not detect a statistically significant difference [30].

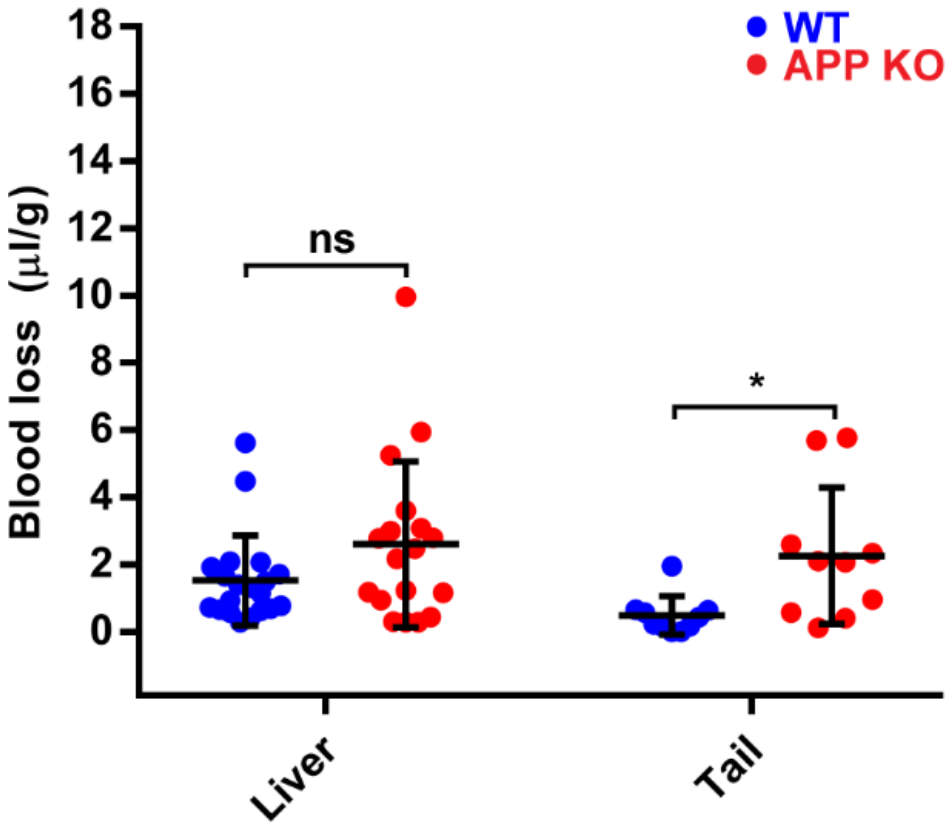

Figure 6.1. APP KO mice have a mild bleeding phenotype. Blood loss in the liver laceration model and tail transection model with WT and APP KO mice. Blood loss was normalized to body weight. In the liver laceration model, each marker indicates one of two bleeds per liver (n = 18 bleeds from 9 mice per group). In the tail transection model, each marker represents a single mouse (n = 10 mice). Error bars represent the mean ± SEM. * $P < 0.05$, ns indicates not significant (P = 0.10).

To test if bleeding in APP KO mice was mediated by differences in thrombin generation, we treated both APP KO mice and WT mice with an inhibitor of coagulation factor Xa (apixaban, 2 mg/kg) and compared their blood loss. When mice were treated with apixaban, APP KO mice bled three-fold more than WT mice ($P < 0.05$, Figure 6.2A). Due to high variability in these groups, we performed a Grubb's test for outliers which excluded one data point in each

group; the differences remained significant (P = 0.02) following exclusion. Apixaban significantly increased blood loss in WT and APP KO mice, confirming that thrombin generation was inhibited in both groups compared to untreated mice. The significant increase in bleeding between APP KO mice and WT mice with apixaban suggests that the bleeding phenotype is not primarily mediated by differences in thrombin generation, but does not rule out the possibility.

To determine if the increased bleeding by APP KO mice was mediated by platelets, we compared blood loss between APP KO and WT mice treated with aspirin+clopidogrel, which inhibited platelet activation. When treated with aspirin+clopidogrel, APP KO mice did not bleed significantly more than WT mice (Figure 6.2A). This suggests the bleeding phenotype in APP KO mice is mediated by platelets.

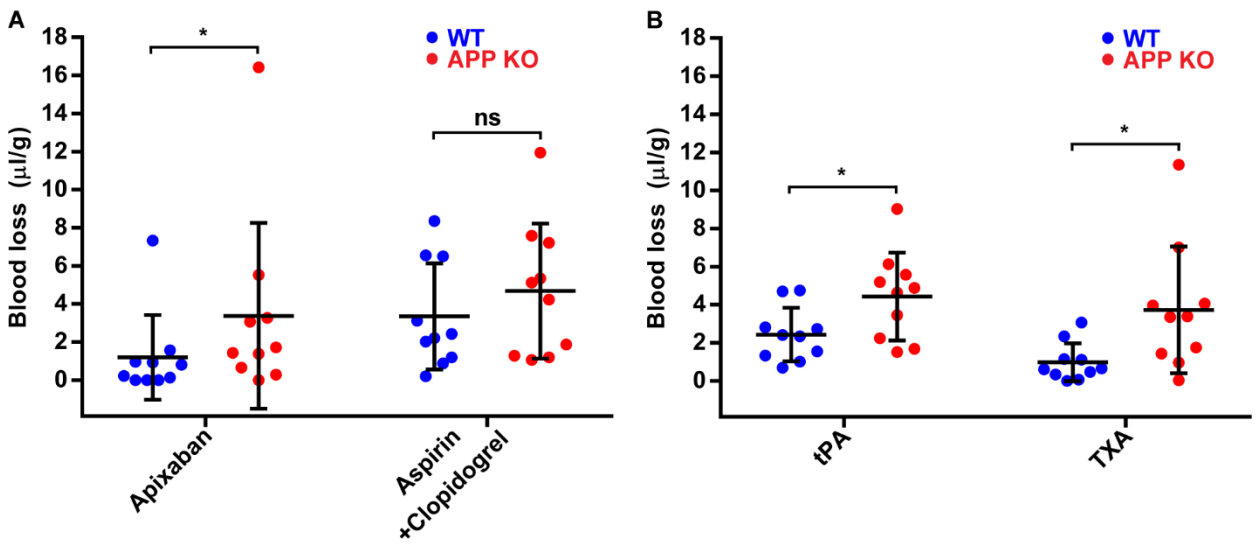

Figure 6.2. Platelet inhibitors abrogate the difference in the bleeding phenotype of APP KO mice, but apixaban, and pro- and anti-fibrinolytic treatments do not. A) Blood loss following tail transection after treating mice with apixaban (2 mg/kg) and aspirin+clopidogrel (100 mg/kg and 5 mg/kg respectively). B) Blood loss following tail transection after treating

mice with tPA (9 mg/kg) and tranexamic acid (TXA, 800 mg/kg). $n = 10$. Error bars represent the mean ± SEM. * $P < 0.05$, ns indicates not significant ($P = 0.40$).

To evaluate if APP KO mice and WT mice bled differently due to differences in fibrinolysis, we compared blood loss under hyper- and hypofibrinolytic conditions. When treated with tPA, APP KO mice bled twice as much as WT mice ($P < 0.05$, Figure 6.2B). When treated with the antifibriolytic tranexamic acid (TXA), APP KO mice bled thrice as much as WT mice ($P < 0.05$). This suggests that the increased bleeding seen in APP KO mice is not primarily mediated by differences in fibrinolytic activity.

All mean and median values for the *in vivo* bleeding experiments are listed in Table 6.1. In some published mouse studies, liver and tail injuries cause similar blood loss [390]. In our liver laceration model, injuries were smaller and caused less-severe capillary bed bleeds. APP KO mice bled more compared to WT in our tail transection model, which causes platelet-dependent arterial bleeding [391], but not our liver laceration model. This suggests that platelet dysfunction may be a potential mechanism [391]. WT mice treated with apixaban, aspirin+clopidogrel, or tPA bled significantly more than WT controls. TXA-treated WT mice also bled slightly more than controls, but the difference was not significant; this may be related to greater volume or tonicity of the injected TXA solution. It was expected that TXA-treated mice would not bleed less, since inhibition of fibrinolysis does not have a strong effect in arterial bleeding models [391, 392]. Apixaban-treated APP KO mice bled significantly more than APP KO controls. While median blood loss in APP KO mice receiving aspirin+clopidogrel was twice that of APP KO controls, the difference was not significant; increased bleeding would suggest that inhibition of platelets by aspirin and clopidogrel can occur independent of APP. These

results do not fully exclude contributions of APP and Aβ to thrombin generation or fibrinolysis, as the tail transection model is more sensitive to changes in platelet activity compared to other aspects of hemostasis [393].

	WT		APP KO	
	mean ± SEM	median (range)	mean ± SEM	median (range)
Liver				
N.T.	1.52 ± 0.30	1.22 (0.28-5.62)	2.60 ± 0.58	2.33 (0.27-9.96)
Tail				
N.T.	0.48 ± 0.18	0.32 (0-1.95)	2.26 ± 0.64	2.08 (0.12-5.77)
Apixaban	1.19 ± 0.70	0.51 (0-7.32)	3.37 ± 1.54	1.57 (0-16.42)
ASA+clop.	3.34 ± 0.88	2.32 (0.19-8.35)	4.68 ± 1.12	4.67 (1.06-11.94)
tPA	2.42 ± 0.45	2.37 (0.68-4.75)	4.43 ± 0.73	4.76 (1.51-9.02)
TXA	0.98 ± 0.32	0.63 (0-3.07)	3.73 ± 1.06	3.37 (0.03-11.35)

* N.T. = no treatment
* all units in µl/g

Table 1. Mean and median values with ranges for *in vivo* bleeding experiments.

We then used TEG to investigate if whole blood from WT and APP KO mice have different clot properties *ex vivo*. Citrated whole blood was collected from mice, and Innovin and tPA were added to allow stable clots to form and lyse. TEG parameters of R-time (clot initiation time), maximum amplitude (MA, clot stiffness), and percent lysis at 30 min (susceptibility to fibrinolysis) were analyzed. Whole blood from APP KO mice had a two-fold increased R-time, 16% decrease in MA, and three-fold increase in percent lysis at 30 min ($P < 0.05$, Figure 6.3). This demonstates that APP KO whole blood clots slower and forms weaker clots compared to WT whole blood. APP KO clots were more suceptible to fibrinolysis, likely because of weaker clot formation due to platelet inhibition, which is consistent with the tail bleed experiments. These results are also consistent with how platelet abnormalities are known to affect bleeding and TEG measurements [394].

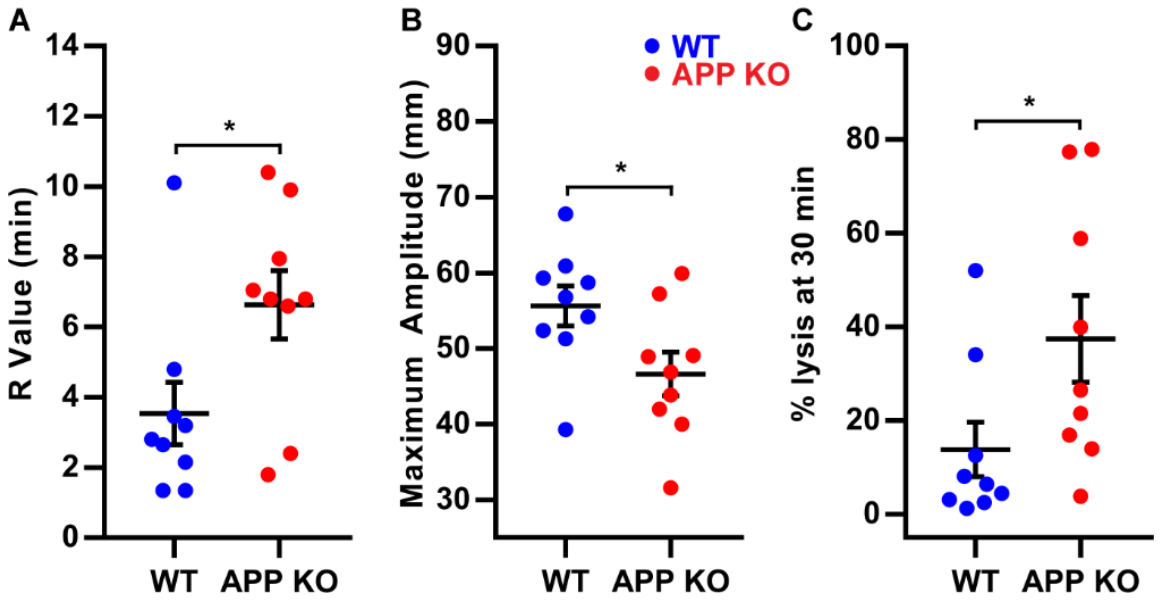

Figure 6.3. TEG analysis of whole blood demonstrating hemostatic abnormalities in APP KO mice. Graphs show clot initiation time (R value, A), clot strength (maximum amplitude, B), and clot stability (percent lysis at 30 min, induced by 3.8 nM tPA, C). *n* = 9 mice. Error bars represent the mean ± SEM. * $P < 0.05$.

There are numerous studies examining the effect of APP and its metabolites on hemostasis, and the characteristics of APP KO platelets. APP has anticoagulant properties through its KPI domain [24], and Aβ-mediated procoagulant properties through increased thrombin generation, platelet activation and aggregation, and resistance to fibrinolysis [25, 28, 169, 278, 386]. Platelets from APP KO mice have normal platelet aggregation, secretion, and αIIbβ3 signaling, but reduced platelet numbers and increased platelet size [30]. To corroborate these findings, we measured platelet concentration, and aggregation and secretion using APP KO mice and the results were consistent with published values. Although we and other groups have not identified major differences in the coagulability of between APP KO and WT platelets *ex vivo*, here we have demonstrated a difference *in vivo*, likely related to the mechanisms previously

published. Overall, APP and its metabolites can affect hemostasis in multiple ways, but in mice its pro-coagulant contributions to hemostasis are most distinct in arterial bleeds where platelet activity is critical.

In this study we investigated the role of APP in hemostasis under physiological and challenged conditions. We found that APP plays a procoagulant role in primary hemostasis and this role is mediated by platelets. APP possessing both procoagulant and anticoagulant properties is consistent with other components of hemostasis; for example fibrin and thrombin are strong drivers of coagulation, but also exhibit anticoagulant properties by inhibiting thrombin and activating protein C, respectively [202, 395]. In conclusion, we found that APP KO mice have a consistent mild bleeding phenotype that is in part mediated by platelets, for which the specific mechanism remains to be validated.

Chapter 7: Conclusions and future directions

7.1 Summary

Platelets are small blood cells but indispensable to several aspects of human physiology. Although their primary role is in hemostasis, platelets also regulate inflammation, innate and acquired immunity, angiogenesis, and tumor progression [67]. Platelets sense and response to their surrounding environment using various surface receptors and release of stored cargo [67]. Most of the various receptors and granule contents in platelets are well characterized and aid in various aspects of hemostasis, to seal damaged vasculature. However, there are still many gaps in knowledge in respect to platelet contents, with some having no clear physiological functions in hemostasis. Understanding how these molecules can modulate hemostasis can aid in the development of therapies to treat uncontrolled bleeding and trauma, which remains the number one global killer of young healthy adults [3-5].

In chapter 2, whether spatial localization of platelet-length polyP could enhance its ability to trigger coagulation was investigated. Numerical simulations predicted the localization of polyP would increase its coagulability at low shear rates. In static conditions, surface localization of polyP greatly accelerated its ability to trigger coagulation, suggesting a mechanism by which platelet-length polyP could also trigger clotting. Under flowing conditions, using a microfluidic device, short-chain polyP accelerated clotting faster when surface-localized compared to dispersed in nanoparticles or in solution. Finally, platelet-length polyP was able to trigger clotting when surface-localized. In addition, surface-localization also accelerated clotting of long-chain polyP. Although a physiological mechanism for the localization of polyP to platelet or vascular surfaces remains unknown, these results suggest a potential new function for platelet-length polyP in hemostasis. In addition, these results suggest a potential pathophysiological role

of platelet polyP to promote thrombosis at sub-physiological shear rates, such as in deep vein thrombosis.

In chapter 3, whether the fibrinolytic system could inactivate FXIIIa was investigated. In purified systems, plasmin was able to degrade active FXIIIa but not the zymogen FXIII. The primary cleavage site of FXIIIa was determined, suggesting a potential mechanism by which the FXIII-B subunit of the zymogen would be protected from inactivation by blocking the cleavage site. The kinetic parameters of plasmin-mediated FXIIIa degradation were determined, suggesting the reaction could occur on a physiologically relevant timescale. Plasmin was able to inactivate both plasma and platelet FXIIIa. Addition of tPA was also able to trigger degradation of plasma FXIIIa. Plasmin did not inactivate FXIIIa during clot formation, but during clot lysis and at thrombolytic tPA concentrations. This work suggests that FXIIIa activity can be modulated by the fibrinolytic system. As FXIIIa plays a role in several platelet functions, this work also suggests how the fibrinolytic system could modulate platelet function, particularly in hemostasis. Also, the significance of this reaction could be exemplified in situations where plasmin activity is abnormal, such as in patients with Quebec platelet disorder, patients undergoing trauma induced coagulopathy, or patients with plasminogen deficiency.

In chapter 4, Aβ was identified as a novel substrate of FXIIIa. In purified systems, FXIIIa covalently cross-linked Aβ into oligomers and higher molecular weight species. The kinetics of the reaction were quantified. FXIIIa was also able to cross-link Aβ to fibrin as well, at rates exceeding Aβ cross-linking to itself, suggesting a likely cross-linking partner in plasma given the high concentrations of fibrin. FXIIIa cross-linked Aβ to platelet proteins under static and flowing conditions. FXIIIa-mediated crosslinking of Aβ increased the clot strength of PRP and PPP. Familial Alzheimer's disease Aβ mutants were also cross-linked by FXIIIa, to itself and to fibrin,

but at different efficiencies, suggesting a pathological mechanism of the reaction. This work suggests a potential pathological mechanism for platelets in AD as they contain both FXIIIa and Aβ. FXIIIa-mediated cross-linking of Aβ could create nucleation sites of Aβ along the cerebrovasculature, promoting further deposition and development of CAA. This novel reaction could also have various implications in hemostasis as Aβ can modulate many aspects of clotting.

In chapter 5, whether FXIIIa could modify platelet APP or its fragments was tested. Endogenous platelet FXIIIa bound to platelet APP upon platelet activation. The binding between APP and FXIIIa did not influence FXIIIa release, activity or degradation when compared in WT and APP KO mouse platelets. FXIIIa activity delayed APP processing and FXIIIa inhibition enhanced APP processing, suggesting FXIIIa activity could modulate APP metabolite generation. Like Aβ in chapter 4, Soluble APPβ was also covalently cross-linked by FXIIIa. In addition, FXIIIa also cross-linked serotonin to APP fragments, suggesting a potential mechanism for the delayed processing of APP. This work suggests a novel mechanism by which FXIIIa can modulate platelet APP processing and fragment generation. This novel link between coagulation and APP processing has implications in both hemostasis and AD, and further describes platelet-mediated mechanisms that modulate hemostasis.

In chapter 6, whether APP contributes to hemostasis *in vivo* was tested. Blood loss was compared between WT and APP KO mice in liver lacerations and tail transections, and APP KO mice bled more in tail transections. Blood loss was further measured following tail transections and the bleeding phenotype in APP KO mice persisted in the presence of apixaban, tPA, and TXA. However, in the presence of aspirin and clopidogrel, the bleeding difference between WT and APP KO mice was abrogated, suggesting a potential platelet function defect in APP KO mice. APP KO whole blood had longer clotting times, the clots had less mechanical strength, and

more susceptible to fibrinolysis compared to WT mice. Although anti-coagulant roles of platelet APP have been described previously, this work demonstrates APP contributes to physiological hemostasis in certain situations. This work is also consistent with *in vitro* studies of pro-coagulant roles of platelet APP and Aβ in clotting, and further demonstrates novel physiological functions of these platelet proteins in hemostasis.

7.2 Future directions

7.2.1 Exploring the impact of platelet-polyP in physiology and pathophysiology

Future work will examine whether *in vitro* findings extend *in vivo*, and their impact to hemostasis and thrombosis under physiological and pathophysiological situations. Initial work should focus on determining whether platelet-polyP localizes to aggregated platelet surfaces or endothelium *in vivo* at sites of clotting. This can be done in mice using intravital microscopy and a fluorescent probe against polyP. In these experiments, thrombosis can be initiated and imaged in the presence of a polyP probe to track the accumulation of polyP at the site of thrombosis. As a negative control, the same experiment can then be done in the presence of a polycationic agent (anti-polyP/polyP inhibitor) which inhibits the accumulation and aggregation of polyP [144, 396]. These experiments will determine whether polyP released from platelets accumulate at the site of clotting. To evaluate to effect of platelet polyP on clotting, the hemostatic process can be measured using intravital microscopy following an injury in inositol hexaphosphate kinse 1 knock-out mice (Ip6k1 KO), [397]which have 10-fold lower platelet polyP [397]. Hemostasis in these mice can be measured via different bleeding models, with and without intravenous platelet-length polyP injection. In a subsequent experiment, mice will be co-administered with both platelet-length polyP and anti-polyP agents (polycationic) as a loss-of-function examination.

While this thesis examined localization of polyP at low and sub-physiological shear rates, the potential effect of polyP localization *in vivo* at higher shear rates should also be examined using the methodology discussed above. This includes imaging platelet polyP deposition using intravital microscopy at arterial (> 1500 s^{-1}) shear rates. If deposition of platelet polyP occurs at arterial shear rates, the potential effect on clotting can be evaluated using WT mice with and without treatment of anti-polyP agents discussed in the previous section. In addition, the impact

of platelet polyP on thrombosis at pathological shear rates, such as in DVT, should be tested in WT and Ip6k1 KO mice using a stenosis model. The hypothesis here is that Ip6k1 KO mice would be protected from thrombosis formation in the stenosis model. The "protected" Ip6k1 KO mice could then be reverted back to the WT stenosis phenotype by injection of exogenous platelet length polyP. These studies would be most relevance in humans as platelet polyP would likely have its greatest effect at these pathological shear rates.

7.2.2 Exploring the implications of plasmin-mediated inactivation of FXIIIa in pathophysiology

Investigations should be done to determine the significance of plasmin-mediated FXIIIa inactivation in situations where fibrinolysis is elevated. One such situation is patients with Quebec platelet disorder (QPD), which have increased platelet uPA levels in α-granules and are hyperfibrinolytic [398]. These patients suffer from increased incidents of bleeding through an increase of fibrinolytic enzymes [398]. However, as the fibrinolytic system (via plasmin) was found to inactivate FXIIIa, the hyperfibrinolytic state in QPD patients could be exacerbated by a depletion of FXIIIa, a key anti-fibrinolytic enzyme. Thus, evaluating the levels of FXIIIa is merited in QPD patients to determine if there is a systemic reduction of circulating FXIIIa. If total circulating FXIIIa levels are depleted in QPD patients, a plausible remedy is prophylactic treatment of recombinant FXIII. Correcting FXIII levels in QPD patients could serve to reduce the bleeding tendency by contributing to clot stability. However, examination of QPD patient FXIII levels might well find that FXIII levels are normal. This is a likely finding as presumably FXIIIa (the active enzyme) would only be susceptible to an increased rate of degradation only at sites of active clotting, where FXIIIa is expected to be generated. In this scenario, the local concentration of FXIIIa could be inadequate to stabilize the clot due to a faster rate of

degradation, without affecting total FXIII levels. If there is an increased rate of FXIIIa degradation at the site of clotting, such that the clot is inadequately stabilized without affected total FXIII levels, prophylactic recombinant FXIII treatment could prove beneficial as well. The reason being is that if physiological FXIII levels are insufficient to counteract the elevated rate of FXIIIa degradation at the site of active clotting, then supra-physiological levels of systemic FXIII might prove sufficient to normalize the local FXIIIa concentration at the site of clotting.

Another relevant hyperfibrinolytic situation, where plasmin-mediated FXIIIa depletion could be taking place, is patients suffering from trauma-induced coagulopathy (TIC). Patients with TIC suffer from significant activation of coagulation (following a traumatic event), hyperfibrinolysis and depletion of key coagulation enzymes [399]. The result is rapid exsanguination and death even after several transfusions [399]. The hyperfibrinolytic state is especially devastating in TIC because not only is acute clot formation at the site of bleeding inhibited, but the systemic activation of the fibrinolytic depletes critical clotting factors systemically. TIC patients could also be suffering from depleted FXIII(a) levels, either systemically (FXIII) or locally at the sites of active clotting (FXIIIa). As such, these patients could benefit with co-administration of recombinant FXIII and blood product transfusions. However, due to the sustained and elevated hyperfibrinolytic nature of TIC, rapid clearance of any administered recombinant FXIII is expected. As such, a recombinant FXIII could be generated with the newly identified primary plasmin cleavage site residue, K468, mutated to increase the half-life of plasmin mediated-FXIIIa degradation in hyperfibrinolytic environments. This strategy could prove beneficial for treatment of TIC as administration of degradation-resistant FXIII will work synergistically with blood product transfusions, particularly during clot

formation at sites of active bleeding to reduce or prevent exsanguination which would buy time for other treatments to take effect.

7.2.3 Exploring the pathological significance of the interactions between platelet FXIIIa and platelet Aβ/APP

Future work should examine the role of FXIIIa-mediated Aβ cross-linking in CAA and AD. This can be done by crossing an AD mouse model (Tg2576) with a FXIII-A KO mouse, to generate a double transgenic AD/FXIII KO model (Tg2576/F13A1$^{-/-}$). These mice will have elevated levels of APP and Aβ as well as associated AD pathological hallmarks such as amyloid plaques in the brain parenchyma and Aβ deposition in the cerebrovasculature [400], but no FXIIIa activity. Accumulation of Aβ in the brain and cerebrovasculature could then be monitored and compared to standard AD mice. The hypothesis being that if FXIIIa activity contributes to Aβ deposition (as in CAA) by cross-linking Aβ, then the absence of FXIIIa could potentially alleviate this pathology. In addition, to further investigate the platelet-specific role to CAA and AD pathology, a platelet-specific knockout of FXIII-A could be done in an AD mouse model, and progression of Aβ accumulation could be monitored. As platelets are a contributing factor in AD and CAA pathogenesis, the purpose here would be to establish the platelet-specific contribution of FXIII to AD and CAA pathogenesis. If a deficiency of FXIIIa activity improves disease progression in AD mice, a strategy for treating AD in humans could be downregulation of platelet FXIIIa using lipid nanoparticles loaded with anti-FXIII-A siRNA targeting the bone marrow. This strategy would allow for controlled downregulation of FXIIIa in MK cells and subsequently platelets to reduce disease AD progression. This strategy could be especially beneficial to patients with FAD, which have a rapidly accelerated rate of Aβ deposition.

An apparent contradiction and a weakness of the above strategy is the work demonstrating reduced levels of FXIIIa activity accelerating platelet APP processing. Thus, downregulation of platelet FXIIIa could have the opposite effect of the intended outcome, resulting in elevated rates of APP processing and Aβ release and deposition in the cerebrovasculature. And so, if downregulation of platelet FXIIIa exacerbates AD and CAA progression, the strategy could then be to upregulate platelet FXIIIa using lipid nanoparticles loaded with FXIII-A mRNA targeting the bone marrow. The elevated platelet FXIIIa levels could protect platelet APP from processing and potentially reduce system Aβ burden and AD progression. The distinction in divergent outcomes comes from the gap in knowledge underlying the platelet-specific contribution of FXIII and APP to the deposition of Aβ in the cerebrovasculature. It is likely that both mechanisms occur simultaneously, i.e. FXIIIa contributes to CAA pathology by cross-linking released Aβ along the cerebrovasculature, as well as, FXIIIa can stabilize platelet APP and inhibit processing and release of Aβ. However, at different stages during AD and CAA pathology, each mechanism could play a dominant role to the overall contribution of disease. For example, early during AD and CAA pathogenesis, before Aβ deposition is prevalent, stabilizing full-length platelet APP could prove beneficial to reduce the local concentration of Aβ at sites of platelet activation, particularly in and around the cerebrovasculature. Alternatively, as AD and CAA pathology progresses, and Aβ deposition along the cerebrovasculature is prevalent, downregulation of platelet FXIII could prove more beneficial by reducing cross-linking of Aβ and deposited fibrinogen which have been found to co-deposit at sites of CAA plaques. As the underlying and temporal molecular mechanisms surrounding CAA pathology remain largely a mystery, the experiments outlined here to

determine the underlying contribution of FXIIIa could prove very insightful in developing a more comprehensive picture of this pathology.

Finally, further investigations should be done into determining the molecular mechanism behind how FXIIIa activity prevents APP processing. Currently, a likely candidate is the FXIIIa-mediated serotonylation of APP at Gln-686, near the α-secretase cleavage site [379]. The significance of FXIIIa-mediated serotonylation of APP at this site should be examined in AD (Tg2576) mice with a residue mutation at that site. The predicted outcome is that without serotonylation of APP at Gln-686, the α-secretase cleavage site remains exposed, and APP processing would be accelerated and AD progression would be exacerbated. If this is the case, then a novel treatment for AD in humans could be developing a monoclonal antibody against Gln-686 on APP. The effect of an antibody binding to Gln-686 on APP would be similar to that of serotonylation at that site, in that it would block the α-secretase cleavage site. Preventing APP processing using antibodies would likely be far more effective and rapid than FXIIIa-mediated serotonylation as FXIIIa has many other competing substrates.

7.2.4 Investigating the molecular mechanism behind the bleeding phenotype in APP KO mice

Further characterization of the bleeding phenotype in APP mice is merited. Initially, studies should be done comparing bleeding in WT and APP KO mice using different models of hemorrhage to determine in what types of injuries APP plays a role in hemostasis [390]. The prediction is that APP is likely to play a pro-coagulant in arterial bleeds as these bleeds are more dependent on platelet function [391]. Furthermore, the specific contribution of platelet APP should be validated as previous experiments were done with APP KO mice, which are

systemically deficient in APP. This can be done by looking at bleeding in WT mice with an APP KO bone marrow transplant. As the MK cell lineage is bone marrow derived, the resulting platelets would also be deficient in APP. The expected outcome would be that mice with platelet specific knockout of APP would have a similar bleeding phenotype as full APP KO mice. Alternatively, if mice with platelet-specific APP KO do not exhibit a bleeding phenotype, the hypothesis would be that circulating APP/Aβ from non-platelet sources contribute to hemostasis concomitantly with platelet activation, as experiments suggest both APP/Aβ and platelets to be contributing factors in the bleeding phenotype of APP KO mice.

There are numerous studies characterizing the effect of APP and its metabolites on hemostasis [24]. Investigations should focus on determining which, if any, of the proposed mechanisms are responsible for the effect on hemostasis. To determine if full-length APP or its metabolites, namely Aβ, are responsible for the bleeding phenotype in APP KO mice, WT mice could be treated with secretase inhibitors to prevent APP processing [401], and compared with untreated mice when subjected to a bleeding challenge. This experiment would determine the specific contribution of full-length APP to hemostasis compared to Aβ. As the contribution of full-length APP is inhibition of coagulation enzymes via the KPI domain [24], or platelet adhesion to deposited Aβ (which would be largely absent with inhibition of APP processing) [364, 388], the expected outcome would likely lead to a bleeding phenotype as seen in APP KO mice. The role of APP in hemostasis should also be evaluated by looking at bleeding in AD mice with accelerated APP processing and elevated Aβ levels, such as in Tg2576 mice [400]. The prediction would be that AD mice are prothrombotic, likely due to procoagulant platelets. The specific contribution of Aβ-mediated platelet activation and aggregation can be investigated by treating WT mice with antibodies targeting $A\beta_{25\text{-}35}$, which is the Aβ fragment responsible platelet

activation and aggregation [402]. The effect of secreted Aβ on platelet activation would be neutralized in these treated mice, and the overall effect on hemostasis through contributions of APP and other procoagulant functions of Aβ could be examined. Further investigations into the roles of platelet APP on hemostasis could further shed light on the procoagulant state of AD patients and lead to novel therapies by modulating platelet functions.

Bibliography

1. Leslie M. Cell biology. Beyond clotting: the powers of platelets. Science. 2010;328(5978):562-4.
2. Broos K, De Meyer SF, Feys HB, Vanhoorelbeke K, Deckmyn H. Blood platelet biochemistry. Thromb Res. 2012;129(3):245-9.
3. Murray CJ, Lopez AD. Evidence-based health policy--lessons from the Global Burden of Disease Study. Science. 1996;274(5288):740-3.
4. Sauaia A, Moore FA, Moore EE, Moser KS, Brennan R, Read RA, et al. Epidemiology of trauma deaths: a reassessment. J Trauma. 1995;38(2):185-93.
5. Tien HC, Spencer F, Tremblay LN, Rizoli SB, Brenneman FD. Preventable deaths from hemorrhage at a level I Canadian trauma center. J Trauma. 2007;62(1):142-6.
6. Pagel O, Walter E, Jurk K, Zahedi RP. Taking the stock of granule cargo: Platelet releasate proteomics. Platelets. 2017;28(2):119-28.
7. Moreno SN, Docampo R. Polyphosphate and its diverse functions in host cells and pathogens. PLoS Pathog. 2013;9(5):e1003230.
8. Choi SH, Smith SA, Morrissey JH. Polyphosphate is a cofactor for the activation of factor XI by thrombin. Blood. 2011;118(26):6963-70.
9. Puy C, Tucker EI, Wong ZC, Gailani D, Smith SA, Choi SH, et al. Factor XII promotes blood coagulation independent of factor XI in the presence of long-chain polyphosphates. Journal of Thrombosis and Haemostasis. 2013;11(7):1341-52.
10. Smith SA, Choi SH, Davis-Harrison R, Huyck J, Boettcher J, Reinstra CM, et al. Polyphosphate exerts differential effects on blood clotting, depending on polymer size. Blood. 2010;116(20):4353-9.
11. Morrissey JH, Choi SH, Smith SA. Polyphosphate: an ancient molecule that links platelets, coagulation, and inflammation. Blood. 2012;119(25):5972-9.
12. Muszbek L, Bereczky Z, Bagoly Z, Komaromi I, Katona E. Factor XIII: a coagulation factor with multiple plasmatic and cellular functions. Physiological Reviews. 2011;91(3):931-72.
13. Muszbek L, Bereczky Z, Bagoly Z, Komaromi I, Katona E. Factor XIII: a coagulation factor with multiple plasmatic and cellular functions. Physiol Rev. 2011;91(3):931-72.
14. Nikolajsen CL, Dyrlund TF, Poulsen ET, Enghild JJ, Scavenius C. Coagulation Factor XIIIa Substrates in Human Plasma Identification and Incorporation into the Clot. J Biol Chem. 2014;289(10):6526-34.
15. Weisel JW, Medved L. The structure and function of the alpha C domains of fibrinogen. Annals of the New York Academy of Sciences. 2001;936:312-27.
16. Rider DM, McDonagh J. Resistance of factor XIII to degradation or activation by plasmin. Biochimica Et Biophysica Acta. 1981;675(2):171-7.
17. Greenberg SM, Bacskai BJ, Hernandez-Guillamon M, Pruzin J, Sperling R, van Veluw SJ. Cerebral amyloid angiopathy and Alzheimer disease - one peptide, two pathways. Nat Rev Neurol. 2020;16(1):30-42.
18. de Jager M, Boot MV, Bol J, Breve JJP, Jongenelen CAM, Drukarch B, et al. The blood clotting Factor XIIIa forms unique complexes with amyloid-beta (A) and colocalizes with deposited A in cerebral amyloid angiopathy. Neuropathology and Applied Neurobiology. 2016;42(3):255-72.

19. Canobbio I, Abubaker AA, Visconte C, Torti M, Pula G. Role of amyloid peptides in vascular dysfunction and platelet dysregulation in Alzheimer's disease. Frontiers in Cellular Neuroscience. 2015;9:15.
20. O'Brien RJ, Wong PC. Amyloid Precursor Protein Processing and Alzheimer's Disease. In: Hyman SE, Jessell TM, Shatz CJ, Stevens CF, Zoghbi HY, editors. Annual Review of Neuroscience, Vol 34. Annual Review of Neuroscience. 34. Palo Alto: Annual Reviews; 2011. p. 185-204.
21. Li QX, Berndt MC, Bush AI, Rumble B, Mackenzie I, Friedhuber A, et al. Membrane-associated forms of the beta-A4 amyloid protein-precursor of Alzheimers-disease in human platelet and brain - surface expression on the activated human platelet. Blood. 1994;84(1):133-42.
22. Li QX, Whyte S, Tanner JE, Evin G, Beyreuther K, Masters CL. Secretion of Alzheimer's disease A beta amyloid peptide by activated human platelets. Laboratory Investigation. 1998;78(4):461-9.
23. Hur WS, Mazinani N, Lu XJD, Yefet LS, Byrnes JR, Ho L, et al. Coagulation factor XIIIa cross-links amyloid β into dimers and oligomers and to blood proteins. J Biol Chem. 2019;294(2):390-6.
24. Schmaier AH. The amyloid beta-precursor protein-The unappreciated cerebral anticoagulant. Thromb Res. 2017;155:149-51.
25. Zamolodchikov D, Renne T, Strickland S. The Alzheimer's disease peptide beta-amyloid promotes thrombin generation through activation of coagulation factor XII. J Thromb Haemost. 2016;14(5):995-1007.
26. Abubaker AA, Vara D, Visconte C, Eggleston I, Torti M, Canobbio I, et al. Amyloid Peptide beta1-42 Induces Integrin alphaIIbbeta3 Activation, Platelet Adhesion, and Thrombus Formation in a NADPH Oxidase-Dependent Manner. Oxid Med Cell Longev. 2019;2019:1050476.
27. Sonkar VK, Kulkarni PP, Dash D. Amyloid beta peptide stimulates platelet activation through RhoA-dependent modulation of actomyosin organization. Faseb Journal. 2014;28(4):1819-29.
28. Zamolodchikov D, Berk-Rauch HE, Oren DA, Stor DS, Singh PK, Kawasaki M, et al. Biochemical and structural analysis of the interaction between beta-amyloid and fibrinogen. Blood. 2016;128(8):1144-51.
29. Wu W, Li H, Navaneetham D, Reichenbach ZW, Tuma RF, Walsh PN. The kunitz protease inhibitor domain of protease nexin-2 inhibits factor XIa and murine carotid artery and middle cerebral artery thrombosis. Blood. 2012;120(3):671-7.
30. Canobbio I, Visconte C, Momi S, Guidetti GF, Zara M, Canino J, et al. Platelet amyloid precursor protein is a modulator of venous thromboembolism in mice. Blood. 2017;130(4):527-36.
31. Kazmi RS, Boyce S, Lwaleed BA. Homeostasis of Hemostasis: The Role of Endothelium. Semin Thromb Hemost. 2015;41(6):549-55.
32. Winter WE, Flax SD, Harris NS. Coagulation Testing in the Core Laboratory. Lab Med. 2017;48(4):295-313.
33. Di Stasio E, De Cristofaro R. The effect of shear stress on protein conformation: Physical forces operating on biochemical systems: The case of von Willebrand factor. Biophys Chem. 2010;153(1):1-8.
34. Nieswandt B, Watson SP. Platelet-collagen interaction: is GPVI the central receptor? Blood. 2003;102(2):449-61.

35. Savage B, Almus-Jacobs F, Ruggeri ZM. Specific synergy of multiple substrate-receptor interactions in platelet thrombus formation under flow. Cell. 1998;94(5):657-66.
36. Nieswandt B, Brakebusch C, Bergmeier W, Schulte V, Bouvard D, Mokhtari-Nejad R, et al. Glycoprotein VI but not alpha2beta1 integrin is essential for platelet interaction with collagen. EMBO J. 2001;20(9):2120-30.
37. Lee D, Fong KP, King MR, Brass LF, Hammer DA. Differential dynamics of platelet contact and spreading. Biophys J. 2012;102(3):472-82.
38. Mills DC. ADP receptors on platelets. Thromb Haemost. 1996;76(6):835-56.
39. Hanasaki K, Arita H. Characterization of thromboxane A2/prostaglandin H2 (TXA2/PGH2) receptors of rat platelets and their interaction with TXA2/PGH2 receptor antagonists. Biochem Pharmacol. 1988;37(20):3923-9.
40. Varga-Szabo D, Pleines I, Nieswandt B. Cell adhesion mechanisms in platelets. Arterioscler Thromb Vasc Biol. 2008;28(3):403-12.
41. Falati S, Gross P, Merrill-Skoloff G, Furie BC, Furie B. Real-time in vivo imaging of platelets, tissue factor and fibrin during arterial thrombus formation in the mouse. Nat Med. 2002;8(10):1175-81.
42. Furie B. Pathogenesis of thrombosis. Hematology Am Soc Hematol Educ Program. 2009:255-8.
43. Mackman N, Tilley RE, Key NS. Role of the extrinsic pathway of blood coagulation in hemostasis and thrombosis. Arterioscler Thromb Vasc Biol. 2007;27(8):1687-93.
44. Owens AP, 3rd, Mackman N. Tissue factor and thrombosis: The clot starts here. Thromb Haemost. 2010;104(3):432-9.
45. Owens AP, Mackman N. Tissue factor and thrombosis: The clot starts here. Thromb Haemost. 2010;104(3):432-9.
46. Dahlback B. Blood coagulation. Lancet. 2000;355(9215):1627-32.
47. Mosesson MW. Fibrinogen and fibrin structure and functions. J Thromb Haemost. 2005;3(8):1894-904.
48. Lane DA, Philippou H, Huntington JA. Directing thrombin. Blood. 2005;106(8):2605-12.
49. Maas C, Renne T. Coagulation factor XII in thrombosis and inflammation. Blood. 2018;131(17):1903-9.
50. Kahn ML, Zheng YW, Huang W, Bigornia V, Zeng D, Moff S, et al. A dual thrombin receptor system for platelet activation. Nature. 1998;394(6694):690-4.
51. Aleman MM, Byrnes JR, Wang JG, Tran R, Lam WA, Di Paola J, et al. Factor XIII activity mediates red blood cell retention in venous thrombi. Journal of Clinical Investigation. 2014;124(8):3590-600.
52. Hoppe B. Fibrinogen and factor XIII at the intersection of coagulation, fibrinolysis and inflammation. Thromb Haemost. 2014;112(4):649-58.
53. Gebbink MF. Tissue-type plasminogen activator-mediated plasminogen activation and contact activation, implications in and beyond haemostasis. J Thromb Haemost. 2011;9 Suppl 1:174-81.
54. Foley JH. Plasmin(ogen) at the Nexus of Fibrinolysis, Inflammation, and Complement. Seminars in thrombosis and hemostasis. 2017;43(2):135-42.
55. Lijnen HR, Zamarron C, Blaber M, Winkler ME, Collen D. Activation of plasminogen by pro-urokinase. I. Mechanism. J Biol Chem. 1986;261(3):1253-8.

56. Di Nisio M, Squizzato A, Rutjes AW, Buller HR, Zwinderman AH, Bossuyt PM. Diagnostic accuracy of D-dimer test for exclusion of venous thromboembolism: a systematic review. Journal of thrombosis and haemostasis : JTH. 2007;5(2):296-304.
57. Foley JH, Cook PF, Nesheim ME. Kinetics of activated thrombin-activatable fibrinolysis inhibitor (TAFIa)-catalyzed cleavage of C-terminal lysine residues of fibrin degradation products and removal of plasminogen-binding sites. J Biol Chem. 2011;286(22):19280-6.
58. van Hinsbergh VWM. Endothelium-role in regulation of coagulation and inflammation. Semin Immunopathol. 2012;34(1):93-106.
59. Marcus AJ, Broekman MJ, Drosopoulos JH, Islam N, Alyonycheva TN, Safier LB, et al. The endothelial cell ecto-ADPase responsible for inhibition of platelet function is CD39. J Clin Invest. 1997;99(6):1351-60.
60. Liu J, Pedersen LC. Anticoagulant heparan sulfate: structural specificity and biosynthesis. Appl Microbiol Biotechnol. 2007;74(2):263-72.
61. Crawley JT, Lane DA. The haemostatic role of tissue factor pathway inhibitor. Arterioscler Thromb Vasc Biol. 2008;28(2):233-42.
62. Mohan Rao LV, Esmon CT, Pendurthi UR. Endothelial cell protein C receptor: a multiliganded and multifunctional receptor. Blood. 2014;124(10):1553-62.
63. Esmon CT. The protein C pathway. Chest. 2003;124(3 Suppl):26S-32S.
64. Quach ME, Chen WC, Li RH. Mechanisms of platelet clearance and translation to improve platelet storage. Blood. 2018;131(14):1512-21.
65. Italiano JE, Lecine P, Shivdasani RA, Hartwig JH. Blood platelets are assembled principally at the ends of proplatelet processes produced by differentiated megakaryocytes. J Cell Biol. 1999;147(6):1299-312.
66. Lefrancais E, Ortiz-Munoz G, Caudrillier A, Mallavia B, Liu FC, Sayah DM, et al. The lung is a site of platelet biogenesis and a reservoir for haematopoietic progenitors. Nature. 2017;544(7648):105-+.
67. Gremmel T, Frelinger AL, Michelson AD. Platelet Physiology. Seminars in Thrombosis and Hemostasis. 2016;42(3):191-204.
68. Broos K, Feys HB, De Meyer SF, Vanhoorelbeke K, Deckmyn H. Platelets at work in primary hemostasis. Blood Rev. 2011;25(4):155-67.
69. Selvadurai MV, Hamilton JR. Structure and function of the open canalicular system - the platelet's specialized internal membrane network. Platelets. 2018;29(4):319-25.
70. Escolar G, Leistikow E, White JG. The Fate of the Open Canalicular System in Surface and Suspension-Activated Platelets. Blood. 1989;74(6):1983-8.
71. Hartwig JH. The platelet: Form and function. Semin Hematol. 2006;43(1):S94-S100.
72. Golebiewska EM, Poole AW. Platelet secretion: From haemostasis to wound healing and beyond. Blood Reviews. 2015;29(3):153-62.
73. Blair P, Flaumenhaft R. Platelet alpha-granules: Basic biology and clinical correlates. Blood Rev. 2009;23(4):177-89.
74. Meyers KM, Holmsen H, Seachord CL. Comparative-Study of Platelet Dense Granule Constituents. American Journal of Physiology. 1982;243(3):R454-R61.
75. Holmsen H, Weiss HJ. Secretable Storage Pools in Platelets. Annu Rev Med. 1979;30:119-34.
76. Rumbaut RE, Thiagarajan P. Platelet-Vessel Wall Interactions in Hemostasis and Thrombosis. Platelet-Vessel Wall Interactions in Hemostasis and Thrombosis. Integrated Systems Physiology: from Molecule to Function to Disease. San Rafael (CA)2010.

77. McCarty OJ, Zhao Y, Andrew N, Machesky LM, Staunton D, Frampton J, et al. Evaluation of the role of platelet integrins in fibronectin-dependent spreading and adhesion. Journal of thrombosis and haemostasis : JTH. 2004;2(10):1823-33.
78. Inoue O, Suzuki-Inoue K, McCarty OJ, Moroi M, Ruggeri ZM, Kunicki TJ, et al. Laminin stimulates spreading of platelets through integrin alpha6beta1-dependent activation of GPVI. Blood. 2006;107(4):1405-12.
79. Mazzucato M, Pradella P, Cozzi MR, De Marco L, Ruggeri ZM. Sequential cytoplasmic calcium signals in a 2-stage platelet activation process induced by the glycoprotein Ibalpha mechanoreceptor. Blood. 2002;100(8):2793-800.
80. Chen H, Kahn ML. Reciprocal signaling by integrin and nonintegrin receptors during collagen activation of platelets. Mol Cell Biol. 2003;23(14):4764-77.
81. Pugh N, Simpson AM, Smethurst PA, de Groot PG, Raynal N, Farndale RW. Synergism between platelet collagen receptors defined using receptor-specific collagen-mimetic peptide substrata in flowing blood. Blood. 2010;115(24):5069-79.
82. Siljander PR, Munnix IC, Smethurst PA, Deckmyn H, Lindhout T, Ouwehand WH, et al. Platelet receptor interplay regulates collagen-induced thrombus formation in flowing human blood. Blood. 2004;103(4):1333-41.
83. Ruggeri ZM, Mendolicchio GL. Adhesion mechanisms in platelet function. Circ Res. 2007;100(12):1673-85.
84. Du X. Signaling and regulation of the platelet glycoprotein Ib-IX-V complex. Current opinion in hematology. 2007;14(3):262-9.
85. Varga-Szabo D, Braun A, Nieswandt B. Calcium signaling in platelets. J Thromb Haemost. 2009;7(7):1057-66.
86. Hollopeter G, Jantzen HM, Vincent D, Li G, England L, Ramakrishnan V, et al. Identification of the platelet ADP receptor targeted by antithrombotic drugs. Nature. 2001;409(6817):202-7.
87. Leon C, Hechler B, Freund M, Eckly A, Vial C, Ohlmann P, et al. Defective platelet aggregation and increased resistance to thrombosis in purinergic P2Y(1) receptor-null mice. J Clin Invest. 1999;104(12):1731-7.
88. Habib A, FitzGerald GA, Maclouf J. Phosphorylation of the thromboxane receptor alpha, the predominant isoform expressed in human platelets. J Biol Chem. 1999;274(5):2645-51.
89. Li N, Wallen NH, Ladjevardi M, Hjemdahl P. Effects of serotonin on platelet activation in whole blood. Blood Coagul Fibrinolysis. 1997;8(8):517-23.
90. Brass LF, Molino M. Protease-activated G protein-coupled receptors on human platelets and endothelial cells. Thromb Haemost. 1997;78(1):234-41.
91. Nieswandt B, Schulte V, Zywietz A, Gratacap MP, Offermanns S. Costimulation of Gi- and G12/G13-mediated signaling pathways induces integrin alpha IIbbeta 3 activation in platelets. J Biol Chem. 2002;277(42):39493-8.
92. Anthis NJ, Wegener KL, Ye F, Kim C, Goult BT, Lowe ED, et al. The structure of an integrin/talin complex reveals the basis of inside-out signal transduction. EMBO J. 2009;28(22):3623-32.
93. Shattil SJ, Kim C, Ginsberg MH. The final steps of integrin activation: the end game. Nat Rev Mol Cell Biol. 2010;11(4):288-300.
94. Berger G, Masse JM, Cramer EM. Alpha-granule membrane mirrors the platelet plasma membrane and contains the glycoproteins Ib, IX, and V. Blood. 1996;87(4):1385-95.

95. Maynard DM, Heijnen HF, Horne MK, White JG, Gahl WA. Proteomic analysis of platelet alpha-granules using mass spectrometry. Journal of thrombosis and haemostasis : JTH. 2007;5(9):1945-55.
96. Periayah MH, Halim AS, Mat Saad AZ. Mechanism Action of Platelets and Crucial Blood Coagulation Pathways in Hemostasis. Int J Hematol Oncol Stem Cell Res. 2017;11(4):319-27.
97. Clark SR, Thomas CP, Hammond VJ, Aldrovandi M, Wilkinson GW, Hart KW, et al. Characterization of platelet aminophospholipid externalization reveals fatty acids as molecular determinants that regulate coagulation. Proc Natl Acad Sci U S A. 2013;110(15):5875-80.
98. Labberton L, Kenne E, Long AT, Nickel KF, Di Gennaro A, Rigg RA, et al. Neutralizing blood-borne polyphosphate in vivo provides safe thromboprotection. Nat Commun. 2016;7:12616.
99. Wijeyewickrema LC, Lameignere E, Hor L, Duncan RC, Shiba T, Travers RJ, et al. Polyphosphate is a novel cofactor for regulation of complement by a serpin, C1 inhibitor. Blood. 2016;128(13):1766-76.
100. Morel O, Morel N, Freyssinet JM, Toti F. Platelet microparticles and vascular cells interactions: a checkpoint between the haemostatic and thrombotic responses. Platelets. 2008;19(1):9-23.
101. Zubairova LD, Nabiullina RM, Nagaswami C, Zuev YF, Mustafin IG, Litvinov RI, et al. Circulating Microparticles Alter Formation, Structure, and Properties of Fibrin Clots. Sci Rep. 2015;5:17611.
102. Stalker TJ, Newman DK, Ma P, Wannemacher KM, Brass LF. Platelet signaling. Handb Exp Pharmacol. 2012(210):59-85.
103. Samson AL, Alwis I, Maclean JAA, Priyananda P, Hawkett B, Schoenwaelder SM, et al. Endogenous fibrinolysis facilitates clot retraction in vivo. Blood. 2017;130(23):2453-62.
104. Smyth SS, McEver RP, Weyrich AS, Morrell CN, Hoffman MR, Arepally GM, et al. Platelet functions beyond hemostasis. J Thromb Haemost. 2009;7(11):1759-66.
105. Zarbock A, Polanowska-Grabowska RK, Ley K. Platelet-neutrophil-interactions: linking hemostasis and inflammation. Blood Rev. 2007;21(2):99-111.
106. Nomura S, Okamae F, Abe M, Hosokawa M, Yamaoka M, Ohtani T, et al. Platelets expressing P-selectin and platelet-derived microparticles in stored platelet concentrates bind to PSGL-1 on filtrated leukocytes. Clin Appl Thromb Hemost. 2000;6(4):213-21.
107. von Hundelshausen P, Koenen RR, Sack M, Mause SF, Adriaens W, Proudfoot AE, et al. Heterophilic interactions of platelet factor 4 and RANTES promote monocyte arrest on endothelium. Blood. 2005;105(3):924-30.
108. Pervushina O, Scheuerer B, Reiling N, Behnke L, Schroder JM, Kasper B, et al. Platelet factor 4/CXCL4 induces phagocytosis and the generation of reactive oxygen metabolites in mononuclear phagocytes independently of Gi protein activation or intracellular calcium transients. J Immunol. 2004;173(3):2060-7.
109. Gleissner CA, von Hundelshausen P, Ley K. Platelet chemokines in vascular disease. Arterioscler Thromb Vasc Biol. 2008;28(11):1920-7.
110. Xia CQ, Kao KJ. Effect of CXC chemokine platelet factor 4 on differentiation and function of monocyte-derived dendritic cells. Int Immunol. 2003;15(8):1007-15.
111. Kasper B, Brandt E, Ernst M, Petersen F. Neutrophil adhesion to endothelial cells induced by platelet factor 4 requires sequential activation of Ras, Syk, and JNK MAP kinases. Blood. 2006;107(5):1768-75.

112. Duerschmied D, Suidan GL, Demers M, Herr N, Carbo C, Brill A, et al. Platelet serotonin promotes the recruitment of neutrophils to sites of acute inflammation in mice. Blood. 2013;121(6):1008-15.
113. Sprague DL, Elzey BD, Crist SA, Waldschmidt TJ, Jensen RJ, Ratliff TL. Platelet-mediated modulation of adaptive immunity: unique delivery of CD154 signal by platelet-derived membrane vesicles. Blood. 2008;111(10):5028-36.
114. Elzey BD, Schmidt NW, Crist SA, Kresowik TP, Harty JT, Nieswandt B, et al. Platelet-derived CD154 enables T-cell priming and protection against Listeria monocytogenes challenge. Blood. 2008;111(7):3684-91.
115. Kissel K, Berber S, Nockher A, Santoso S, Bein G, Hackstein H. Human platelets target dendritic cell differentiation and production of proinflammatory cytokines. Transfusion. 2006;46(5):818-27.
116. Kraemer BF, Campbell RA, Schwertz H, Cody MJ, Franks Z, Tolley ND, et al. Novel anti-bacterial activities of beta-defensin 1 in human platelets: suppression of pathogen growth and signaling of neutrophil extracellular trap formation. PLoS Pathog. 2011;7(11):e1002355.
117. Valle-Jimenez X, Ramirez-Cosmes A, Aquino-Dominguez AS, Sanchez-Pena F, Bustos-Arriaga J, Romero-Tlalolini MLA, et al. Human platelets and megakaryocytes express defensin alpha 1. Platelets. 2019:1-11.
118. Yeaman MR. Platelets: at the nexus of antimicrobial defence. Nat Rev Microbiol. 2014;12(6):426-37.
119. Clark SR, Ma AC, Tavener SA, McDonald B, Goodarzi Z, Kelly MM, et al. Platelet TLR4 activates neutrophil extracellular traps to ensnare bacteria in septic blood. Nat Med. 2007;13(4):463-9.
120. Jenne CN, Wong CH, Zemp FJ, McDonald B, Rahman MM, Forsyth PA, et al. Neutrophils recruited to sites of infection protect from virus challenge by releasing neutrophil extracellular traps. Cell Host Microbe. 2013;13(2):169-80.
121. Gaertner F, Ahmad Z, Rosenberger G, Fan S, Nicolai L, Busch B, et al. Migrating Platelets Are Mechano-scavengers that Collect and Bundle Bacteria. Cell. 2017;171(6):1368-82 e23.
122. Battinelli EM, Markens BA, Italiano JE, Jr. Release of angiogenesis regulatory proteins from platelet alpha granules: modulation of physiologic and pathologic angiogenesis. Blood. 2011;118(5):1359-69.
123. Li L, Blumenthal DK, Terry CM, He Y, Carlson ML, Cheung AK. PDGF-induced proliferation in human arterial and venous smooth muscle cells: molecular basis for differential effects of PDGF isoforms. Journal of cellular biochemistry. 2011;112(1):289-98.
124. Massberg S, Konrad I, Schurzinger K, Lorenz M, Schneider S, Zohlnhoefer D, et al. Platelets secrete stromal cell-derived factor 1alpha and recruit bone marrow-derived progenitor cells to arterial thrombi in vivo. J Exp Med. 2006;203(5):1221-33.
125. Salvucci O, Yao L, Villalba S, Sajewicz A, Pittaluga S, Tosato G. Regulation of endothelial cell branching morphogenesis by endogenous chemokine stromal-derived factor-1. Blood. 2002;99(8):2703-11.
126. Gawaz M, Vogel S. Platelets in tissue repair: control of apoptosis and interactions with regenerative cells. Blood. 2013;122(15):2550-4.
127. Erpenbeck L, Schon MP. Deadly allies: the fatal interplay between platelets and metastasizing cancer cells. Blood. 2010;115(17):3427-36.

128. Dvorak HF, Detmar M, Claffey KP, Nagy JA, van de Water L, Senger DR. Vascular permeability factor/vascular endothelial growth factor: an important mediator of angiogenesis in malignancy and inflammation. Int Arch Allergy Immunol. 1995;107(1-3):233-5.
129. Goel HL, Mercurio AM. VEGF targets the tumour cell. Nat Rev Cancer. 2013;13(12):871-82.
130. Bambace NM, Holmes CE. The platelet contribution to cancer progression. Journal of thrombosis and haemostasis : JTH. 2011;9(2):237-49.
131. Morrell CN, Sun H, Swaim AM, Baldwin WM, 3rd. Platelets an inflammatory force in transplantation. Am J Transplant. 2007;7(11):2447-54.
132. Zarbock A, Ley K. The role of platelets in acute lung injury (ALI). Front Biosci (Landmark Ed). 2009;14:150-8.
133. McCormack G, Moriarty D, O'Donoghue DP, McCormick PA, Sheahan K, Baird AW. Tissue cytokine and chemokine expression in inflammatory bowel disease. Inflamm Res. 2001;50(10):491-5.
134. Ulfman LH, Joosten DP, van Aalst CW, Lammers JW, van de Graaf EA, Koenderman L, et al. Platelets promote eosinophil adhesion of patients with asthma to endothelium under flow conditions. Am J Respir Cell Mol Biol. 2003;28(4):512-9.
135. Docampo R, Ulrich P, Moreno SN. Evolution of acidocalcisomes and their role in polyphosphate storage and osmoregulation in eukaryotic microbes. Philos Trans R Soc Lond B Biol Sci. 2010;365(1541):775-84.
136. Travers RJ, Smith SA, Morrissey JH. Polyphosphate, platelets, and coagulation. Int J Lab Hematol. 2015;37 Suppl 1:31-5.
137. Ruiz FA, Lea CR, Oldfield E, Docampo R. Human platelet dense granules contain polyphosphate and are similar to acidocalcisomes of bacteria and unicellular eukaryotes. J Biol Chem. 2004;279(43):44250-7.
138. Choi SH, Smith SA, Morrissey JH. Polyphosphate accelerates factor V activation by factor XIa. Thromb Haemost. 2015;113(3):599-604.
139. Puy C, Tucker EI, Ivanov IS, Gailani D, Smith SA, Morrissey JH, et al. Platelet-Derived Short-Chain Polyphosphates Enhance the Inactivation of Tissue Factor Pathway Inhibitor by Activated Coagulation Factor XI. Plos One. 2016;11(10):e0165172.
140. Mutch NJ, Engel R, Uitte de Willige S, Philippou H, Ariens RA. Polyphosphate modifies the fibrin network and down-regulates fibrinolysis by attenuating binding of tPA and plasminogen to fibrin. Blood. 2010;115(19):3980-8.
141. Smith SA, Mutch NJ, Baskar D, Rohloff P, Docampo R, Morrissey JH. Polyphosphate modulates blood coagulation and fibrinolysis. Proc Natl Acad Sci U S A. 2006;103(4):903-8.
142. Muller F, Mutch NJ, Schenk WA, Smith SA, Esterl L, Spronk HM, et al. Platelet Polyphosphates Are Proinflammatory and Procoagulant Mediators In Vivo. Cell. 2009;139(6):1143-56.
143. Verhoef JJ, Barendrecht AD, Nickel KF, Dijkxhoorn K, Kenne E, Labberton L, et al. Polyphosphate nanoparticles on the platelet surface trigger contact system activation. Blood. 2017;129(12):1707-17.
144. Smith SA, Choi SH, Collins JNR, Travers RJ, Cooley BC, Morrissey JH. Inhibition of polyphosphate as a novel strategy for preventing thrombosis and inflammation. Blood. 2012;120(26):5103-10.

145. Travers RJ, Shenoi RA, Kalathottukaren MT, Kizhakkedathu JN, Morrissey JH. Nontoxic polyphosphate inhibitors reduce thrombosis while sparing hemostasis. Blood. 2014;124(22):3183-90.
146. Kudela D, Smith SA, May-Masnou A, Braun GB, Pallaoro A, Nguyen CK, et al. Clotting Activity of Polyphosphate-Functionalized Silica Nanoparticles. Angew Chem-Int Edit. 2015;54(13):4018-22.
147. Weidmann H, Heikaus L, Long AT, Naudin C, Schluter H, Renne T. The plasma contact system, a protease cascade at the nexus of inflammation, coagulation and immunity. Biochim Biophys Acta Mol Cell Res. 2017;1864(11 Pt B):2118-27.
148. Naudin C, Burillo E, Blankenberg S, Butler L, Renne T. Factor XII Contact Activation. Seminars in thrombosis and hemostasis. 2017;43(8):814-26.
149. Kannemeier C, Shibamiya A, Nakazawa F, Trusheim H, Ruppert C, Markart P, et al. Extracellular RNA constitutes a natural procoagulant cofactor in blood coagulation. Proc Natl Acad Sci U S A. 2007;104(15):6388-93.
150. von Bruhl ML, Stark K, Steinhart A, Chandraratne S, Konrad I, Lorenz M, et al. Monocytes, neutrophils, and platelets cooperate to initiate and propagate venous thrombosis in mice in vivo. J Exp Med. 2012;209(4):819-35.
151. van der Meijden PE, Munnix IC, Auger JM, Govers-Riemslag JW, Cosemans JM, Kuijpers MJ, et al. Dual role of collagen in factor XII-dependent thrombus formation. Blood. 2009;114(4):881-90.
152. Sala-Cunill A, Bjorkqvist J, Senter R, Guilarte M, Cardona V, Labrador M, et al. Plasma contact system activation drives anaphylaxis in severe mast cell-mediated allergic reactions. J Allergy Clin Immunol. 2015;135(4):1031-43 e6.
153. Engel R, Brain CM, Paget J, Lionikiene AS, Mutch NJ. Single-chain factor XII exhibits activity when complexed to polyphosphate. J Thromb Haemost. 2014;12(9):1513-22.
154. Renne T, Schmaier AH, Nickel KF, Blomback M, Maas C. In vivo roles of factor XII. Blood. 2012;120(22):4296-303.
155. Colman RW, Schmaier AH. Contact system: a vascular biology modulator with anticoagulant, profibrinolytic, antiadhesive, and proinflammatory attributes. Blood. 1997;90(10):3819-43.
156. Schmaier AH, McCrae KR. The plasma kallikrein-kinin system: its evolution from contact activation. Journal of thrombosis and haemostasis : JTH. 2007;5(12):2323-9.
157. Wheeler AP, Gailani D. The Intrinsic Pathway of Coagulation as a Target for Antithrombotic Therapy. Hematol Oncol Clin North Am. 2016;30(5):1099-114.
158. Fernandes HD, Newton S, Rodrigues JM. Factor XII Deficiency Mimicking Bleeding Diathesis: A Unique Presentation and Diagnostic Pitfall. Cureus. 2018;10(6):e2817.
159. Kleinschnitz C, Stoll G, Bendszus M, Schuh K, Pauer HU, Burfeind P, et al. Targeting coagulation factor XII provides protection from pathological thrombosis in cerebral ischemia without interfering with hemostasis. J Exp Med. 2006;203(3):513-8.
160. Worm M, Kohler EC, Panda R, Long A, Butler LM, Stavrou EX, et al. The factor XIIa blocking antibody 3F7: a safe anticoagulant with anti-inflammatory activities. Ann Transl Med. 2015;3(17):247.
161. Tans G, Rosing J. Structural and Functional-Characterization of Factor-Xii. Seminars in thrombosis and hemostasis. 1987;13(1):1-14.
162. Renne T, Stavrou EX. Roles of Factor XII in Innate Immunity. Front Immunol. 2019;10:2011.

163. Borissoff JI, Heeneman S, Kilinc E, Kassak P, Van Oerle R, Winckers K, et al. Early atherosclerosis exhibits an enhanced procoagulant state. Circulation. 2010;122(8):821-30.
164. Renne T, Pozgajova M, Gruner S, Schuh K, Pauer HU, Burfeind P, et al. Defective thrombus formation in mice lacking coagulation factor XII. J Exp Med. 2005;202(2):271-81.
165. Nickel KF, Ronquist G, Langer F, Labberton L, Fuchs TA, Bokemeyer C, et al. The polyphosphate-factor XII pathway drives coagulation in prostate cancer-associated thrombosis. Blood. 2015;126(11):1379-89.
166. Persson K, Morgelin M, Lindbom L, Alm P, Bjorck L, Herwald H. Severe lung lesions caused by Salmonella are prevented by inhibition of the contact system. J Exp Med. 2000;192(10):1415-24.
167. McLaren M, Alkaabi J, Connacher M, Belch JJ, Valenete E. Activated factor XII in rheumatoid arthritis. Rheumatol Int. 2002;22(5):182-4.
168. Dewald G, Bork K. Missense mutations in the coagulation factor XII (Hageman factor) gene in hereditary angioedema with normal C1 inhibitor. Biochem Biophys Res Commun. 2006;343(4):1286-9.
169. Zamolodchikov D, Chen ZL, Conti BA, Renne T, Strickland S. Activation of the factor XII-driven contact system in Alzheimer's disease patient and mouse model plasma. Proc Natl Acad Sci U S A. 2015;112(13):4068-73.
170. Muszbek L, Bereczky Z, Bagoly Z, Komáromi I, Katona É. Factor XIII: a coagulation factor with multiple plasmatic and cellular functions. Physiol Rev. 2011;91(3):931-72.
171. Shi DY, Wang SJ. Advances of Coagulation Factor XIII. Chin Med J (Engl). 2017;130(2):219-23.
172. Schroeder V, Kohler HP. New developments in the area of factor XIII. Journal of thrombosis and haemostasis : JTH. 2013;11(2):234-44.
173. Greenberg CS, Shuman MA. The zymogen forms of blood coagulation factor XIII bind specifically to fibrinogen. J Biol Chem. 1982;257(11):6096-101.
174. Souri M, Osaki T, Ichinose A. The Non-catalytic B Subunit of Coagulation Factor XIII Accelerates Fibrin Cross-linking. J Biol Chem. 2015;290(19):12027-39.
175. Lorand L, Jeong JM, Radek JT, Wilson J. Human plasma factor XIII: subunit interactions and activation of zymogen. Methods in enzymology. 1993;222:22-35.
176. Pedersen LC, Yee VC, Bishop PD, Le Trong I, Teller DC, Stenkamp RE. Transglutaminase factor XIII uses proteinase-like catalytic triad to crosslink macromolecules. Protein Sci. 1994;3(7):1131-5.
177. Duval C, Allan P, Connell SD, Ridger VC, Philippou H, Ariens RA. Roles of fibrin alpha- and gamma-chain specific cross-linking by FXIIIa in fibrin structure and function. Thromb Haemost. 2014;111(5):842-50.
178. Fraser SR, Booth NA, Mutch NJ. The antifibrinolytic function of factor XIII is exclusively expressed through alpha(2)-antiplasmin cross-linking. Blood. 2011;117(23):6371-4.
179. Sixma JJ, van den Berg A, Schiphorst M, Geuze HJ, McDonagh J. Immunocytochemical localization of albumin and factor XIII in thin cryo sections of human blood platelets. Thromb Haemost. 1984;51(3):388-91.
180. Mitchell JL, Lionikiene AS, Fraser SR, Whyte CS, Booth NA, Mutch NJ. Functional factor XIII-A is exposed on the stimulated platelet surface. Blood. 2014;124(26):3982-90.
181. Reed GL, Matsueda GR, Haber E. Fibrin-fibrin and alpha 2-antiplasmin-fibrin cross-linking by platelet factor XIII increases the resistance of platelet clots to fibrinolysis. Trans Assoc Am Physicians. 1991;104:21-8.

182. Hevessy Z, Haramura G, Boda Z, Udvardy M, Muszbek L. Promotion of the crosslinking of fibrin and alpha 2-antiplasmin by platelets. Thromb Haemost. 1996;75(1):161-7.
183. Serrano K, Devine DV. Intracellular factor XIII crosslinks platelet cytoskeletal elements upon platelet activation. Thromb Haemost. 2002;88(2):315-20.
184. Kasahara K, Kaneda M, Miki T, Iida K, Sekino-Suzuki N, Kawashima I, et al. Clot retraction is mediated by factor XIII-dependent fibrin-alphaIIbbeta3-myosin axis in platelet sphingomyelin-rich membrane rafts. Blood. 2013;122(19):3340-8.
185. Mitchell JL, Mutch NJ. Let's cross-link: diverse functions of the promiscuous cellular transglutaminase factor XIII-A. Journal of thrombosis and haemostasis : JTH. 2019;17(1):19-30.
186. Dale GL, Friese P, Batar P, Hamilton SF, Reed GL, Jackson KW, et al. Stimulated platelets use serotonin to enhance their retention of procoagulant proteins on the cell surface. Nature. 2002;415(6868):175-9.
187. Szasz R, Dale GL. Thrombospondin and fibrinogen bind serotonin-derivatized proteins on COAT-platelets. Blood. 2002;100(8):2827-31.
188. Soendergaard C, Kvist PH, Seidelin JB, Nielsen OH. Tissue-regenerating functions of coagulation factor XIII. Journal of thrombosis and haemostasis : JTH. 2013;11(5):806-16.
189. Al-Jallad HF, Myneni VD, Piercy-Kotb SA, Chabot N, Mulani A, Keillor JW, et al. Plasma membrane factor XIIIA transglutaminase activity regulates osteoblast matrix secretion and deposition by affecting microtubule dynamics. Plos One. 2011;6(1):e15893.
190. Inbal A, Muszbek L. Coagulation factor deficiencies and pregnancy loss. Seminars in thrombosis and hemostasis. 2003;29(2):171-4.
191. Asahina T, Kobayashi T, Okada Y, Goto J, Terao T. Maternal blood coagulation factor XIII is associated with the development of cytotrophoblastic shell. Placenta. 2000;21(4):388-93.
192. Board PG, Losowsky MS, Miloszewski KJ. Factor XIII: inherited and acquired deficiency. Blood Rev. 1993;7(4):229-42.
193. Dorgalaleh A, Rashidpanah J. Blood coagulation factor XIII and factor XIII deficiency. Blood Rev. 2016;30(6):461-75.
194. Naderi M, Dorgalaleh A, Alizadeh S, Tabibian S, Hosseini S, Shamsizadeh M, et al. Clinical manifestations and management of life-threatening bleeding in the largest group of patients with severe factor XIII deficiency. Int J Hematol. 2014;100(5):443-9.
195. de Maat MP, Verschuur M. Fibrinogen heterogeneity: inherited and noninherited. Current opinion in hematology. 2005;12(5):377-83.
196. Redman CM, Xia H. Fibrinogen biosynthesis. Assembly, intracellular degradation, and association with lipid synthesis and secretion. Ann N Y Acad Sci. 2001;936:480-95.
197. Weisel JW, Veklich Y, Gorkun O. The sequence of cleavage of fibrinopeptides from fibrinogen is important for protofibril formation and enhancement of lateral aggregation in fibrin clots. J Mol Biol. 1993;232(1):285-97.
198. Okumura N, Terasawa F, Haneishi A, Fujihara N, Hirota-Kawadobora M, Yamauchi K, et al. B:b interactions are essential for polymerization of variant fibrinogens with impaired holes 'a'. Journal of thrombosis and haemostasis : JTH. 2007;5(12):2352-9.
199. Siebenlist KR, Meh DA, Mosesson MW. Plasma factor XIII binds specifically to fibrinogen molecules containing gamma chains. Biochemistry. 1996;35(32):10448-53.
200. Coller BS, Shattil SJ. The GPIIb/IIIa (integrin alphaIIbbeta3) odyssey: a technology-driven saga of a receptor with twists, turns, and even a bend. Blood. 2008;112(8):3011-25.

201. Tutwiler V, Litvinov RI, Lozhkin AP, Peshkova AD, Lebedeva T, Ataullakhanov FI, et al. Kinetics and mechanics of clot contraction are governed by the molecular and cellular composition of the blood. Blood. 2016;127(1):149-59.
202. Mosesson MW. Antithrombin I. Inhibition of thrombin generation in plasma by fibrin formation. Thromb Haemost. 2003;89(1):9-12.
203. Richardson DL, Pepper DS, Kay AB. Chemotaxis for human monocytes by fibrinogen-derived peptides. British journal of haematology. 1976;32(4):507-13.
204. Senior RM, Skogen WF, Griffin GL, Wilner GD. Effects of Fibrinogen Derivatives Upon the Inflammatory Response - Studies with Human Fibrinopeptide-B. J Clin Invest. 1986;77(3):1014-9.
205. Singh TM, Kadowaki MH, Glagov S, Zarins CK. Role of fibrinopeptide B in early atherosclerotic lesion formation. Am J Surg. 1990;160(2):156-9.
206. Jennewein C, Tran N, Paulus P, Ellinghaus P, Eble JA, Zacharowski K. Novel aspects of fibrin(ogen) fragments during inflammation. Mol Med. 2011;17(5-6):568-73.
207. Ho PP, Lee LY, Zhao X, Tomooka BH, Paniagua RT, Sharpe O, et al. Autoimmunity against fibrinogen mediates inflammatory arthritis in mice. J Immunol. 2010;184(1):379-90.
208. Adams RA, Schachtrup C, Davalos D, Tsigelny I, Akassoglou K. Fibrinogen signal transduction as a mediator and therapeutic target in inflammation: lessons from multiple sclerosis. Curr Med Chem. 2007;14(27):2925-36.
209. Chen R, Doolittle RF. - cross-linking sites in human and bovine fibrin. Biochemistry. 1971;10(24):4487-91.
210. Sobel JH, Gawinowicz MA. Identification of the alpha chain lysine donor sites involved in factor XIIIa fibrin cross-linking. J Biol Chem. 1996;271(32):19288-97.
211. Siebenlist KR, Mosesson MW. Evidence of intramolecular cross-linked A alpha.gamma chain heterodimers in plasma fibrinogen. Biochemistry. 1996;35(18):5817-21.
212. Francis CW, Marder VJ. Increased resistance to plasmic degradation of fibrin with highly crosslinked alpha-polymer chains formed at high factor XIII concentrations. Blood. 1988;71(5):1361-5.
213. Rijken DC, Abdul S, Malfliet JJ, Leebeek FW, Uitte de Willige S. Compaction of fibrin clots reveals the antifibrinolytic effect of factor XIII. Journal of thrombosis and haemostasis : JTH. 2016;14(7):1453-61.
214. Wolberg AS, Campbell RA. Thrombin generation, fibrin clot formation and hemostasis. Transfus Apher Sci. 2008;38(1):15-23.
215. Undas A, Zawilska K, Ciesla-Dul M, Lehmann-Kopydlowska A, Skubiszak A, Ciepluch K, et al. Altered fibrin clot structure/function in patients with idiopathic venous thromboembolism and in their relatives. Blood. 2009;114(19):4272-8.
216. Mills JD, Ariens RA, Mansfield MW, Grant PJ. Altered fibrin clot structure in the healthy relatives of patients with premature coronary artery disease. Circulation. 2002;106(15):1938-42.
217. Zabczyk M, Plens K, Wojtowicz W, Undas A. Prothrombotic Fibrin Clot Phenotype Is Associated With Recurrent Pulmonary Embolism After Discontinuation of Anticoagulant Therapy. Arterioscler Thromb Vasc Biol. 2017;37(2):365-73.
218. Tziomalos K, Vakalopoulou S, Perifanis V, Garipidou V. Treatment of congenital fibrinogen deficiency: overview and recent findings. Vasc Health Risk Manag. 2009;5:843-8.

219. Arcagok BC, Ozdemir N, Tekin A, Ozcan R, Elicevik M, Senyuz OF, et al. Spontaneous splenic rupture in a patient with congenital afibrinogenemia. Turk Pediatri Ars. 2014;49(3):247-9.
220. Rodriguez-Merchan EC. Surgical wound healing in bleeding disorders. Haemophilia. 2012;18(4):487-90.
221. van Meegeren ME, de Rooy JW, Schreuder HW, Brons PP. Bone cysts in patients with afibrinogenaemia: a literature review and two new cases. Haemophilia. 2014;20(2):244-8.
222. de Moerloose P, Casini A, Neerman-Arbez M. Congenital fibrinogen disorders: an update. Seminars in thrombosis and hemostasis. 2013;39(6):585-95.
223. Forsgren M, Raden B, Israelsson M, Larsson K, Heden LO. Molecular cloning and characterization of a full-length cDNA clone for human plasminogen. FEBS Lett. 1987;213(2):254-60.
224. Castellino FJ, Ploplis VA. Structure and function of the plasminogen/plasmin system. Thromb Haemost. 2005;93(4):647-54.
225. Law RHP, Abu-Ssaydeh D, Whisstock JC. New insights into the structure and function of the plasminogen/plasmin system. Current Opinion in Structural Biology. 2013;23(6):836-41.
226. Miles LA, Castellino FJ, Gong Y. Critical role for conversion of glu-plasminogen to Lys-plasminogen for optimal stimulation of plasminogen activation on cell surfaces. Trends Cardiovasc Med. 2003;13(1):21-30.
227. Violand BN, Castellino FJ. Mechanism of the urokinase-catalyzed activation of human plasminogen. J Biol Chem. 1976;251(13):3906-12.
228. Backes BJ, Harris JL, Leonetti F, Craik CS, Ellman JA. Synthesis of positional-scanning libraries of fluorogenic peptide substrates to define the extended substrate specificity of plasmin and thrombin. Nat Biotechnol. 2000;18(2):187-93.
229. Ponting CP, Marshall JM, Cederholm-Williams SA. Plasminogen: a structural review. Blood Coagul Fibrinolysis. 1992;3(5):605-14.
230. Law RH, Sofian T, Kan WT, Horvath AJ, Hitchen CR, Langendorf CG, et al. X-ray crystal structure of the fibrinolysis inhibitor alpha2-antiplasmin. Blood. 2008;111(4):2049-52.
231. Rehman AA, Ahsan H, Khan FH. alpha-2-Macroglobulin: a physiological guardian. J Cell Physiol. 2013;228(8):1665-75.
232. Bajzar L, Manuel R, Nesheim ME. Purification and characterization of TAFI, a thrombin-activable fibrinolysis inhibitor. J Biol Chem. 1995;270(24):14477-84.
233. Schouten ES, van de Pol AC, Schouten AN, Turner NM, Jansen NJ, Bollen CW. The effect of aprotinin, tranexamic acid, and aminocaproic acid on blood loss and use of blood products in major pediatric surgery: a meta-analysis. Pediatr Crit Care Med. 2009;10(2):182-90.
234. Schuster V, Mingers AM, Seidenspinner S, Nussgens Z, Pukrop T, Kreth HW. Homozygous mutations in the plasminogen gene of two unrelated girls with ligneous conjunctivitis. Blood. 1997;90(3):958-66.
235. Schuster V, Seidenspinner S, Muller C, Rempen A. Prenatal diagnosis in a family with severe type I plasminogen deficiency, ligneous conjunctivitis and congenital hydrocephalus. Prenat Diagn. 1999;19(5):483-7.
236. Brandt JT. Plasminogen and tissue-type plasminogen activator deficiency as risk factors for thromboembolic disease. Arch Pathol Lab Med. 2002;126(11):1376-81.
237. Kruithof EK, Dunoyer-Geindre S. Human tissue-type plasminogen activator. Thromb Haemost. 2014;112(2):243-54.

238. Emeis JJ, van den Eijnden-Schrauwen Y, van den Hoogen CM, de Priester W, Westmuckett A, Lupu F. An endothelial storage granule for tissue-type plasminogen activator. J Cell Biol. 1997;139(1):245-56.
239. Tate KM, Higgins DL, Holmes WE, Winkler ME, Heyneker HL, Vehar GA. Functional role of proteolytic cleavage at arginine-275 of human tissue plasminogen activator as assessed by site-directed mutagenesis. Biochemistry. 1987;26(2):338-43.
240. Rijken DC, Hoylaerts M, Collen D. Fibrinolytic properties of one-chain and two-chain human extrinsic (tissue-type) plasminogen activator. J Biol Chem. 1982;257(6):2920-5.
241. Chapin JC, Hajjar KA. Fibrinolysis and the control of blood coagulation. Blood Rev. 2015;29(1):17-24.
242. Kuiper J, Otter M, Voorschuur AH, van Zonneveld AJ, Rijken DC, van Berkel TJ. Characterization of the interaction of a complex of tissue-type plasminogen activator and plasminogen activator inhibitor type 1 with rat liver cells. Thromb Haemost. 1995;74(5):1298-304.
243. Tabrizi P, Wang L, Seeds N, McComb JG, Yamada S, Griffin JH, et al. Tissue plasminogen activator (tPA) deficiency exacerbates cerebrovascular fibrin deposition and brain injury in a murine stroke model: studies in tPA-deficient mice and wild-type mice on a matched genetic background. Arterioscler Thromb Vasc Biol. 1999;19(11):2801-6.
244. Coutts SB, Berge E, Campbell BC, Muir KW, Parsons MW. Tenecteplase for the treatment of acute ischemic stroke: A review of completed and ongoing randomized controlled trials. Int J Stroke. 2018;13(9):885-92.
245. Sappino AP, Wohlwend A, Huarte J, Belin D, Vassalli JD. The PA-plasmin system during murine embryogenesis. Annals of the New York Academy of Sciences. 1992;667:41.
246. Pawlak R, Nagai N, Urano T, Napiorkowska-Pawlak D, Ihara H, Takada Y, et al. Rapid, specific and active site-catalyzed effect of tissue-plasminogen activator on hippocampus-dependent learning in mice. Neuroscience. 2002;113(4):995-1001.
247. Tsirka SE. Tissue plasminogen activator as a modulator of neuronal survival and function. Biochem Soc Trans. 2002;30(2):222-5.
248. Herczenik E, Gebbink MF. Molecular and cellular aspects of protein misfolding and disease. Faseb J. 2008;22(7):2115-33.
249. Jacobsen JS, Comery TA, Martone RL, Elokdah H, Crandall DL, Oganesian A, et al. Enhanced clearance of Abeta in brain by sustaining the plasmin proteolysis cascade. Proc Natl Acad Sci U S A. 2008;105(25):8754-9.
250. Melchor JP, Pawlak R, Strickland S. The tissue plasminogen activator-plasminogen proteolytic cascade accelerates amyloid-beta (Abeta) degradation and inhibits Abeta-induced neurodegeneration. J Neurosci. 2003;23(26):8867-71.
251. Tucker HM, Kihiko M, Caldwell JN, Wright S, Kawarabayashi T, Price D, et al. The plasmin system is induced by and degrades amyloid-beta aggregates. J Neurosci. 2000;20(11):3937-46.
252. Liu RM, van Groen T, Katre A, Cao D, Kadisha I, Ballinger C, et al. Knockout of plasminogen activator inhibitor 1 gene reduces amyloid beta peptide burden in a mouse model of Alzheimer's disease. Neurobiol Aging. 2011;32(6):1079-89.
253. Tucker HM, Simpson J, Kihiko-Ehmann M, Younkin LH, McGillis JP, Younkin SG, et al. Plasmin deficiency does not alter endogenous murine amyloid beta levels in mice. Neurosci Lett. 2004;368(3):285-9.
254. Lane CA, Hardy J, Schott JM. Alzheimer's disease. Eur J Neurol. 2018;25(1):59-70.

255. Kumar A, Singh A, Ekavali. A review on Alzheimer's disease pathophysiology and its management: an update. Pharmacol Rep. 2015;67(2):195-203.
256. Gandy S. The role of cerebral amyloid beta accumulation in common forms of Alzheimer disease. J Clin Invest. 2005;115(5):1121-9.
257. Thinakaran G, Koo EH. Amyloid precursor protein trafficking, processing, and function. J Biol Chem. 2008;283(44):29615-9.
258. Oh ES, Savonenko AV, King JF, Fangmark Tucker SM, Rudow GL, Xu G, et al. Amyloid precursor protein increases cortical neuron size in transgenic mice. Neurobiol Aging. 2009;30(8):1238-44.
259. Young-Pearse TL, Bai J, Chang R, Zheng JB, LoTurco JJ, Selkoe DJ. A critical function for beta-amyloid precursor protein in neuronal migration revealed by in utero RNA interference. J Neurosci. 2007;27(52):14459-69.
260. Kamenetz F, Tomita T, Hsieh H, Seabrook G, Borchelt D, Iwatsubo T, et al. APP processing and synaptic function. Neuron. 2003;37(6):925-37.
261. Abramov E, Dolev I, Fogel H, Ciccotosto GD, Ruff E, Slutsky I. Amyloid-beta as a positive endogenous regulator of release probability at hippocampal synapses. Nat Neurosci. 2009;12(12):1567-76.
262. Zhang W, Huang W, Jing F. Contribution of blood platelets to vascular pathology in Alzheimer's disease. J Blood Med. 2013;4:141-7.
263. Charidimou A, Gang Q, Werring DJ. Sporadic cerebral amyloid angiopathy revisited: recent insights into pathophysiology and clinical spectrum. J Neurol Neurosurg Psychiatry. 2012;83(2):124-37.
264. Cortes-Canteli M, Paul J, Norris EH, Bronstein R, Ahn HJ, Zamolodchikov D, et al. Fibrinogen and beta-amyloid association alters thrombosis and fibrinolysis: a possible contributing factor to Alzheimer's disease. Neuron. 2010;66(5):695-709.
265. Shen MY, Hsiao G, Fong TH, Chen HM, Chou DS, Lin CH, et al. Amyloid beta peptide-activated signal pathways in human platelets. Eur J Pharmacol. 2008;588(2-3):259-66.
266. de Jager M, Boot MV, Bol JG, Breve JJ, Jongenelen CA, Drukarch B, et al. The blood clotting Factor XIIIa forms unique complexes with amyloid-beta (Abeta) and colocalizes with deposited Abeta in cerebral amyloid angiopathy. Neuropathology and applied neurobiology. 2016;42(3):255-72.
267. Li QX, Berndt MC, Bush AI, Rumble B, Mackenzie I, Friedhuber A, et al. Membrane-associated forms of the beta A4 amyloid protein precursor of Alzheimer's disease in human platelet and brain: surface expression on the activated human platelet. Blood. 1994;84(1):133-42.
268. Burkhart JM, Vaudel M, Gambaryan S, Radau S, Walter U, Martens L, et al. The first comprehensive and quantitative analysis of human platelet protein composition allows the comparative analysis of structural and functional pathways. Blood. 2012;120(15):e73-82.
269. Tanzi RE, McClatchey AI, Lamperti ED, Villa-Komaroff L, Gusella JF, Neve RL. Protease inhibitor domain encoded by an amyloid protein precursor mRNA associated with Alzheimer's disease. Nature. 1988;331(6156):528-30.
270. Van Nostrand WE, Wagner SL, Farrow JS, Cunningham DD. Immunopurification and protease inhibitory properties of protease nexin-2/amyloid beta-protein precursor. J Biol Chem. 1990;265(17):9591-4.
271. Smith RP, Higuchi DA, Broze GJ, Jr. Platelet coagulation factor XIa-inhibitor, a form of Alzheimer amyloid precursor protein. Science. 1990;248(4959):1126-8.

272. Schmaier AH, Dahl LD, Rozemuller AJ, Roos RA, Wagner SL, Chung R, et al. Protease nexin-2/amyloid beta protein precursor. A tight-binding inhibitor of coagulation factor IXa. J Clin Invest. 1993;92(5):2540-5.
273. Mahdi F, Van Nostrand WE, Schmaier AH. Protease nexin-2/amyloid beta-protein precursor inhibits factor Xa in the prothrombinase complex. J Biol Chem. 1995;270(40):23468-74.
274. Mahdi F, Rehemtulla A, Van Nostrand WE, Bajaj SP, Schmaier AH. Protease nexin-2/Amyloid beta-protein precursor regulates factor VIIa and the factor VIIa-tissue factor complex. Thromb Res. 2000;99(3):267-76.
275. Xu F, Davis J, Miao J, Previti ML, Romanov G, Ziegler K, et al. Protease nexin-2/amyloid beta-protein precursor limits cerebral thrombosis. Proc Natl Acad Sci U S A. 2005;102(50):18135-40.
276. Xu F, Previti ML, Van Nostrand WE. Increased severity of hemorrhage in transgenic mice expressing cerebral protease nexin-2/amyloid beta-protein precursor. Stroke. 2007;38(9):2598-601.
277. Visconte C, Canino J, Guidetti GF, Zara M, Seppi C, Abubaker AA, et al. Amyloid precursor protein is required for in vitro platelet adhesion to amyloid peptides and potentiation of thrombus formation. Cell Signal. 2018;52:95-102.
278. Canobbio I, Guidetti GF, Oliviero B, Manganaro D, Vara D, Torti M, et al. Amyloid beta-peptide-dependent activation of human platelets: essential role for Ca2+ and ADP in aggregation and thrombus formation. Biochem J. 2014;462(3):513-23.
279. Smith SA, Mutch NJ, Baskar D, Rohloff P, Docampo R, Morrissey JH. Polyphosphate modulates blood coagulation and fibrinolysis. Proc Natl Acad Sci U S A. 2006;103(4):903-8.
280. Kumble KD, Kornberg A. Inorganic Polyphosphate in Mammalian-Cells and Tissues. J Biol Chem. 1995;270(11):5818-22.
281. Moreno-Sanchez D, Hernandez-Ruiz L, Ruiz FA, Docampo R. Polyphosphate Is a Novel Pro-inflammatory Regulator of Mast Cells and Is Located in Acidocalcisomes. J Biol Chem. 2012;287(34):28435-44.
282. Donovan AJ, Kalkowski J, Smith SA, Morrissey JH, Liu Y. Size-Controlled Synthesis of Granular Polyphosphate Nanoparticles at Physiologic Salt Concentrations for Blood Clotting. Biomacromolecules. 2014;15(11):3976-84.
283. Zhu S, Travers RJ, Morrissey JH, Diamond SL. FXIa and platelet polyphosphate as therapeutic targets during human blood clotting on collagen/tissue factor surfaces under flow. Blood. 2015;126(12):1494-502.
284. Kastrup CJ, Runyon MK, Lucchetta EM, Price JM, Ismagilov RF. Using chemistry and microfluidics to understand the spatial dynamics of complex biological networks. Accounts Chem Res. 2008;41(4):549-58.
285. Szymusiak M, Donovan AJ, Smith SA, Ransom R, Shen H, Kalkowski J, et al. Colloidal Confinement of Polyphosphate on Gold Nanoparticles Robustly Activates the Contact Pathway of Blood Coagulation. Bioconjug Chem. 2016;27(1):102-9.
286. Okorie UM, Denney WS, Chatterjee MS, Neeves KB, Diamond SL. Determination of surface tissue factor thresholds that trigger coagulation at venous and arterial shear rates: amplification of 100 fM circulating tissue factor requires flow. Blood. 2008;111(7):3507-13.
287. Balandina AN, Shibeko AM, Kireev DA, Novikova AA, Shmirev II, Panteleev MA, et al. Positive Feedback Loops for Factor V and Factor VII Activation Supply Sensitivity to Local Surface Tissue Factor Density During Blood Coagulation. Biophys J. 2011;101(8):1816-24.

288. Kastrup CJ, Runyon MK, Shen F, Ismagilov RF. Modular chemical mechanism predicts spatiotemporal dynamics of initiation in the complex network of hemostasis. Proc Natl Acad Sci U S A. 2006;103(43):15747-52.
289. Kastrup CJ, Boedicker JQ, Pomerantsev AP, Moayeri M, Bian Y, Pompano RR, et al. Spatial localization of bacteria controls coagulation of human blood by 'quorum acting'. Nat Chem Biol. 2008;4(12):742-50.
290. Chatterjee MS, Denney WS, Jing HY, Diamond SL. Systems Biology of Coagulation Initiation: Kinetics of Thrombin Generation in Resting and Activated Human Blood. PLoS Comput Biol. 2010;6(9):24.
291. Rana K, Neeves KB. Blood flow and mass transfer regulation of coagulation. Blood Rev. 2016.
292. Fogelson AL, Hussain YH, Leiderman K. Blood Clot Formation under Flow: The Importance of Factor XI Depends Strongly on Platelet Count. Biophys J. 2012;102(1):10-8.
293. Haynes LM, Dubief YC, Orfeo T, Mann KG. Dilutional Control of Prothrombin Activation at Physiologically Relevant Shear Rates. Biophys J. 2011;100(3):765-73.
294. Runyon MK, Kastrup CJ, Johnson-Kerner BL, Van Ha TG, Ismagilov RF. Effects of shear rate on propagation of blood clotting determined using microfluidics and numerical simulations. J Am Chem Soc. 2008;130(11):3458-64.
295. Cheng CP, Herfkens RJ, Taylor CA. Inferior vena caval hemodynamics quantified in vivo at rest and during cycling exercise using magnetic resonance imaging. Am J Physiol-Heart C. 2003;284(4):H1161-H7.
296. Karino T, Motomiya M. Flow through a Venous Valve and Its Implication for Thrombus Formation. Thromb Res. 1984;36(3):245-57.
297. Papaioannou TG, Stefanadis C. Vascular wall shear stress: basic principles and methods. Hellenic journal of cardiology : HJC = Hellenike kardiologike epitheorese. 2005;46(1):9-15.
298. Hathcock JJ. Flow effects on coagulation and thrombosis. Arterioscler Thromb Vasc Biol. 2006;26(8):1729-37.
299. Goel MS, Diamond SL. Adhesion of normal erythrocytes at depressed venous shear rates to activated neutrophils, activated platelets, and fibrin polymerized from plasma. Blood. 2002;100(10):3797-803.
300. Gallus AS. Travel, venous thromboembolism, and thrombophilia. Seminars in thrombosis and hemostasis. 2005;31(1):90-6.
301. Casa LDC, Deaton DH, Ku DN. Role of high shear rate in thrombosis. J Vasc Surg. 2015;61(4):1068-80.
302. Aghourian MN, Lemarie CA, Blostein MD. In vivo monitoring of venous thrombosis in mice. J Thromb Haemost. 2012;10(3):447-52.
303. Wilson JS, Virag L, Di Achille P, Karsaj I, Humphrey JD. Biochemomechanics of Intraluminal Thrombus in Abdominal Aortic Aneurysms. J Biomech Eng-Trans ASME. 2013;135(2):14.
304. Stavrou E, Schmaier AH. Factor XII: What does it contribute to our understanding of the physiology and pathophysiology of hemostasis & thrombosis. Thromb Res. 2010;125(3):210-5.
305. Yau JW, Liao P, Fredenburgh JC, Stafford AR, Revenko AS, Monia BP, et al. Selective depletion of factor XI or factor XII with antisense oligonucleotides attenuates catheter thrombosis in rabbits. Blood. 2014;123(13):2102-7.
306. Choi SH, Collins JNR, Smith SA, Davis-Harrison RL, Rienstra CM, Morrissey JH. Phosphoramidate End Labeling of Inorganic Polyphosphates: Facile Manipulation of

Polyphosphate for Investigating and Modulating Its Biological Activities. Biochemistry. 2010;49(45):9935-41.
307. Whitesides GM, Ostuni E, Takayama S, Jiang XY, Ingber DE. Soft lithography in biology and biochemistry. Annu Rev Biomed Eng. 2001;3:335-73.
308. Kenis PJA, Ismagilov RF, Whitesides GM. Microfabrication inside capillaries using multiphase laminar flow patterning. Science. 1999;285(5424):83-5.
309. Colace TV, Tormoen GW, McCarty OJT, Diamond SL. Microfluidics and Coagulation Biology. Annu Rev Biomed Eng. 2013;15:283-303.
310. Mann KG, Whelihan MF, Butenas S, Orfeo T. Citrate anticoagulation and the dynamics of thrombin generation. J Thromb Haemost. 2007;5(10):2055-61.
311. Sakariassen KS, Orning L, Turitto VT. The impact of blood shear rate on arterial thrombus formation. Future Sci OA. 2015;1(4).
312. Morrissey JH, Macik BG, Neuenschwander PF, Comp PC. Quantitation of Activated Factor-Vii Levels in Plasma Using a Tissue Factor Mutant Selectively Deficient in Promoting Factor-Vii Activation. Blood. 1993;81(3):734-44.
313. Riddell A, Abdul-Kadir R, Pollard D, Tuddenham E, Gomez K. Monitoring low dose recombinant factor VIIa therapy in patients with severe factor XI deficiency undergoing surgery. Thromb Haemost. 2011;106(3):521-7.
314. Hendriks HGD, van der Maaten JMAA, de Wolf J, Waterbolk TW, Slooff MJH, van der Meer J. An effective treatment of severe intractable bleeding after valve repair by one single dose of activated recombinant factor VII. Anesth Analg. 2001;93(2):287-9.
315. Mackman N. New insights into the mechanisms of venous thrombosis. J Clin Invest. 2012;122(7):2331-6.
316. Smith SA, Morrissey JH. Polyphosphate: a new player in the field of hemostasis. Curr Opin Hematol. 2014;21(5):388-94.
317. Colace TV, Tormoen GW, McCarty OJ, Diamond SL. Microfluidics and coagulation biology. Annu Rev Biomed Eng. 2013;15:283-303.
318. Geddings JE, Mackman N. New players in haemostasis and thrombosis. Thromb Haemost. 2014;111(4):570-4.
319. Becattini C, Agnelli G. Aspirin for prevention and treatment of venous thromboembolism. Blood Rev. 2014;28(3):103-8.
320. Mekaj YH, Daci FT, Mekaj AY. New insights into the mechanisms of action of aspirin and its use in the prevention and treatment of arterial and venous thromboembolism. Ther Clin Risk Manag. 2015;11.
321. Collaborative Overview of Randomized Trials of Antiplatelet Therapy .3. Reduction in Venous Thrombosis and Pulmonary-Embolism by Antiplatelet Prophylaxis among Surgical and Medical Patients. Brit Med J. 1994;308(6923):235-46.
322. Jensen TE, Baxter M, Rachlin JW, Jani V. Uptake of Heavy-Metals by Plectonema-Boryanum (Cyanophyceae) into Cellular-Components, Especially Polyphosphate Bodies - an X-Ray-Energy Dispersive Study. Environ Pollut A. 1982;27(2):119-27.
323. Yamaguchi T, Hasegawa M, Niimi R, Sudo A. Incidence and time course of asymptomatic deep vein thrombosis with fondaparinux in patients undergoing total joint arthroplasty. Thromb Res. 2010;126(4):E323-E6.
324. Katona E, Penzes K, Csapo A, Fazakas F, Udvardy ML, Bagoly Z, et al. Interaction of factor XIII subunits. Blood. 2014;123(11):1757-63.

325. Siebenlist KR, Meh DA, Mosesson MW. Plasma factor XIII binds specifically to fibrinogen molecules containing gamma' chains. Biochemistry. 1996;35(32):10448-53.
326. Takahashi N, Takahashi Y, Putnam FW. Primary Structure of Blood-coagulation Factor-XIIIa (Fibrinoligase, Transglutaminase) from Human-Placenta. Proceedings of the National Academy of Sciences of the United States of America. 1986;83(21):8019-23.
327. Bagoly Z, Haramura G, Muszbek L. Down-regulation of activated factor XIII by polymorphonuclear granulocyte proteases within fibrin clot. Thrombosis and Haemostasis. 2007;98(2):359-67.
328. Dunn CJ, Goa KL. Tranexamic acid - A review of its use in surgery and other indications. Drugs. 1999;57(6):1005-32.
329. Hsu JL, Huang SY, Chow NH, Chen SH. Stable-isotope dimethyl labeling for quantitative proteomics. Analytical Chemistry. 2003;75(24):6843-52.
330. Foster LJ, de Hoog CL, Mann M. Unbiased quantitative proteomics of lipid rafts reveals high specificity for signaling factors. Proceedings of the National Academy of Sciences of the United States of America. 2003;100(10):5813-8.
331. Rappsilber J, Ishihama Y, Mann M. Stop and go extraction tips for matrix-assisted laser desorption/ionization, nanoelectrospray, and LC/MS sample pretreatment in proteomics. Analytical Chemistry. 2003;75(3):663-70.
332. Fox BA, Yee VC, Pedersen LC, Le Trong I, Bishop PD, Stenkamp RE, et al. Identification of the calcium binding site and a novel ytterbium site in blood coagulation factor XIII by X-ray crystallography. Journal of Biological Chemistry. 1999;274(8):4917-23.
333. Stieler M, Weber J, Hils M, Kolb P, Heine A, Buchold C, et al. Structure of Active Coagulation Factor XIII Triggered by Calcium Binding: Basis for the Design of Next-Generation Anticoagulants. Angewandte Chemie-International Edition. 2013;52(45):11930-4.
334. Komorowicz E, Kolev K, Machovich R. Fibrinolysis with des-kringle derivatives of plasmin and its modulation by plasma protease inhibitors. Biochemistry. 1998;37(25):9112-8.
335. Kopec M, Latallo ZS, Stahl M, Wegrzyno.Z. Effect of Proteolytic Enzymes on Fibrin Stabilizing Factor. Biochimica Et Biophysica Acta. 1969;181(2):437-&.
336. Bucay I, O'Brien ET, Wulfe SD, Superfine R, Wolberg AS, Falvo MR, et al. Physical Determinants of Fibrinolysis in Single Fibrin Fibers. Plos One. 2015;10(2):15.
337. Schaller J, Gerber SS. The plasmin-antiplasmin system: structural and functional aspects. Cellular and Molecular Life Sciences. 2011;68(5):785-801.
338. Inbal A, Oldenburg J, Carcao M, Rosholm A, Tehranchi R, Nugent D. Recombinant factor XIII: a safe and novel treatment for congenital factor XIII deficiency. Blood. 2012;119(22):5111-7.
339. Adams HP, Leira EC, Torner JC, Barnathan E, Padgett L, Effron MB, et al. Treating patients with 'wake-up' stroke the experience of the AbESTT-II Trial. Stroke. 2008;39(12):3277-82.
340. Brott T, Broderick J, Kothari R, Odonoghue M, Barsan W, Tomsick T, et al. Intracerebral hemorrhage after intravenous t-PA therapy for ischemic stroke. Stroke. 1997;28(11):2109-18.
341. Cannon CP, McCabe CH, Gibson CM, Ghali M, Sequeira RF, McKendall GR, et al. TNK-tissue plasminogen activator in acute myocardial infarction - Results of the Thrombolysis in Myocardial Infarction (TIMI) 10A dose-ranging trial. Circulation. 1997;95(2):351-6.
342. Acheampong P, Ford GA. Pharmacokinetics of alteplase in the treatment of ischaemic stroke. Expert Opinion on Drug Metabolism & Toxicology. 2012;8(2):271-81.

343. Kahr WHA, Zheng SL, Sheth PM, Pai M, Cowie A, Bouchard M, et al. Platelets from patients with the Quebec platelet disorder contain and secrete abnormal amounts of urokinase-type plasminogen activator. Blood. 2001;98(2):257-65.
344. Thelwell C, Longstaff C. The regulation by fibrinogen and fibrin of tissue plasminogen activator kinetics and inhibition by plasminogen activator inhibitor 1. Journal of Thrombosis and Haemostasis. 2007;5(4):804-11.
345. Alonzo NC, Hyman BT, Rebeck GW, Greenberg SM. Progression of cerebral amyloid angiopathy: Accumulation of amyloid-beta 40 in affected vessels. Journal of Neuropathology and Experimental Neurology. 1998;57(4):353-9.
346. Love S, Miners S, Palmer J, Chalmers K, Kehoe P. Insights into the pathogenesis and pathogenicity of cerebral amyloid angiopathy. Frontiers in Bioscience. 2009;14:4778-92.
347. Ahn HJ, Zamolodchikov D, Cortes-Canteli M, Norris EH, Glickman JF, Strickland S. Alzheimer's disease peptide beta-amyloid interacts with fibrinogen and induces its oligomerization. Proceedings of the National Academy of Sciences of the United States of America. 2010;107(50):21812-7.
348. Zamolodchikov D, Renne T, Strickland S. The Alzheimer's disease peptide beta-amyloid promotes thrombin generation through activation of coagulation factor XII. Journal of Thrombosis and Haemostasis. 2016;14(5):995-1007.
349. Zamolodchikov D, Strickland S. A beta delays fibrin clot lysis by altering fibrin structure and attenuating plasminogen binding to fibrin. Blood. 2012;119(14):3342-51.
350. Donner L, Falker K, Gremer L, Klinker S, Pagani G, Ljungberg LU, et al. Platelets contribute to amyloid-beta aggregation in cerebral vessels through integrin alpha(IIb)beta(3)-induced outside-in signaling and clusterin release. Science Signaling. 2016;9(429):16.
351. Murphy MP, LeVine H. Alzheimer's Disease and the Amyloid-beta Peptide. Journal of Alzheimers Disease. 2010;19(1):311-23.
352. Nilsberth C, Westlind-Danielsson A, Eckman CB, Condron MM, Axelman K, Forsell C, et al. The 'Arctic' APP mutation (E693G) causes Alzheimer's disease by enhanced A beta protofibril formation. Nature Neuroscience. 2001;4(9):887-93.
353. Bugiani O, Giaccone G, Rossi G, Mangieri M, Capobianco R, Morbin M, et al. Hereditary Cerebral Hemorrhage With Amyloidosis Associated With the E693K Mutation of APP. Archives of Neurology. 2010;67(8):987-95.
354. Fernandezmadrid I, Levy E, Marder K, Frangione B. Codon-618 variant of Alzheimer amyloid gene associated with inherited cerebral-hemorrhage. Annals of Neurology. 1991;30(5):730-3.
355. Grabowski TJ, Cho HS, Vonsattel JPG, Rebeck GW, Greenberg SM. Novel amyloid precursor protein mutation in an Iowa family with dementia and severe cerebral amyloid angiopathy. Annals of Neurology. 2001;49(6):697-705.
356. Hendriks L, Vanduijn CM, Cras P, Cruts M, Vanhul W, Vanharskamp F, et al. Presenile-dementia and cerebral-hemorrhage linked to a mutation at codon-692 of the beta-amyloid precursor protein gene. Nature Genetics. 1992;1(3):218-21.
357. Benilova I, Karran E, De Strooper B. The toxic A beta oligomer and Alzheimer's disease: an emperor in need of clothes. Nature Neuroscience. 2012;15(3):349-57.
358. Hartley DM, Zhao CH, Speier AC, Woodard GA, Li SM, Li ZL, et al. Transglutaminase induces protofibril-like amyloid beta-protein assemblies that are protease-resistant and inhibit long-term potentiation. Journal of Biological Chemistry. 2008;283(24):16790-800.

359. Hur WS, Mazinani N, Lu XJD, Britton HM, Byrnes JR, Wolberg AS, et al. Coagulation factor XIIIa is inactivated by plasmin. Blood. 2015;126(20):2329-37.
360. Whitesides GM. The origins and the future of microfluidics. Nature. 2006;442(7101):368-73.
361. Yeon JH, Mazinani N, Schlappi TS, Chan KYT, Baylis JR, Smith SA, et al. Localization of Short-Chain Polyphosphate Enhances its Ability to Clot Flowing Blood Plasma. Scientific Reports. 2017;7:10.
362. Bochsen L, Johansson PI, Kristensen AT, Daugaard G, Ostrowski SR. The influence of platelets, plasma and red blood cells on functional haemostatic assays. Blood Coagulation & Fibrinolysis. 2011;22(3):167-75.
363. Lewis KB, Teller DC, Fry J, Lasser GW, Bishop PD. Crosslinking kinetics of the human transglutaminase, factor XIII A(2) , acting on fibrin gels and gamma-chain peptides. Biochemistry. 1997;36(5):995-1002.
364. Kucheryavykh LY, Davila-Rodriguez J, Rivera-Aponte DE, Zueva LV, Washington AV, Sanabria P, et al. Platelets are responsible for the accumulation of beta-amyloid in blood clots inside and around blood vessels in mouse brain after thrombosis. Brain Research Bulletin. 2017;128:98-105.
365. Biere AL, Ostaszewski B, Stimson ER, Hyman BT, Maggio JE, Selkoe DJ. Amyloid beta-peptide is transported on lipoproteins and albumin in human plasma. Journal of Biological Chemistry. 1996;271(51):32916-22.
366. Milojevic J, Costa M, Ortiz AM, Jorquera JI, Melacini G. In Vitro Amyloid-beta Binding and Inhibition of Amyloid-beta Self-Association by Therapeutic Albumin. Journal of Alzheimers Disease. 2014;38(4):753-65.
367. Ahn HJ, Glickman JF, Poon KL, Zamolodchikov D, Jno-Charles OC, Norris EH, et al. A novel A beta-fibrinogen interaction inhibitor rescues altered thrombosis and cognitive decline in Alzheimer's disease mice. Journal of Experimental Medicine. 2014;211(6):1049-62.
368. Gerardino L, Papaleo P, Flex A, Gaetani E, Fioroni G, Pola P, et al. Coagulation factor XIII Val34Leu gene polymorphism and Alzheimer's disease. Neurological Research. 2006;28(8):807-9.
369. Nalivaeva NN, Turner AJ. The amyloid precursor protein: A biochemical enigma in brain development, function and disease. Febs Letters. 2013;587(13):2046-54.
370. Rice HC, de Malmazet D, Schreurs A, Frere S, Van Molle I, Volkov AN, et al. Secreted amyloid-β precursor protein functions as a GABA. Science. 2019;363(6423).
371. Serrano K, Devine DV. Intracellular factor XIII crosslinks platelet cytoskeletal elements upon platelet activation. Thrombosis and Haemostasis. 2002;88(2):315-20.
372. Mitchell JL, Lionikiene AS, Fraser SR, Whyte CS, Booth NA, Mutch NJ. Functional factor XIII-A is exposed on the stimulated platelet surface. Blood. 2014;124(26):3982-90.
373. Boersema PJ, Aye TT, van Veen TA, Heck AJ, Mohammed S. Triplex protein quantification based on stable isotope labeling by peptide dimethylation applied to cell and tissue lysates. Proteomics. 2008;8(22):4624-32.
374. Cox J, Mann M. MaxQuant enables high peptide identification rates, individualized p.p.b.-range mass accuracies and proteome-wide protein quantification. Nat Biotechnol. 2008;26(12):1367-72.
375. Bale MD, Müller MF, Ferry JD. Effects of fibrinogen-binding tetrapeptides on mechanical properties of fine fibrin clots. Proc Natl Acad Sci U S A. 1985;82(5):1410-3.

376. Investigators PGIIiUARSUITPT. Inhibition of platelet glycoprotein IIb/IIIa with eptifibatide in patients with acute coronary syndromes. N Engl J Med. 1998;339(7):436-43.
377. Casoli T, Di Stefano G, Giorgetti B, Grossi Y, Balietti M, Fattoretti P, et al. Release of beta-amyloid from high-density platelets - Implications for Alzheimer's disease pathology. Signal Transduction Pathways, Pt D: Inflammatory Signaling Pathways and Neuropathology. 2007;1096:170-8.
378. De Strooper B, Vassar R, Golde T. The secretases: enzymes with therapeutic potential in Alzheimer disease. Nat Rev Neurol. 2010;6(2):99-107.
379. Prodan CI, Szasz R, Vincent AS, Ross ED, Dale GL. Coated-platelets retain amyloid precursor protein on their surface. Platelets. 2006;17(1):56-60.
380. Van Nostrand WE, Schmaier AH, Farrow JS, Cines DB, Cunningham DD. Protease nexin-2/amyloid beta-protein precursor in blood is a platelet-specific protein. Biochem Biophys Res Commun. 1991;175(1):15-21.
381. O'Brien RJ, Wong PC. Amyloid precursor protein processing and Alzheimer's disease. Annu Rev Neurosci. 2011;34:185-204.
382. Catricala S, Torti M, Ricevuti G. Alzheimer disease and platelets: how's that relevant. Immun Ageing. 2012;9(1):20.
383. Evin G, Li QX. Platelets and Alzheimer's disease: Potential of APP as a biomarker. World J Psychiatry. 2012;2(6):102-13.
384. Van Nostrand WE, Wagner SL, Suzuki M, Choi BH, Farrow JS, Geddes JW, et al. Protease nexin-II, a potent antichymotrypsin, shows identity to amyloid beta-protein precursor. Nature. 1989;341(6242):546-9.
385. Xu F, Davis J, Hoos M, Van Nostrand WE. Mutation of the Kunitz-type proteinase inhibitor domain in the amyloid beta-protein precursor abolishes its anti-thrombotic properties in vivo. Thromb Res. 2017;155:58-64.
386. Sonkar VK, Kulkarni PP, Dash D. Amyloid beta peptide stimulates platelet activation through RhoA-dependent modulation of actomyosin organization. Faseb J. 2014;28(4):1819-29.
387. Kucheryavykh LY, Davila-Rodriguez J, Rivera-Aponte DE, Zueva LV, Washington AV, Sanabria P, et al. Platelets are responsible for the accumulation of beta-amyloid in blood clots inside and around blood vessels in mouse brain after thrombosis. Brain Res Bull. 2017;128:98-105.
388. Canobbio I, Catricala S, Di Pasqua LG, Guidetti G, Consonni A, Manganaro D, et al. Immobilized amyloid Abeta peptides support platelet adhesion and activation. FEBS Lett. 2013;587(16):2606-11.
389. Hur WS, Mazinani N, Lu XJD, Yefet LS, Byrnes JR, Ho L, et al. Coagulation factor XIIIa cross-links amyloid beta into dimers and oligomers and to blood proteins. J Biol Chem. 2019;294(2):390-6.
390. Elg M, Gustafsson D, Carlsson S. Antithrombotic effects and bleeding time of thrombin inhibitors and warfarin in the rat. Thromb Res. 1999;94(3):187-97.
391. Stagaard R, Flick MJ, Bojko B, Gorynski K, Gorynska PZ, Ley CD, et al. Abrogating fibrinolysis does not improve bleeding or rFVIIa/rFVIII treatment in a non-mucosal venous injury model in haemophilic rodents. J Thromb Haemost. 2018;16(7):1369-82.
392. Stagaard R, Ley CD, Almholt K, Olsen LH, Knudsen T, Flick MJ. Absence of functional compensation between coagulation factor VIII and plasminogen in double-knockout mice. Blood Adv. 2018;2(22):3126-36.

393. Vaezzadeh N, Ni R, Kim PY, Weitz JI, Gross PL. Comparison of the effect of coagulation and platelet function impairments on various mouse bleeding models. Thromb Haemost. 2014;112(2):412-8.
394. Swallow RA, Agarwala RA, Dawkins KD, Curzen NP. Thromboelastography: potential bedside tool to assess the effects of antiplatelet therapy? Platelets. 2006;17(6):385-92.
395. Dahlback B, Villoutreix BO. The anticoagulant protein C pathway. FEBS Lett. 2005;579(15):3310-6.
396. Jain S, Pitoc GA, Holl EK, Zhang Y, Borst L, Leong KW, et al. Nucleic acid scavengers inhibit thrombosis without increasing bleeding. Proc Natl Acad Sci U S A. 2012;109(32):12938-43.
397. Ghosh S, Shukla D, Suman K, Lakshmi BJ, Manorama R, Kumar S, et al. Inositol hexakisphosphate kinase 1 maintains hemostasis in mice by regulating platelet polyphosphate levels. Blood. 2013;122(8):1478-86.
398. McKay H, Derome F, Haq MA, Whittaker S, Arnold E, Adam F, et al. Bleeding risks associated with inheritance of the Quebec platelet disorder. Blood. 2004;104(1):159-65.
399. Chang R, Cardenas JC, Wade CE, Holcomb JB. Advances in the understanding of trauma-induced coagulopathy. Blood. 2016;128(8):1043-9.
400. Elder GA, Gama Sosa MA, De Gasperi R. Transgenic mouse models of Alzheimer's disease. Mt Sinai J Med. 2010;77(1):69-81.
401. Maia MA, Sousa E. BACE-1 and gamma-Secretase as Therapeutic Targets for Alzheimer's Disease. Pharmaceuticals (Basel). 2019;12(1).
402. Canobbio I, Abubaker AA, Visconte C, Torti M, Pula G. Role of amyloid peptides in vascular dysfunction and platelet dysregulation in Alzheimer's disease. Front Cell Neurosci. 2015;9:65.